U.S. Department of Transportation

Federal Railroad Administration

Developing a Reliable Signal Wire Attachment Method for Rail

Office of Research
and Development
Washington, DC 20590

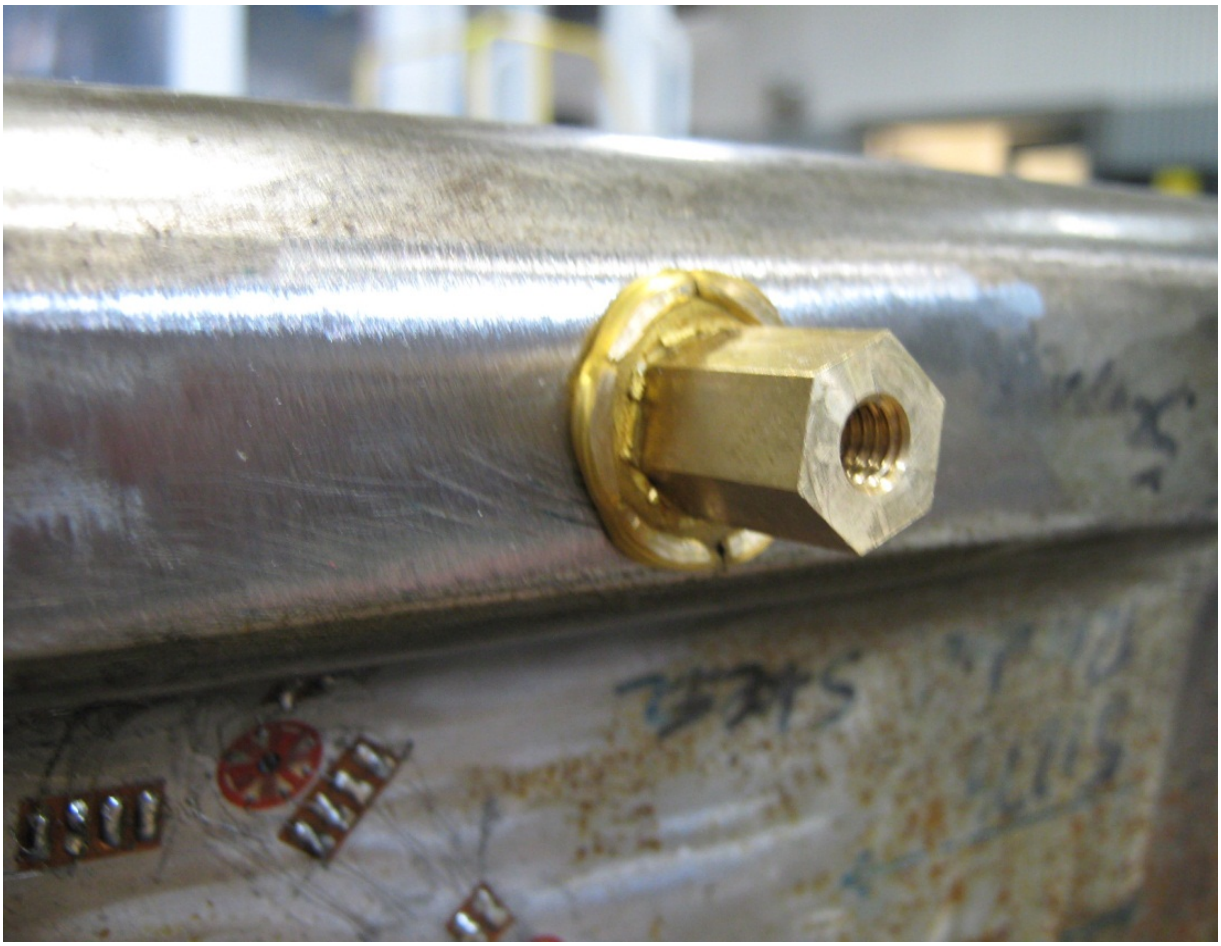

DOT/FRA/ORD-14/33

Final Report
November 2014

REPORT DOCUMENTATION PAGE

Form Approved
OMB No. 0704-0188

1. AGENCY USE ONLY (Leave blank)	2. REPORT DATE	3. REPORT TYPE AND DATES COVERED
	November 2014	Final (September 2011–June 2013)

4. TITLE AND SUBTITLE
Developing a Reliable Signal Wire Attachment Method

5. FUNDING NUMBERS
DTFR53-12-C-00002

6. AUTHOR(S)
Dave Workman, Cameron Stuart

7. PERFORMING ORGANIZATION NAME(S) AND ADDRESS(ES)
EWI
1250 Arthur E. Adams Drive
Columbus, OH 43221

8. PERFORMING ORGANIZATION REPORT NUMBER
EWI Project No. 53167GTH

9. SPONSORING/MONITORING AGENCY NAME(S) AND ADDRESS(ES)
U.S. Department of Transportation
Federal Railroad Administration
Office of Railroad Policy and Development
Office of Research and Development
Washington, DC 20590

10. SPONSORING/MONITORING AGENCY REPORT NUMBER
DOT/FRA/ORD-14/33

11. SUPPLEMENTARY NOTES
COR: Cameron Stuart

12a. DISTRIBUTION/AVAILABILITY STATEMENT
This document is available to the public through the FRA Web site at http://www.fra.dot.gov.

12b. DISTRIBUTION CODE

13. ABSTRACT (Maximum 200 words)
The goal of this project was to develop a better attachment method for rail signal wires to improve the reliability of signaling systems. EWI conducted basic research into the failure mode of current attachment methods and developed and tested a new process that provides improved performance over current techniques. EWI studied currently available stud alloys and developed a solid state inertia friction welding (IFW) process to better control the joining process and reduce the likelihood of forming martensite in the rail head. C464 Naval Brass exhibited high strength without the formation of martensite under manageable process parameters.

EWI developed the new welding process and conducted a series of tests to address any barriers to implementation. The testing included comparative tests between current exothermic welding techniques and the new IFW process. These tests included tensile testing, fatigue testing of welded joints, impact testing of weld joints, shear testing, microstructural analysis, and hardness testing in the rail steel immediately adjacent to the joint. In these tests, no martensite was found in the rail using the newly developed IFW process conditions. The mechanical tests showed a joint strength comparable to exothermic processes and fatigue performance that was as good, or better than, existing methods. This suggests the IFW approach should allow placement of the weld on the rail head with low risk of rail steel damage. A conceptual design for a portable IFW machine was completed.

14. SUBJECT TERMS
Railroad; rail; rail head; rail head defect; train control; signal wire attachment; liquid metal embrittlement; heat affected zone; solid state welding; naval brass; rail wire interface; martensite; inertial welding

15. NUMBER OF PAGES
100

16. PRICE CODE

17. SECURITY CLASSIFICATION OF REPORT	18. SECURITY CLASSIFICATION OF THIS PAGE	19. SECURITY CLASSIFICATION OF ABSTRACT	20. LIMITATION OF ABSTRACT
Unclassified	Unclassified	Unclassified	

NSN 7540-01-280-5500

Standard Form 298 (Rev. 2-89)
Prescribed by ANSI Std. 239-18
298-102

METRIC/ENGLISH CONVERSION FACTORS

ENGLISH TO METRIC	METRIC TO ENGLISH
LENGTH (APPROXIMATE)	**LENGTH (APPROXIMATE)**
1 inch (in) = 2.5 centimeters (cm)	1 millimeter (mm) = 0.04 inch (in)
1 foot (ft) = 30 centimeters (cm)	1 centimeter (cm) = 0.4 inch (in)
1 yard (yd) = 0.9 meter (m)	1 meter (m) = 3.3 feet (ft)
1 mile (mi) = 1.6 kilometers (km)	1 meter (m) = 1.1 yards (yd)
	1 kilometer (km) = 0.6 mile (mi)
AREA (APPROXIMATE)	**AREA (APPROXIMATE)**
1 square inch (sq in, in^2) = 6.5 square centimeters (cm^2)	1 square centimeter (cm^2) = 0.16 square inch (sq in, in^2)
1 square foot (sq ft, ft^2) = 0.09 square meter (m^2)	1 square meter (m^2) = 1.2 square yards (sq yd, yd^2)
1 square yard (sq yd, yd^2) = 0.8 square meter (m^2)	1 square kilometer (km^2) = 0.4 square mile (sq mi, mi^2)
1 square mile (sq mi, mi^2) = 2.6 square kilometers (km^2)	10,000 square meters (m^2) = 1 hectare (ha) = 2.5 acres
1 acre = 0.4 hectare (he) = 4,000 square meters (m^2)	
MASS - WEIGHT (APPROXIMATE)	**MASS - WEIGHT (APPROXIMATE)**
1 ounce (oz) = 28 grams (gm)	1 gram (gm) = 0.036 ounce (oz)
1 pound (lb) = 0.45 kilogram (kg)	1 kilogram (kg) = 2.2 pounds (lb)
1 short ton = 2,000 pounds (lb) = 0.9 tonne (t)	1 tonne (t) = 1,000 kilograms (kg) = 1.1 short tons
VOLUME (APPROXIMATE)	**VOLUME (APPROXIMATE)**
1 teaspoon (tsp) = 5 milliliters (ml)	1 milliliter (ml) = 0.03 fluid ounce (fl oz)
1 tablespoon (tbsp) = 15 milliliters (ml)	1 liter (l) = 2.1 pints (pt)
1 fluid ounce (fl oz) = 30 milliliters (ml)	1 liter (l) = 1.06 quarts (qt)
1 cup (c) = 0.24 liter (l)	1 liter (l) = 0.26 gallon (gal)
1 pint (pt) = 0.47 liter (l)	
1 quart (qt) = 0.96 liter (l)	
1 gallon (gal) = 3.8 liters (l)	
1 cubic foot (cu ft, ft^3) = 0.03 cubic meter (m^3)	1 cubic meter (m^3) = 36 cubic feet (cu ft, ft^3)
1 cubic yard (cu yd, yd^3) = 0.76 cubic meter (m^3)	1 cubic meter (m^3) = 1.3 cubic yards (cu yd, yd^3)
TEMPERATURE (EXACT)	**TEMPERATURE (EXACT)**
[(x-32)(5/9)] °F = y °C	[(9/5) y + 32] °C = x °F

QUICK INCH - CENTIMETER LENGTH CONVERSION

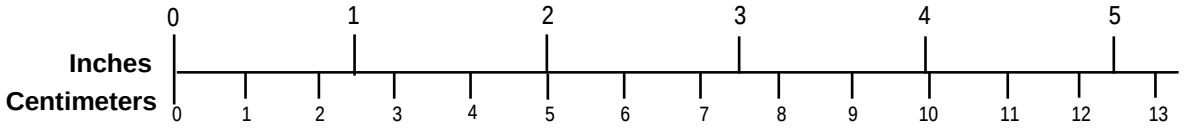

QUICK FAHRENHEIT - CELSIUS TEMPERATURE CONVERSIO

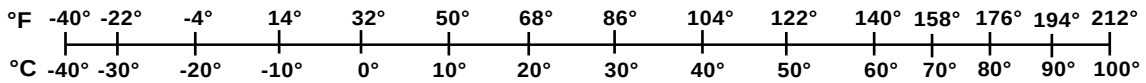

For more exact and or other conversion factors, see NIST Miscellaneous Publication 286, Units of Weights and Measures. Price $2.50 SD Catalog No. C13 10286

Updated 6/17/98

Contents

Illustrations

Tables

Executive Summary

The goal of this project was to develop a better attachment method for rail signal wires to improve the reliability of signaling systems. EWI conducted basic research to determine the failure modes of current methods and developed a list of process characteristics needed to improve the attachment methods. The key characteristics needed for an improved process include:

- No martensite or other deleterious microstructural damage formed in the rail during the joining process
- A simple, operator-independent process
- No preheating of the rail
- Weld strength sufficient to break the wire rather than the attachment to the rail
- Process reparability
- Portable tooling

Based on these process characteristics, EWI investigated the use of inertia friction welding (IFW) for this application. EWI experimented with a collection of metal alloys to determine the most suitable material for the stud attachment hardware. One alloy, C464 Naval Brass, exhibited high strength without the formation of martensite. In addition, the IFW process parameters for this alloy allow the use of a portable welding machine. Using this alloy, welds can be produced with a range of weld parameters with good results. Metallographic inspections revealed that the lamellae (thin layer) of pearlite in rail is unaffected by the welding process immediately adjacent to the C464 material. These welds have a tensile strength of 4,800 pounds (lb), which is more than adequate to cause failure of the wire prior to failure of the stud-to-rail attachment. A reparability test conducted on the weld showed that 10 repeat welds could be made with no martensite formation in the adjacent rail steel, while maintaining consistent weld strength.

After the welding process was developed, EWI conducted a series of tests to address any barriers to implementation. The testing included comparative tests between current exothermic welding techniques and the new IFW process. These tests included tensile testing, fatigue testing of welded joints, impact testing of weld joints, shear testing, microstructural analysis, and hardness testing in the rail steel immediately adjacent to the joint. In these tests, no martensite was found in the rail when using the newly developed IFW process conditions. The mechanical tests showed joint strength comparable to exothermic processes and fatigue performance equal to, or better than existing joining methods. The results indicate that the IFW process for stud welding results in a safe and secure signal wire attachment to the rail head.

Based on these results, EWI created a conceptual design for a portable IFW machine. This design will be used in future phases of development to validate the approach for field welding trials.

1. Introduction

1.1 Background

Electrical signals are sent through rail sections in order to detect trains on the track, identify broken rails to prevent derailments, and alert signal crossing stations when a train approaches. Studs are attached to rails so that bond wires can be installed to bridge rail joints, thus completing the electrical circuits. Railroad industry input indicates that signal attachments fail at a rather high rate. This creates uncertainty in the system, resulting in reduced train speeds, additional required inspections to identify the cause of the failures, and reinstallation of attachment studs.

Ideally, the studs for signal connection should be attached on the head of the rail, placing the bond wires clear of maintenance equipment. However, several train derailments and rail breaks have been associated with welded/brazed joints used on the head of the rail. These track failures were due to the high heat input associated with joining processes such as pin brazing and exothermic weld processes. These processes can produce a temperature profile in the rail that results in the formation of untempered martensite directly beneath the joint. Untempered martensite in rail steel is particularly brittle and can fracture easily when strain is applied as a train passes over the rails. Once a crack is present in the rail head, it will progressively increase in size with each passing wheelset and may result in rail fracture.

As a result of the known risk of untempered martensite in stud-to-rail joints, the stud locations have been moved to the neutral axis of the rail (the web area) to reduce the bending strain. This has alleviated the problem, but the undesirable microstructure is still present—just in a less critical position. One drawback of this lower risk option is that the cables and studs are now in an area where regular track maintenance work can snag the wires or studs, resulting in detachment of the stud from the track. This detachment results in the loss of the electrical signal conduction and requires repair before efficient train velocity can be regained.

1.2 Objectives

The objective of this research program is to develop a procedure that substantially reduces variability in the quality of stud-to-rail welds, allows stud attachments to occur at consistent locations on the rails, and reduces the risk of microstructural damage and premature failure. Project success can (1) restore the preferred (rail head) location of the stud while preserving rail fatigue life by avoiding the formation of undesirable metallurgical phases, (2) reduce the incidents related to signal wires interfering with maintenance of way (MOW) equipment, and (3) reduce the number of signal track failure incidents by increasing the life expectancy of a stud-to-rail attachment.

Specific project goals are as follows:

- Investigate failure modes of current rail signal wire attachment techniques.
- Develop a signal wire attachment method that is operator independent to guarantee joint quality.

- Design a solid-state operation to prevent formation of martensite or liquid metal embrittlement in the rail during welding and a break-away feature to prevent rail damage in a wire snag scenario.
- Create portable process that can be applied easily in the field.
- Complete testing of the new process so as to compare it with existing attachment methods.

1.3 Scope

The project work was conducted in three phases. Phase 1 consisted of literature reviews, surveys, and a failure analysis to assess the current signal wire attachment methods. Advantages and disadvantages of various signal wire attachment methods were documented along with industry performance requirements. In Phase 2, EWI completed the developmental work to create a portable friction welding process for signal wire attachment to the rail head. Various attachment stud materials were evaluated. Welds were performed on laboratory equipment at operational parameters that could be transitioned to portable applications. Test welds were evaluated for metallurgical and mechanical performance. In Phase 3, EWI completed testing and analysis of the inertia friction welding method and compared this new process against the industry accepted exothermic signal wire joining method.

1.4 Technical Approach

1.4.1 Phase 1—Literature Review

The approach for Phase 1 was to perform a literature review, survey railroads, and conduct a failure analysis on a sample that failed in service. Interviews were conducted with major railroads and experts from organizations such as the Federal Railroad Administration (FRA), the John A. Volpe National Transportation Systems Center (Volpe), and Transportation Technology Center Inc. (TTCI). The literature review included prior research results from TTCI. A review of the National Transportation Safety Board (NTSB) Railroad Accident Report was also conducted. The results were used to determine failure mechanisms of current stud-to-rail attachment techniques and their effect on the efficiency and safety of rail operations. In addition, we compiled a list of desired stud attachment characteristics and summarized their performance.

1.4.2 Phase 2—Process Development

In Phase 2, EWI identified candidate stud alloy materials with the desired material characteristics, corrosion properties, and electrical performance and created a new IFW. Approximately 100 studs were produced from the top three candidate materials. Selected studs were used to determine welding parameters such as spindle revolutions per minute (RPM), welding force, upset speed, upset force, spindle inertia, and stud extension from the spindle. EWI performed metallurgical and mechanical analyses of these trial welds to determine preliminary process parameters. Using the preferred process procedures, welding trials were repeated to assess any underlying rail damage from repeated welds at the same location.

1.4.3 Phase 3—Weld Testing and Evaluation

In Phase 3, one stud material was down-selected from the results of Phase 2 to perform further analysis and characterization of the weld joint. More than 100 weld samples were produced for testing. EWI completed testing of both the IFW samples and samples made with the industry standard exothermic weld process. Corrosion testing was conducted on both weld samples using industry standard accelerated corrosion techniques. To ensure adequate service life, fatigue testing was conducted by loading welded samples in a servo-hydraulic fatigue apparatus. Additional mechanical tests were conducted to provide impact and shear strength data for the weld joints. Based on these results, EWI created a conceptual design for a portable IFW machine.

2. Experimental Studies

2.1 Phase 1: Examination of Current Signal Wire Techniques and Issues

Railroad signaling systems detect trains on the track, identify broken rails to prevent derailments, and alert signal crossing stations when trains approach. These systems are vital to safe train operation; therefore, each component of this system has to be extremely reliable. Current methods of rail-wire attachment have shortcomings that are creating reliability problems for the railroads. Failures in signal cable attachments create uncertainty in the signaling system, resulting in reduced train speeds, additional inspection time to identify the cause of the failures, and reinstallation efforts that result in train delays, lost productivity, and reduced operational safety.

Signaling systems are based on the closed-circuit principle and fail-safe characteristics founded on and expanded from William Robinson's original 1872 patent for "Improvements in Electrical Signaling Apparatus for Railroads" (U.S. Patent 130,661). These systems require a rugged and dependable interconnection from the rail to the electronic equipment. The connection where the wayside signaling and grade crossing warning systems interface with the rail is referred to as the rail-wire interface (RWI). The RWI is an integral part of the operating system. RWI failures, particularly signal bond RWI failures, cause train delays that can affect operations over a large segment of the system.

This section begins with a discussion of the various signal wire attachment methods, their advantages, disadvantages, and known failure mechanisms. It continues with a summary of the findings from the NTSB Railroad Accident Report "Derailment of Canadian National Freight Train M33371 and Subsequent Release of Hazardous Materials in Tamaroa, Illinois." This section also includes a literature review, which shows the results of the testing that has been conducted to advance signal wire reliability, and highlights areas of continued interest. Additionally, EWI conducted interviews with railroad personnel to compare with the literature review findings. These reports and findings show that signal wire failures are a significant problem, and a new method of attachment is worth exploring. Portable friction welding of the rail wires addresses the shortcomings of the other bonding approaches, while providing a portable, repeatable, and reliable solution that can be applied in the field. This report concludes with an outline of the proposed evaluation and testing approach for portable friction welding of signal wires to the head of the rail.

2.1.1 Current Signal Wire Attachment Methods

Railroads commonly use exothermic welding and/or pin brazing to create RWI bonds. Other methods are in limited use, or experimental. These methods include mechanical tapered-pin plug bonds, hard or soft solder, amalgamated contacts, bolted contacts, conductive epoxy bonding (experimental), stud welding (experimental), and driven-in threaded stud (experimental).

2.1.1.1 Exothermic Weld Bonds

Exothermic bonds are produced using a set of molds containing molten metal that is cast between a signal wire and the rail itself. This process requires a field operator to successfully perform initial installation and adjustment of the mold against the rail. An aluminum powder and copper oxide mixture is ignited in a crucible to form molten copper. Once the molten copper forms, it travels through a tube into the mold, filling the mold and forming a weld or braze joint. Figure 1 shows a photograph of an exothermic bond joint. Exothermic weld bonds are one of the most common RWI bonding methods because there are no external power requirements and the equipment is portable.

Welded bonds require heat to make the weld and this heat can change the microstructure of the rail steel. Martensite, a hard and brittle microstructure, is formed as a result of rapid cooling (quenching) of the heated steel. Untempered martensite weakens the steel and can lead to cracking under load. In general, the exothermic weld/braze joints can perform well if they are properly executed. However, there are many critical steps in the process to guarantee quality of the joint, making it a risky process to perform in the field. Thorough cleaning of the rail and fit-up of the mold to rail are critical to the success of the operation.

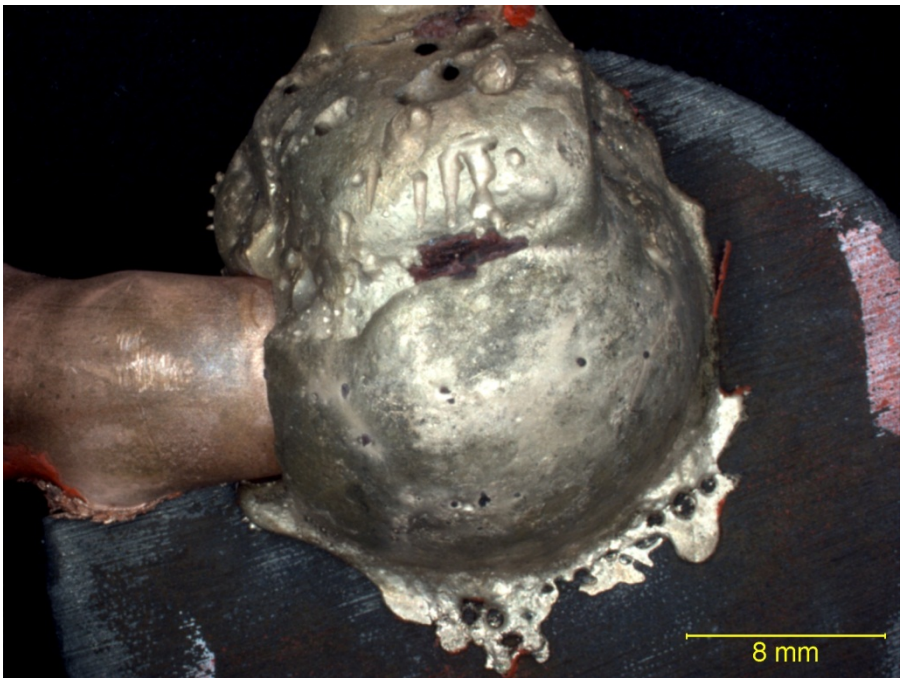

Figure 1. Exothermic RWI Joint

2.1.1.2 Pin Brazing

Pin brazing is a variation of a drawn arc stud welding process. A pin braze can be produced with an alloy that drastically reduces the peak temperature of the process required to reflow the braze joint. A section of track is initially cleaned thoroughly to remove all dirt and oxides. A flux is applied to a special pin and to the track to ensure that the area is chemically cleaned to ensure good quality bonding. A pin is heated, then with an arc heating process, the backside of a cable lug is heated; this process melts the brazing alloy, allowing it to flow between the RWI and

solidify. A picture of the process is shown in Figure 2. The equipment required to perform pin brazing is more bulky than exothermic welding and requires a vehicle or cart for transportation to a job site.

More procedure variables are required for pin brazing than for exothermic bonding, and the operator needs to maintain a properly ground surface, proper application of fluxing agents, and appropriate brazing parameters to form a quality joint. It is important to note that pin brazing is performed at high enough temperatures to affect the underlying rail material with the potential to form untempered martensite.

Figure 2. Pin Brazing

2.1.1.3 Plug Bonds

Plug bonds or chicken heads have been used for nearly a century; however, they are no longer commonly used by most railroads. Where flammable materials are handled, there is limited use of these mechanical tapered-pin plug bonds. Plug bonds are installed by broaching the soft steel plug into a sharp-edged hole drilled into the rail web with a slight interference fit. This type of bond does not leave much material to be worn away before failure of the plug bond begins to occur from loosening. Plug bonds have an advantage over welded or brazed bonds since the bond is mechanical and, therefore, not likely to cause microstructure transformations in the rail steel. Research has concluded that drilling holes in the neutral axis of rails does not damage the steel in the rail. However, repeated installation and removal cycles may result in a loose-fitting plug bond due to frictional wear.

2.1.1.4 Bolted Contacts

Bolted contacts are installed in the web of the rail and require drilling equipment to drill a hole through the web of the rail. These joints offer excellent attachment and detachment characteristics because you can simply loosen and retighten a bolt to fix a broken wire. The joint strength will be consistently as high as the strength of the bolt, so it is possible to size the bolt to

carry the required loads. The bolting does require drilling a hole in the web of the rail, which can lead to a geometric notch if procedures are not followed or the hole is not properly placed.

2.1.1.5 Adhesive Bonds

The adhesive bonding process typically requires many steps to successfully bond the signal wires to rail steel. The steel must be cleaned, primed, and a corrosion inhibitor applied to ensure that the adhesive joint performs well. These joints are advantageous since bonding does not require the rail to be exposed to heat above any critical temperatures. Most adhesive solutions are still in the experimental stage and have not proven to be as reliable as the methods mentioned above.

2.1.2 NTSB Railroad Accident Report Summary

Much of the recent emphasis on researching improved signal wire joining techniques can be traced back to the Tamaroa, IL, train derailment in 2003.

On February 9, 2003, a Canadian National freight train derailed 22 of its 108 cars in Tamaroa, IL. Some cars released methanol, fueling a fire, and other cars released phosphoric acid, hydrochloric acid, formaldehyde, and vinyl chloride. Approximately 850 residents were evacuated from an area within a 3-mile radius of the derailment. No one was injured in the accident, although one contract employee was injured during the cleanup activities. Damages to track, signals, equipment, as well as clearing costs associated with the accident, totaled nearly $1.9 million. The NTSB determined that the probable cause for the accident was placement of bond wire welds on the head of the rail just outside the joint bars, where untempered martensite associated with the welds led to fatigue and subsequent cracking and rapidly progressed to rail failure.

The NTSB report indicates that the exothermic welding system requires no external power source and is highly portable, quick, effective, relatively inexpensive, and widely used among railroads. However, several instances of exothermic bond wire welds produced conditions that left untempered martensite in the rail heat-affected zone (HAZ).[6] The report also identifies a need for a separate classification for rail cracks originating from bond wire attachments for defects identified in 49 CFR Part 213, “Track Safety Standards.” Furthermore, NTSB suggests that FRA should require 49 CFR Part 225, “Guide for Preparing Accident/Incident Reports,” to report a specific cause code for derailments caused by rail cracks originating from bond wire attachments. The report also recommends that ERICO Products, Inc. revise instructions for exothermic (CADWELD) welding systems to address proper placement of exothermic bond wire welds, especially in the vicinity of joint bars. The report further recommends that users be made aware that these welds create untempered martensite that could, under certain conditions, lead to fatigue cracking and rail failure. NTSB also recommended that the American Railway Engineering and Maintenance-of-Way Association (AREMA) modify the Railroad Engineering Manual and/or the Communications and Signals Manual to address the proper placement of exothermic bond wire welds and high-temperature pin brazings and to include information that these welds and brazings create untempered martensite that could, under certain conditions, lead to fatigue cracking and rail failure.

2.1.3 TTCI Signal Wire Attachment Research Review

Research has been conducted over the last 5 years by the Association of American Railroads (AAR) and TTCI for improved signal wire reliability, particularly in the area of rail-to-wire bonding. TTCI estimates that there are 25,000 train stops in North America per year due to track wire connections. This data is congruent with FRA statistical safety data. FRA reported 50,000 signal track failures in 2009, and approximately 22,000 of these were caused by stud or RWI failure. TTCI has published several Technology Digests on the evaluation of track wire connections. The following digests were reviewed under and summarized within this report:

- TD-08-016 – "Improved Signal Reliability: Rail-To-Wire Bonding"
- TD-08-058 – "Rail-Wire Interface Performance Issues"
- TD-10-025 – "Evaluation of the Effects of Track Wire Connections on Rail Fatigue Life"
- TD-11-010 – "Maintenance Resistant Track Wire Connections"
- TD-11-026 – "In-Service Evaluation of Track-to-Wire Connections for Signals"

2.1.3.1 TD-08-016 – "Improved Signal Reliability: Rail-To-Wire Bonding"

This report summarizes information gathered from an investigation into the problem of track signal wire failures and their potential to contribute to train service disruption [1]. Interviews were conducted as part of this research and the following conclusions were drawn:

- The present RWI attachment methods all have shortcomings that are creating reliability problems for railroads.
- Newer methods have not provided solutions.
- The train delays due to RWI failures warrant further investigation and the development of better attachment methods and materials.

RWI analysis for this report included ten RWI technologies, of which seven were currently accepted methods of attachment, and three were experimental. The investigation revealed the following list of desired attributes for new bonding designs:

- Low Contact Resistance—the contact resistance should be as low as, or lower than, a properly installed plug bond.
- Bond Strand Retention—the mechanical strength of the bond should be at least equal to the "pull-out" strength of a crimped-sleeve connection.
- Ease of Installation—the weight of the equipment required to install the bond should be carefully considered as a significant parameter, along with the number of tools and consumables required to complete the process.
- Application during Inclement Weather—an ideal bonding technology will not be adversely affected by extremes of temperature, humidity, and precipitation.
- Temporary Disconnection of Track Wire from Track—disconnecting the track wires from the rails serves to isolate expensive electronic signaling equipment from potentially damaging voltages and currents during welded track repair and is also standard practice for several signal maintainers when MOW or tamping crews are working in the area. This key feature has kept plug bonds viable for many years.

- No Damage to Rails—each new rail bonding technology should be evaluated by sectioning and etching the bond area to determine the impact of the bonding method on the steel of the rails.
- Cost—as always, the installed cost-per-bond, including the amortized equipment cost and labor costs, should be considered.

2.1.3.2 TD-08-058 – "Rail-Wire Interface Performance Issues"

This report summarizes several interviews that TTCI conducted with signal maintenance personnel from a number of railroads regarding RWI performance issues. The interviews were conducted to obtain a perspective on the known or suspected root causes of RWI problems and failures, to learn more about RWI installation and maintenance practices, and to identify potential improvements to current RWI technology.

The following information was noted from the interviews:

- The most common types of RWIs in use on freight railroads were exothermic welds and pin brazing.
- Tapered-pin plug bonds were used in limited applications, particularly applications near flammable materials.
- Failure of exothermic or pin-brazed welds can be associated with improper procedure adherence such as grinding and/or preheating.
- Exothermic molds will fail to seal against the adjacent rail surface as the mold materials degrade when used past their working life.
- Rail defects are detected adjacent to exothermic welds.
- Crimping of the wire pigtails is often insufficient or improper.
- Improper lengths of pigtails cause failures due to thermal movements or train-induced rail movements.
- Excessive track deflections under heavy loads can cause RWI failures.

From the information gathered in these interviews the TTCI authors concluded that a bolted connection rather than a crimped connection is preferred for ease of replacement. The industry expressed considerable frustration with exothermic mold reuse practices in the field. One of the most significant findings was that nearly half of the RWI failures occur during track maintenance. System designs that facilitate RWI removal and reinstallation during maintenance are desired. [(2)]

The authors suggested improved methods of quality control, improved materials, and enhanced training to provide incremental improvements to the RWI technologies currently in use. Additionally, they suggested that new RWI technologies need to be pursued through research.

2.1.3.3 TD-10-025 – "Evaluation of the Effects of Track Wire Connections on Rail Fatigue Life"

This work involved finite-element modeling of the effects of hole geometry and RWI placement in the web of the rail. Both round holes and irregular-shaped holes were evaluated to simulate multiple RWI interface conditions. Rough holes were used to simulate either a poorly drilled hole or a weld that thermally damaged the rail. The modeling showed that holes in the rail web do create a stress riser that will reduce the fatigue life of the rail; however, if the holes are

properly installed, this effect will not affect rail service life.[3] The researchers determined that the effects of dynamic loading, cracks propagating from weld metal, or other hole shapes may be more significant than suggested by the models simulated in this study. The researchers thus concluded that further development into track wire connections is necessary, particularly where technologies that do not require significant heating of the rail or drilling of holes in the rail are concerned.

2.1.3.4 TD-11-010 – "Maintenance Resistant Track Wire Connections"

This article reviewed and suggested methods for sizing and setting up RWI joints and fusible links in the wire to avoid damaging the wire bond itself. This is a critical set of tests because it defines how strong rail-to-wire interface joints should be and how strong the break away or fusible line should be in order to protect the joint. The study showed that a RWI joint, with a more than 1,000-pound pull strength, will remove a portion of the rail during failure, resulting in a geometric defect.[4] The study also found that a 550-pound target strength for the wire-to-connector joint was adequate to resist in-service loading and incidents with wire movement while maintaining a constant wire conductivity. This data can be used to size the strength of any newly developed process.

2.1.3.5 TD-11-026 – "In-Service Evaluation of Track-to-Wire Connections for Signals"

This document discusses the results of long-term in-service testing conducted by TTCI at the Facility for Accelerated Service Testing (FAST) and two revenue service locations. The findings of the study showed that conventional track wire connections, such as welded, brazed, bolted, and drilled technologies, exhibited low rates of failure. All technologies experienced some type of failure when subjected to ballast maintenance, but most had some form of wire connection remaining.[5] This finding suggests that a "fused, repairable link" may offer easier repair and replacement at the same location on the rail. Welded and brazed connections performed the best over the long term in all the different environments tested. The report also concluded that the joints in one of the revenue service locations failed sooner due to the high-frequency vibration and perhaps corrosive (salt spray) environment.

2.1.3.6 TTCI Report Summary

TTCI reports a number of different failure modes—at the RWI, the wire, and at connections between links of wire. Broken track wires seem to indicate MOW equipment snagging. This is suggested as the cause of 50 percent of the wire failures or trouble codes; improved location and routing of the wires would alleviate many of these failures. Additionally, some railroads have a policy which necessitates removal of the wires before the MOW activity is initiated; therefore, a reliable method of attaching and reattaching the wires is needed.

Currently used RWI attachment methods are also heavily dependent on human operator performance. The processes require many steps, pieces of equipment, and different materials to make a joint. Variability in procedure execution can result in varying joint quality. All reports indicate human factors as the major source of variation in the current bonding methods. This implies that an automated RWI process may be preferred.

TTCI's extensive interviews and findings can be summarized in three statements:

1. The present methods of rail-wire attachment all have shortcomings that are creating signal and rail reliability problems for the railroads.
2. The newer methods have not provided ideal solutions.
3. The problem of train delays resulting from rail-wire interfaces may not be urgent but is significant enough to warrant further investigation and the development of better attachment methods and materials.

2.1.4 Railroad Personnel Interviews and Feedback

EWI approached the major railroads in the list below with a questionnaire on rail-wire attachments:

- Amtrak
- Union Pacific
- Burlington Northern Santa Fe
- CSX
- Canadian Pacific
- Norfolk Southern

The questions related to signal wire stud attachments and associated challenges were:

1. What method is typically used to attach signal wire studs?
2. Does the method currently provide adequate performance when properly used?
3. What failure rate is associated with signal wire studs?
4. What is the #1 cause of failure?
5. What is the most challenging part of attachment in the current process?
6. Are there any rail section failures associated with single wire stud attachment?

A combination of pin brazing and exothermic welding is predominantly used to create the RWI. Clamp-on type joints are used, but only for temporary closure of the circuit. These two methods are common in Union Pacific, Amtrak, Canadian Pacific, and CSX.

All railroads discussed the need to improve the reliability of the signal wire attachment methods currently in use. Two railroads responded and provided further insight into the issues associated with current signal wire attachment methods. Guidance on equipment-type solutions was also provided by both parties. Additionally, a staff member of the Canadian Pacific railroad was interviewed during a rail conference. The most frequent comments by railroad staff regarding equipment was the need to keep it lightweight, make installation one simple step, and limit the number of parts used.

Rail section failures were noted as occurring close to RWI joints (but, in general, are not tracked as a specific failure). One railroad noted that three rail section failures have occurred from the center of the rail where a current return stud was attached. These failures were associated with martensite formation in the rail steel. Another railroad provided a sample where the rail section itself indicated a crack at the signal wire attachment location. A failure analysis of this sample is presented later in this report, highlighting metallurgical issues with the current RWI methods.

Railroads have conducted projects to try to move the signal wire attachment onto the rail head to avoid MOW interactions with the wires. Cracking has been occasionally detected around the

signal wire attachments when pin brazing or exothermic processes were used. No permanent, viable solution has been developed. The biggest concern from an implementation standpoint is process complexity. A simple, yet robust and field-deployable technology solution is needed to guarantee that the quality of the joints is consistent and acceptable.

It should be reported that the railroads investigated all noted rail failures or flaw indications around RWI joints as an issue mostly because they could not identify the root cause of the failures.

2.1.5 Failure Analysis of a Sample Rail Section

A section of rail with an ultrasonic testing (UT) indication next to the RWI joint was provided for evaluation. This section was obtained from a freight line. The presence of defects next to RWI joints was noted in the TTCI work as a concern. This section was removed before fracture of the rail occurred by drilling from the backside of the RWI joint in the web. A group of photos of the extracted crack-containing section is shown in Figures 3–5. The crack is apparent in Figure 5 where it is running into and parallel with the round column of material.

Figure 3. Removed Section

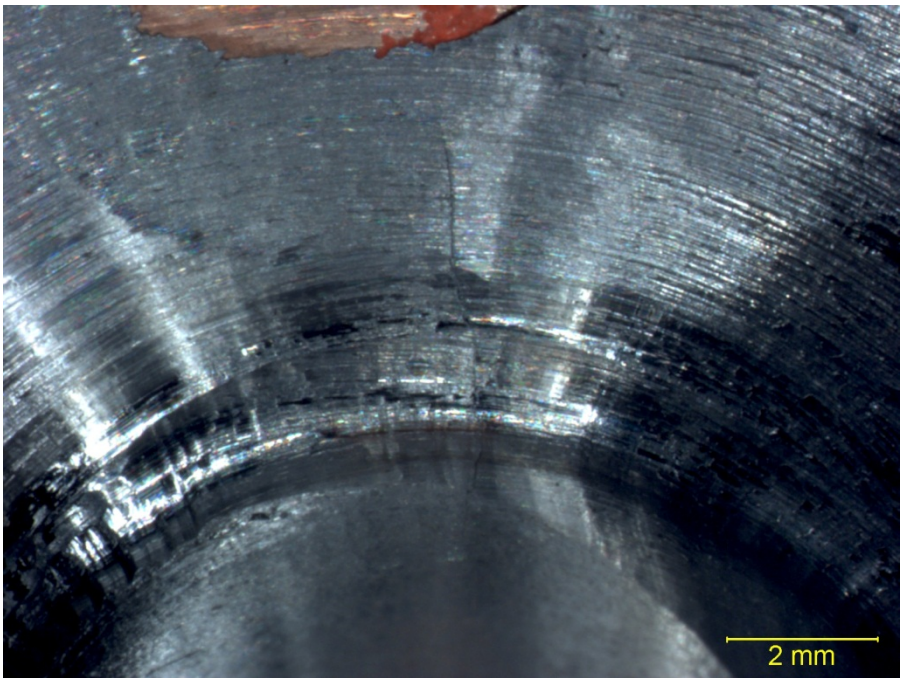

Figure 4. Perspective View of Crack on Backside of Sample

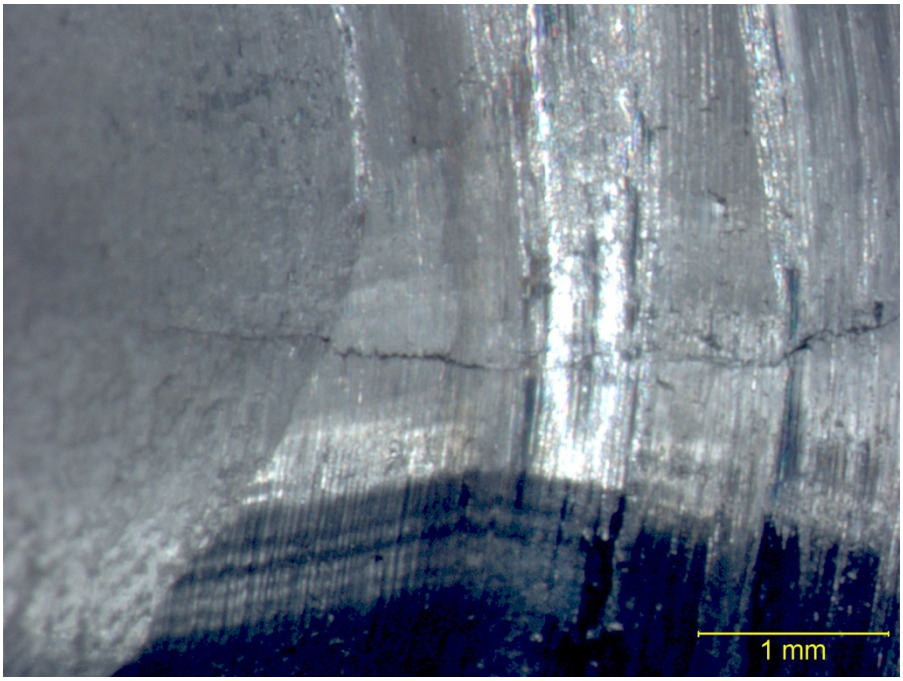

Figure 5. Detail View of Crack in Section

The crack was parted at the edge of the cylindrical section normal to it to allow for metallographic examination. The larger section of the crack was prepared using standard metallographic techniques for examination of the crack and surrounding microstructure. Photos were taken at two different grinding levels to get an idea of the crack morphology.

The smaller section of the crack was broken open and viewed optically to determine what the fracture face contained. As shown in Figure 6, copper decorates the surface of the crack face. Others areas of the sample showed similar evidence of copper on the crack face, clearly indicating copper contamination or liquid metal embrittlement (LME). LME occurs when a lower melting metal flows across a higher melting metal under tensile stress. Note that a tensile stress is present in the rail in order to maintain the neutral rail temperature and the braze and solder materials used are known to cause LME in steel.

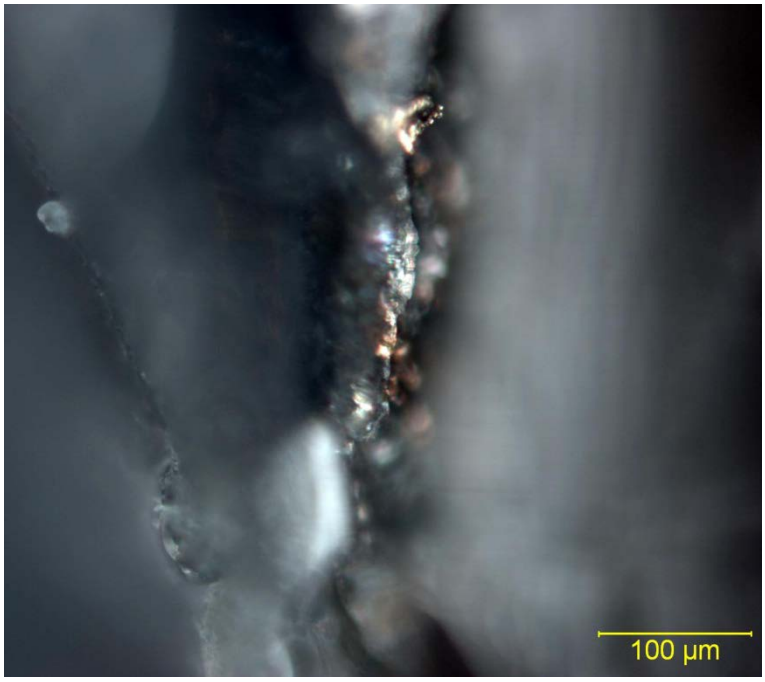

Figure 6. View of Crack Face Showing Copper on the Surface

The results of the initial grinding of the crack section are shown in Figures 7 and 8. Additional photos of the area adjacent to the crack are shown in Figures 9–11, where areas of possible LME are present.

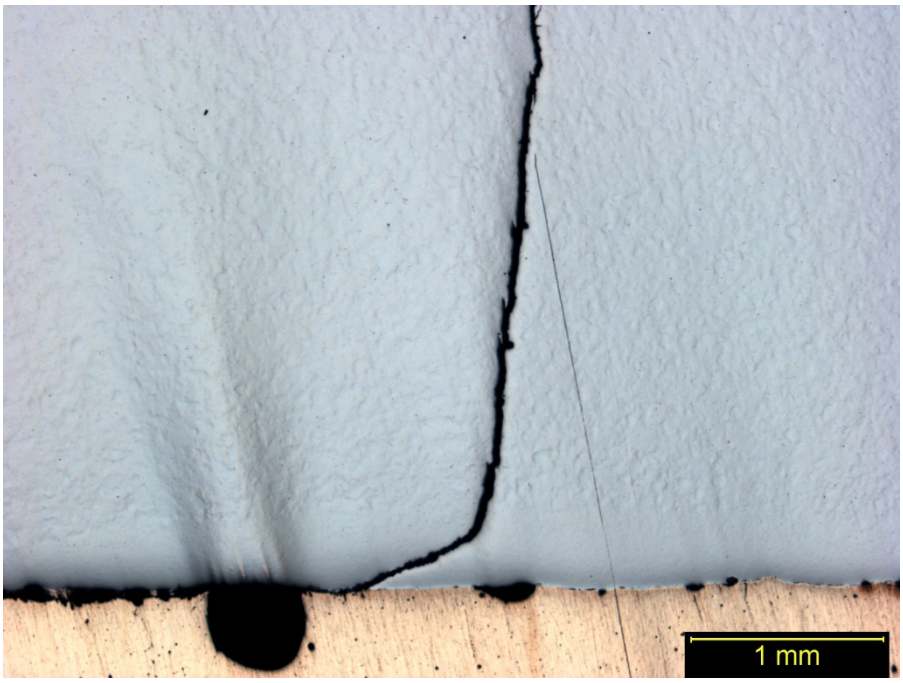

Figure 7. Macro View of Crack at First Grind Level

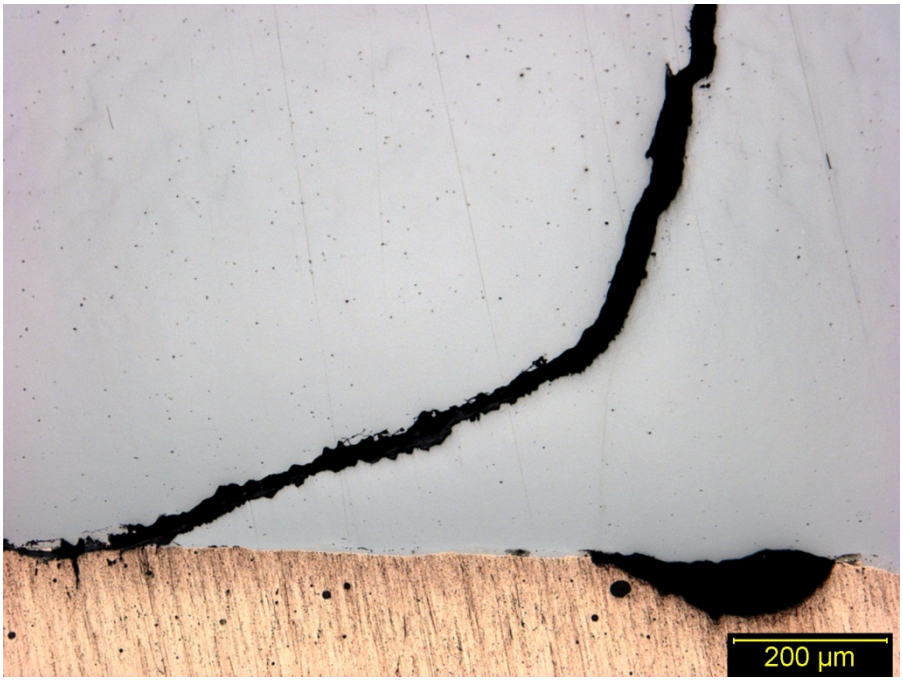

Figure 8. Close-Up of Crack Area at First Grind Level

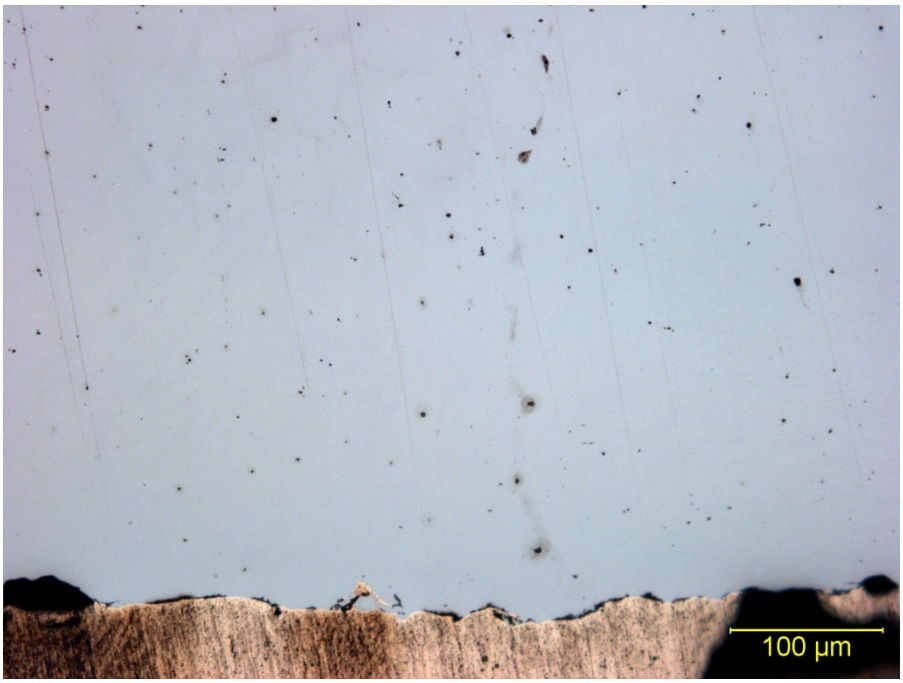

Figure 9. Adjacent Area of Suspected LME Copper Contamination

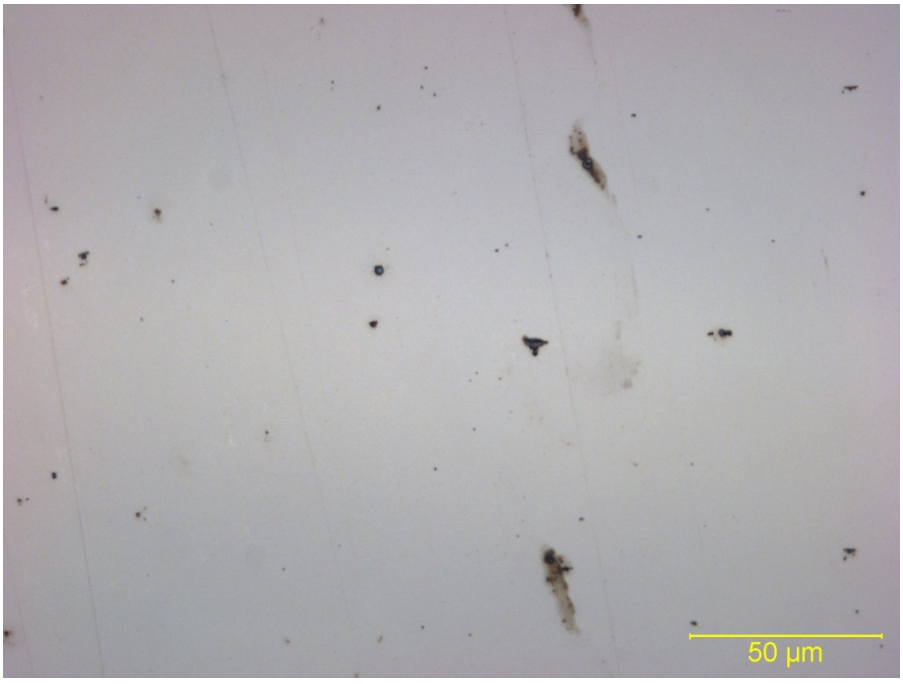

Figure 10. Suspected LME Area Detail

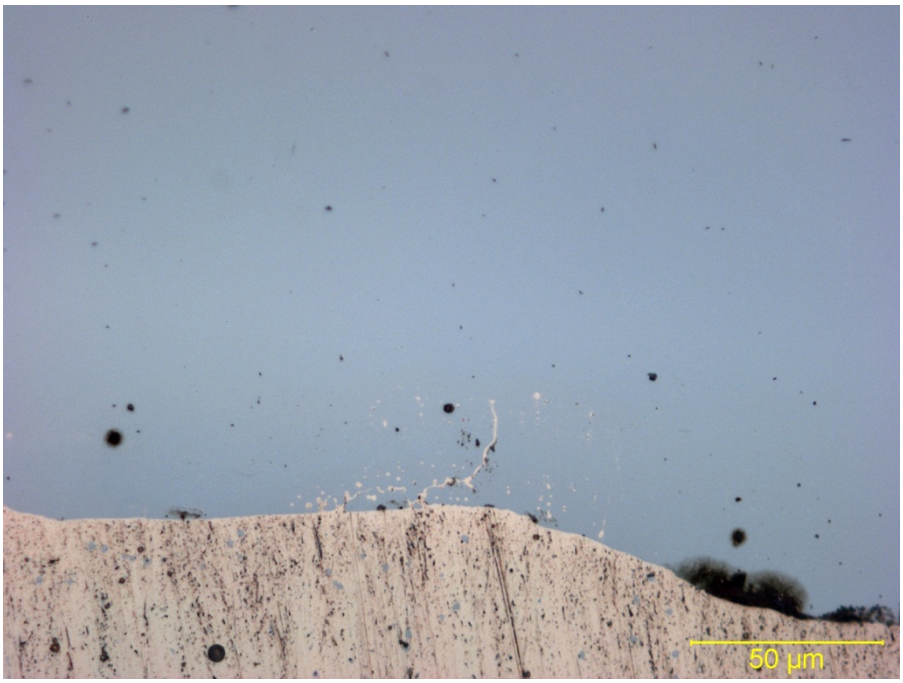

Figure 11. Adjacent Area of Suspected LME in Stage 1 Grind

The secondary grind macro view is shown in Figure 12, and a detailed image of the secondary crack that develops at greater grind depth is shown in Figure 13. Figure 14 shows an area where copper appears to be attached to the crack edge although there is a possibility of contamination from the grinding process. More detailed photos in Figures 15 and 16 show the copper migrating along the fusion boundary between the weld alloy and the steel at shallow depths.

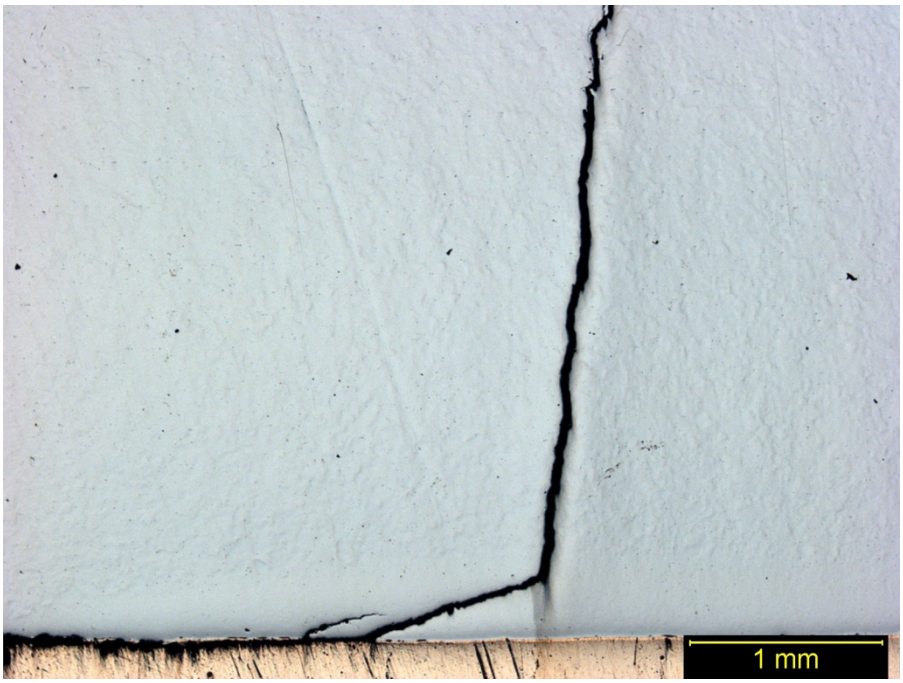

Figure 12. Macro View of Crack at Stage 2 Grind

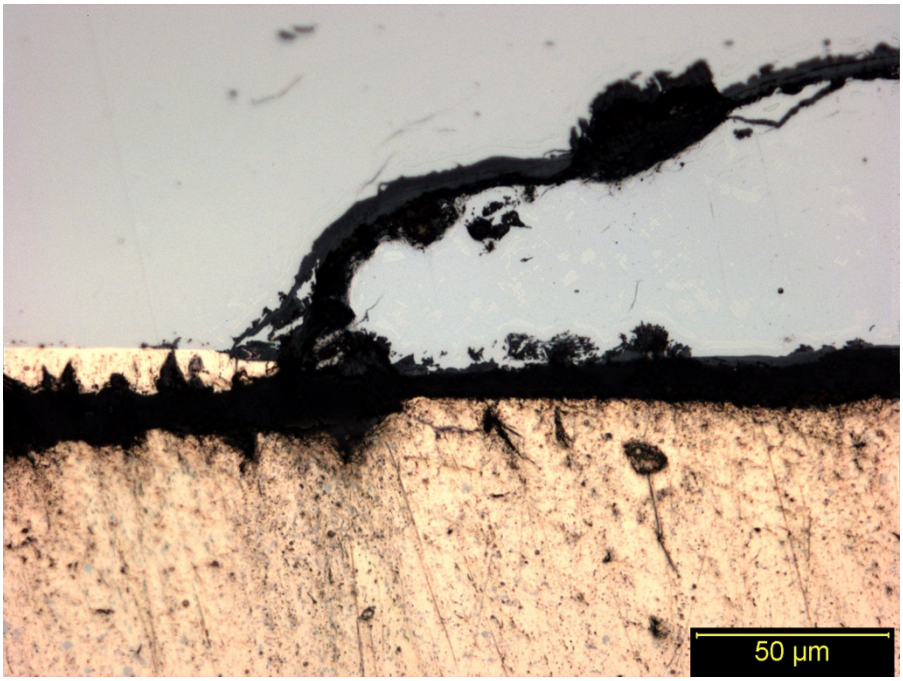

Figure 13. More Detailed View of Secondary Crack

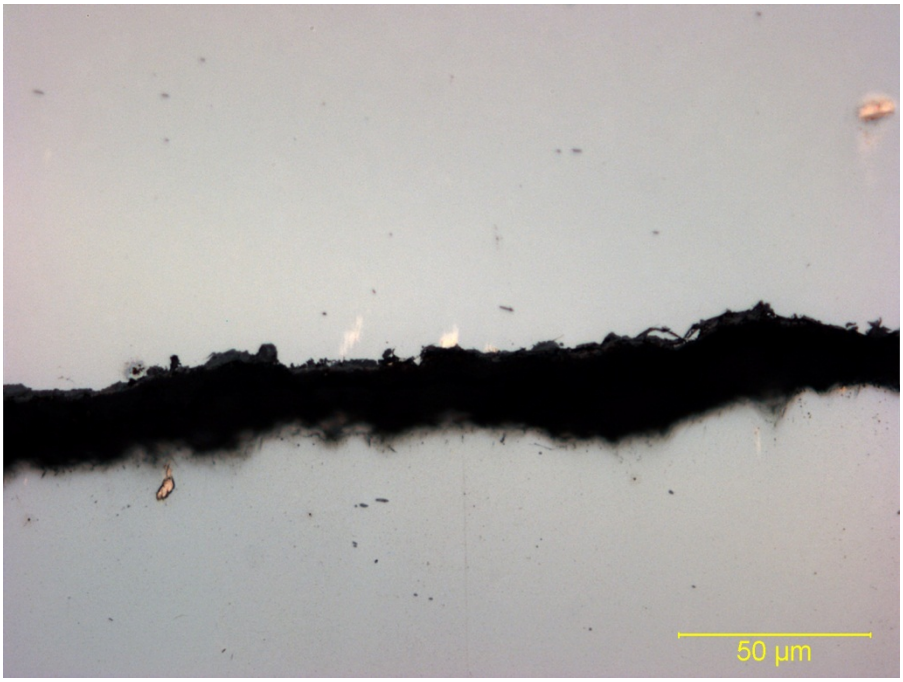

Figure 14. Area of Crack Showing Potential Copper Contamination on Crack Edges

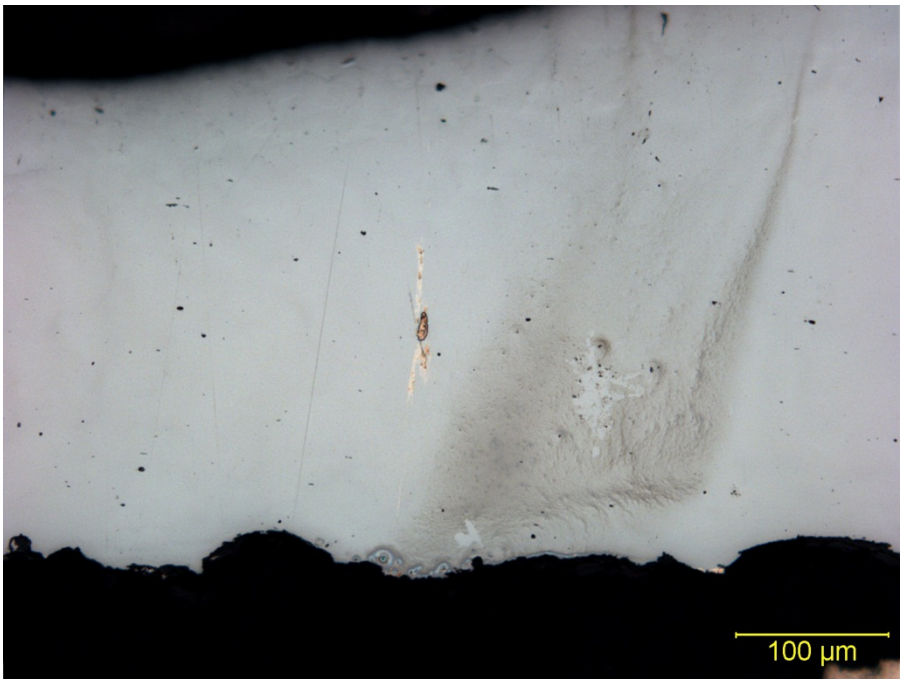

Figure 15. Adjacent Area to Crack Showing More Typical LME

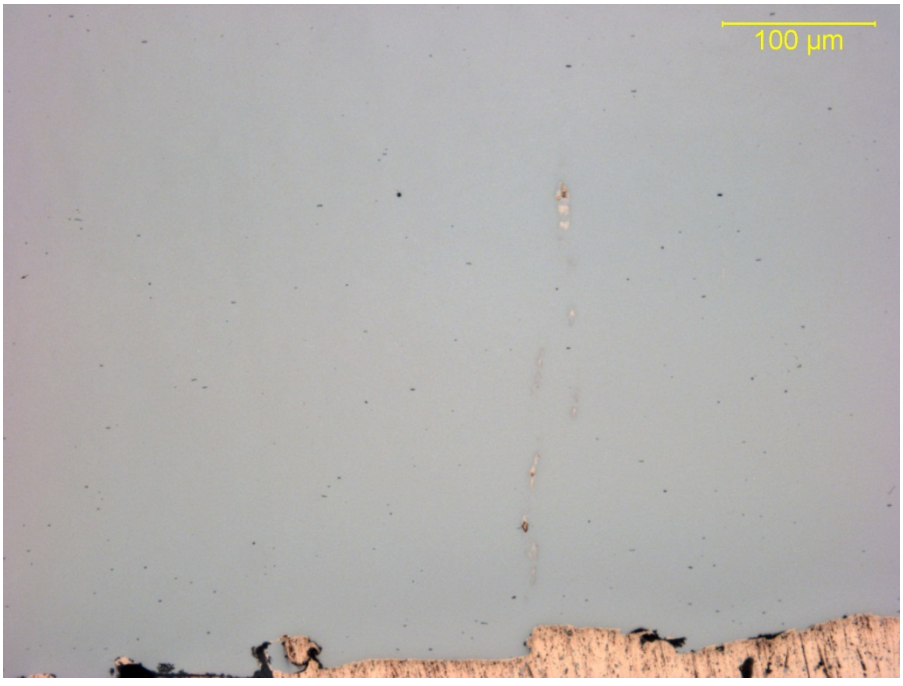

Figure 16. Potential Copper Penetration into the Steel

Figure 17 is a macro view of the crack area next to the RWI joint that clearly exhibits a transformation in the heat-affected zone (HAZ). The etched specimen in Figure 18 shows the rail steel immediately adjacent to the RWI joint. The steel appears to have been heated above its critical temperature and likely above the melting temperature of the steel before cooling. This heating and cooling cycle transformed the microstructure to martensite. This structural change in the steel is the likely source of crack initiation.

In addition, there is an area of microstructurally modified steel at the copper-to-steel interface. The round copper inclusions and the grain structure in the fusion zone indicate that the steel in this area was melted and re-solidified with the copper being rejected during terminal solidification. Additional images of this area are provided in Figures 19 and 20.

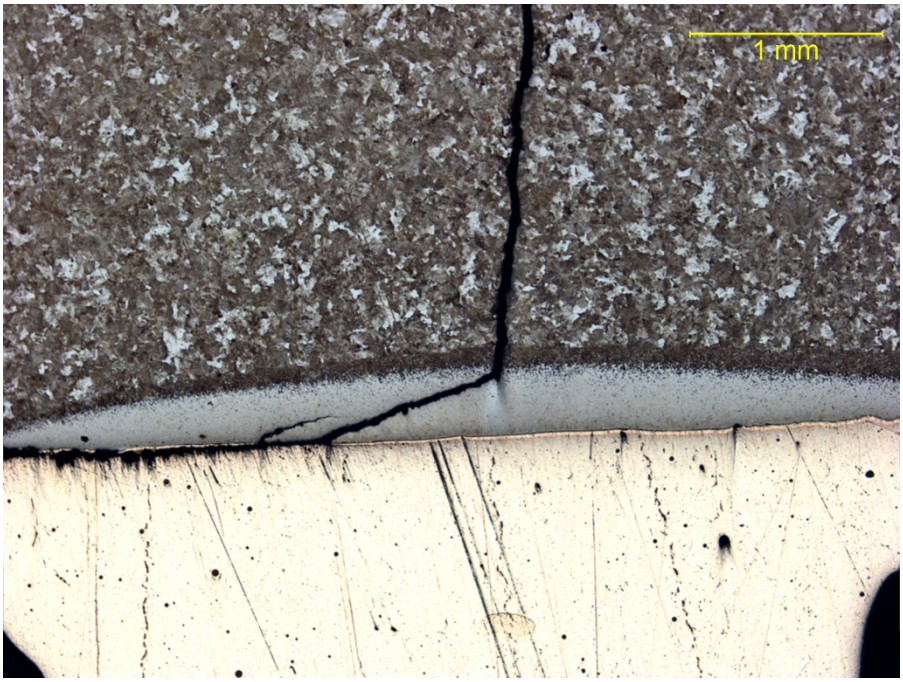

Figure 17. Etched Section of Crack Area

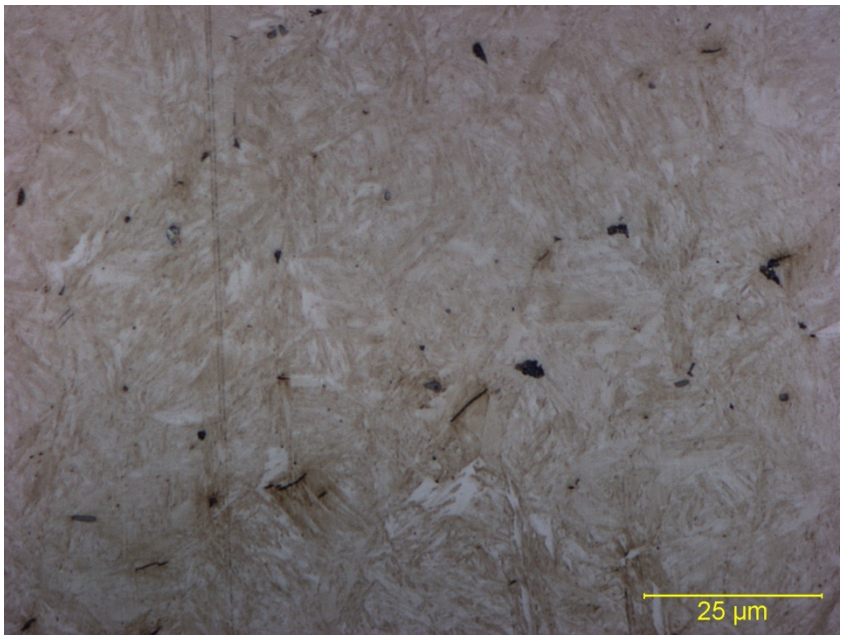

Figure 18. Microstructure in HAZ

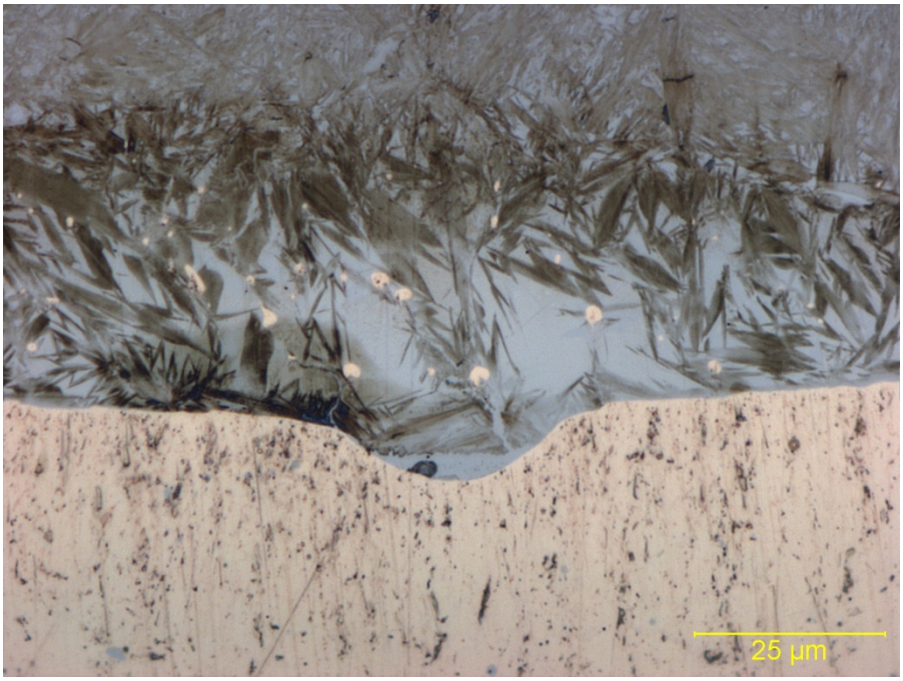

Figure 19. Detail of Copper Globules in HAZ

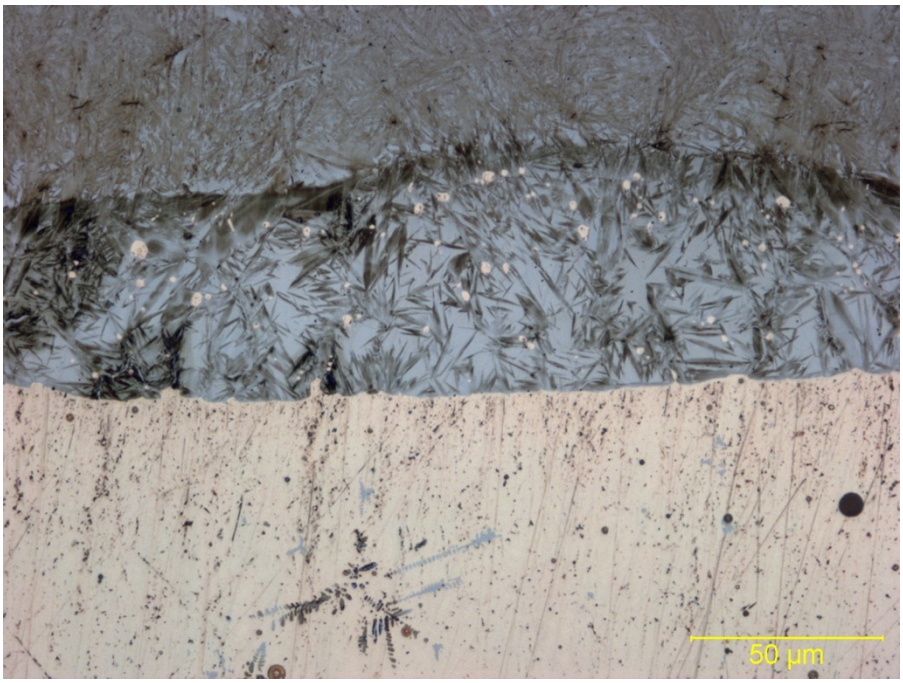

Figure 20. Copper Globules in HAZ

It is possible that the steel immediately adjacent to the weld interface was melted by an overheated weld alloy. This condition allows the copper to dissolve into the molten steel and, upon cooling, decorate the grain boundaries in inter-dendritic regions. It is possible that the increase in temperature allowed the copper to go into solution in the steel in the areas adjacent to the fusion boundary. This theory is supported by the copper-iron phase data shown in Figure 21. Copper solubility decreases upon cooling and it is rejected along the grain boundaries. Figure 22 shows the presence of copper in the HAZ next to the crack.

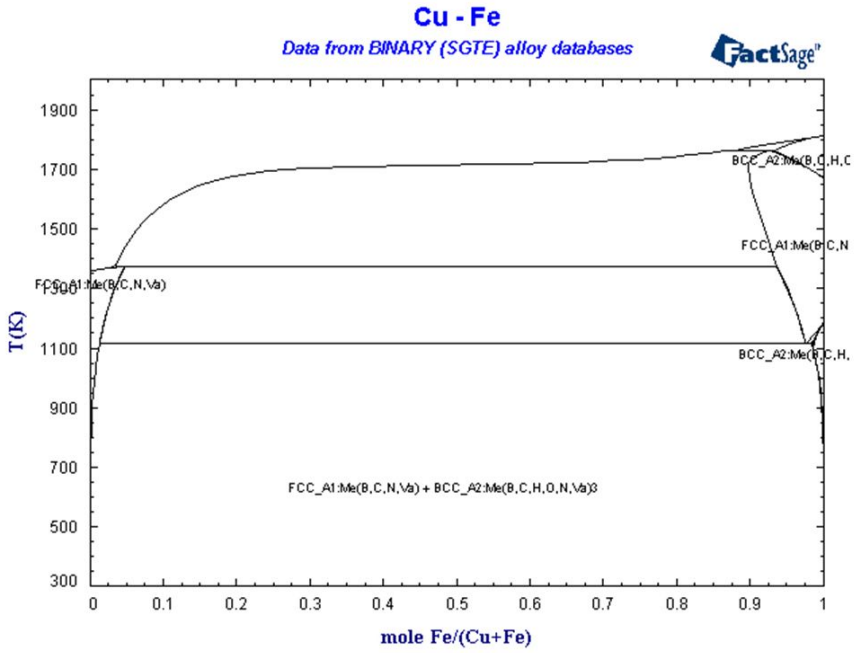

Figure 21. Phase Diagram: Copper Solubility in Iron at Elevated Temperatures

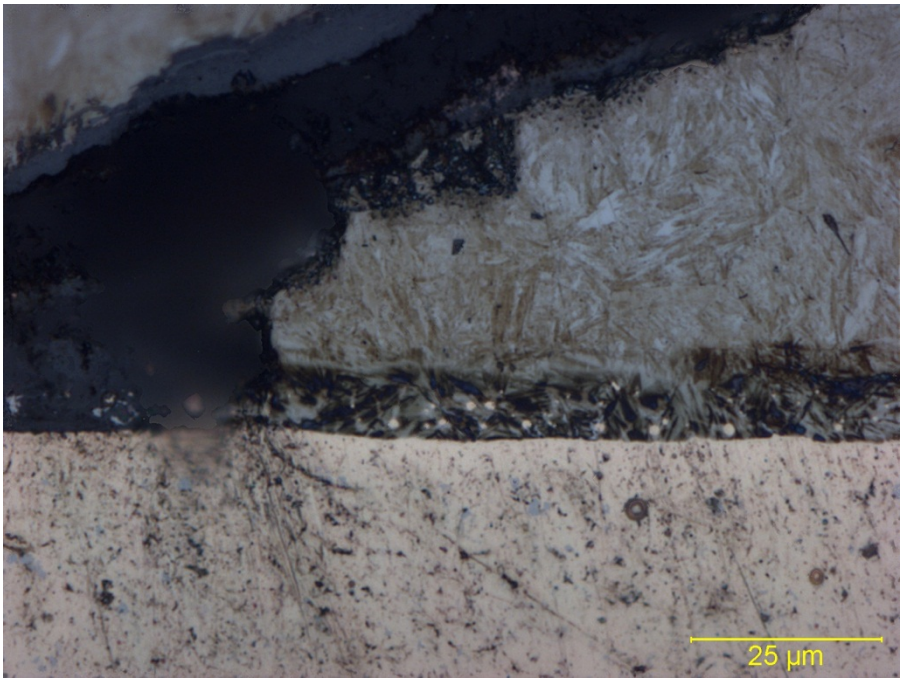

Figure 22. Crack Area Showing Copper Globules Next to Fusion Boundary

Based on the presence of copper in the RWI interface, TTCI believed that localized melting occurred and resulted in copper contamination. The increased copper content will alter the steel metallurgically, leading to a stabilization of the austenite. Upon strain, or during very cold temperatures, this retained austenite in the joint can transform to pure martensite. TTCI cannot determine whether copper is solely responsible for the crack, or it if is simply a contributing factor to the brittle microstructure. Researchers do, however, know that without special procedures and controls in place, melting and solidification of rail steel in an uncontrolled fashion leads to cracking.

General conclusions and findings from this work:

1. The formation of martensite will lead to a brittle microstructure immediately beneath the RWI joint. This can result in the development of a transverse defect during loading or panning out of the RWI joint, leaving a geometric void in the rail.

2. LME can form in the rail steel in the presence of a molten copper-based alloy and tensile stresses. The copper decorates the grain boundaries and acts as a microstructural notch that can be the source of a crack.

3. Solidification-type cracking of the rail steel is possible when the superheated liquid metal is poured into the joint molds. Solidification cracking would be driven by the copper RWI material being segregated into the liquid steel, leading to solidification cracking during cooling.

4. Quench cracking of the steel beneath the RWI joint is possible, as thermal strains developed during the process cannot be relieved unless a proper cooling rate is maintained. Note that this cooling rate is not controlled in the current methods.

2.1.6 Findings of Situational Research

Based on interviews conducted for this project and its own research in the area of signal wire attachment, TTCI has drawn the following conclusions. A welded or brazed joint is desired at the RWI location for durability and corrosion resistance. MOW equipment snags still account for many wire or RWI interface failures because of wire location requirements. In the work conducted by TTCI, it would appear that approximately 50 percent of the required wire repairs can be traced to MOW activity. The current exothermic and pin brazing systems used in the field can produce martensite in the RWI joint. This martensite can lead to rail section failure even though it is on the neutral axis of the rail. Additionally, the RWI joint can lead to formation of a hard disk at the attachment point that can lead to a dishing, or planar failure, releasing the RWI from the rail web because of the underlying brittle nature of the attachment. Cleaning and preheating are reportedly required for best use of the exothermic attachment systems. However, it is unclear whether signal crews have the tools and training to regulate and use preheat effectively.

The failure analysis of the RWI joint provided with a crack indication showed both overheating of the steel to the point of melting resulting in martensite formation and LME in the joints. In particular, the crack face itself was decorated with copper. The most critical flaw in this joint, the flaw that initiated failure, could not be positively identified with the material provided. However, two issues capable of initiating crack development and growth were present in the sample.

A weld process must be developed that creates a solid-state bond while controlling the peak temperature in the rail steel. The process must require very few preparation steps and should be very portable. It would be ideal for the process to eliminate the need for preheating, as this feature of all welding and brazing processes used on rail is cited as undesirable. The number of RWI joints in the field is estimated in Appendix A. The failure rate is relatively low; however, the impact is large.

2.1.7 Description of Improved Welding Process and Method

A metallurgical bond between the stud and the rail head is the most desirable and durable solution because it can deliver the necessary electrical performance. The stud is a preferred attachment technique because it allows for easy detachment and reattachment of wires to the rail. A metallurgical bond will also be able to tolerate rail movement better than a pressure-type bond which can loosen in time.

In order to improve signal wire attachment reliability and durability, there are several items that need to be addressed in the current wire and wire attachment system. The wire system must be easily removable, and the installation and removal technique must be simple, minimizing the probability of operator-induced variation. The wire should be installed on the head so that it is less likely to interact with MOW equipment. Ideally, the wires would be attached to a common connector type that could be metallurgically bonded to the rail head.

The use of a method that creates liquid metal during the RWI attachment process is discouraged because LME can occur when the rail is under tension. This statement implies that a solid-state welding process did not perform well in TTCI research. The RWI joining system must be automatic in the sense that it requires minimal operator tasks to achieve a good quality joint. A single consumable process is preferred to reduce the chances of items like flux being applied in error, which would result in a poor quality RWI joint. This preference was highlighted in the TTCI studies and reinforced in the EWI railroad signal crew discussions.

The proposed solution to the current signal wire attachment methods involves two changes to the approach. First, the wires should not be attached using a crimp joint. A bolted connection is easily controlled from a quality control perspective and the bolts and screws are a well-established technology in all fields. Additionally, a bolted connection will allow for easy attachment and disconnection over multiple iterations without requiring replacement of the wires or leads. This provides a more permanent type of joint. The innovative solution that addresses these changes is shown in Figure 23. For a standardized joint connection, factory-made lengths of the cables could be produced so that no field connections would be required.

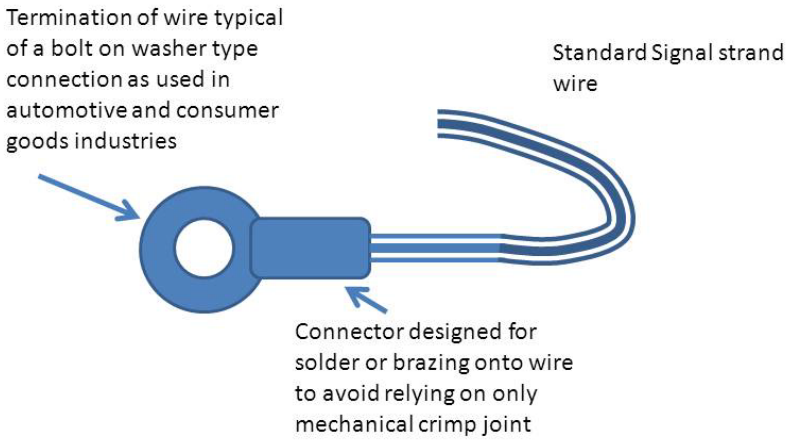

Figure 23. Suggest Bolt-On Connection Wire Termination (Typical)

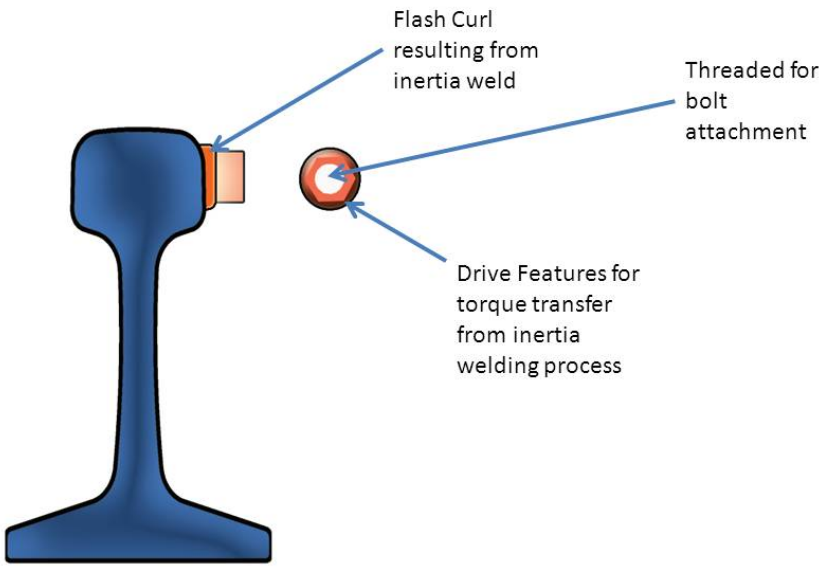

Figure 24. Inertia Weld Showing Lug Attached to Rail Head

The recommended RWI joint is a friction-type weld created using a portable inertia welding system. This process will create a solid-state weld, and with careful selection of a copper-based alloy, the weld can be produced without melting and without overheating the rail steel.

The inertia welding process can be operator independent. The equipment controls the heat input and other key parameters. A single consumable will be used. The attached lug will have a direct connection to the wires using a specially designed bolt system. The lug will be friction-welded directly onto the rail head with minimal surface preparation. The equipment package will be lightweight and easily carried by maintenance personnel.

2.2 Phase 2 Development of Welding Process

2.2.1 Materials Selection

The steel composition determines the transformation temperatures at which austenite in rail steel forms. The transformation temperature (Ac1) in rail steel is a critical temperature that must be avoided by the new process.

The critical performance requirement for the new process is to avoid forming martensite in the rail steel. Martensite can form if the rail temperature is raised sufficiently to first generate the formation of austenite. Unless stringent conditions are employed, the austenite phase, upon cooling, gives way to the formation of martensite. The critical temperature for austenite formation in any steel that will form austenite is called the Ac1 temperature. The approach taken in this work was to avoid crossing the critical temperature, or Ac1, in the rail steel. This set a

thermal profile limit for the process. The Ac1 temperature of pearlitic rail steels is between 705°C and 725°C, based on the JMatPro® modeling software predictions. JMatPro® is software that uses computational methods to determine transformation temperatures and microstructural make-up of steels based on chemistry, temperatures, and cooling rates. The observed variation in transformation temperature is driven by variations in the steel chemistry. All rail steel chemistries available and historically documented were assessed in these calculations.

Using this threshold temperature as a guide, EWI completed a materials review for the lug material, examining different materials based on many factors, including: melting point, forging temperature, galvanic corrosion couple, materials strength, and commercial availability. Other factors such as thermal conductivity, electrical conductivity, and tensile strength were also examined as they can affect welding processes.

EWI examined databases on material properties, such as the Copper Development Association, MatWeb, and ASM handbooks, to collect data on a variety of materials and their respective mechanical and metallurgical characteristics. A key factor in the search for a stud material was that it could be welded to the rail steel without crossing or exceeding the 705°C (Ac1) temperature threshold. The forging temperature must not be crossed when making a friction weld or the material will break during processing as the weld formation is based on extensive deformation of one or both materials.[9] The best materials identified in this work are shown in Table 1.

Table 1. Collection of Best Alloys Identified with Promising Properties

Material	Alloy No. (UNS)	Melting Temp (°C)	Forging Temp. Min °C	Forging Temp. Max °C	High Galvanic Potential to Steel	UTS (ksi)	%IACS Conductivity
CL2 Cu	C18200	1070	816	927	Minimal	72	75%
CL 4	C172	980	650	810	Minimal	125	20%
CL 3	C17510	1040	650	955	Minimal	110+	65%
Amp 940	C1800	1038	816	927	Minimal	50	48%
90-10 Bronze	C22000	1043	760	870	Minimal		44%
360 Brass	C36000	899	705	788	Minimal		26%
6061 Al		651	500	600	Yes	45	55%
Steel	AISI 1018	1150	890	~1100	Minimal	Varies	11%
Ni-12 p		880	N/A	N/A	Minimal	Varies	10%
Phosphor Bronze	C52100	1027	800	930	Minimal	80	95%
N/A	C67000	900	N/A	N/A	Minimal	100+	22%
N/A	C90500	999	N/A	N/A	Minimal	45	11%
Muntz Metal	C28000	900	622	788	Minimal	70	28%
Tin Brass	C41100	1041	830	890	Minimal	42	32%
Cartridge Brass	C26000	916-954	733	844	Minimal	48	28%
Jewel Brass	C22600	1035	760	900	Minimal	68	40%
N/A	66930	940	801			131	2%
N/A	C63600	1032	760	870		60	12%
Tin	Pure	231	N/A	N/A	Potential	31	15%
Zinc	Pure	420	N/A	N/A	Yes	5.3	27%
Naval Brass	C46400	900	650	816	Minimal	75	26%

Some material choices shown in Table 1 were not viable because they are not commercially available. For example, Muntz Metal has the desired material characteristics, but is only available in sheets up to 0.250 inches thick and was not in rod form as required for sample production. Cartridge Brass shows similarly desirable material characteristics with slightly higher working temperatures, but a source of material suitable for this process development could not be identified.

Four materials were selected from Table 1 for further study in process development trials. The four materials selected were:

- C172 Class 4 Copper (low melting point, high strength, and low? forging temperature)
- Naval Brass C464 (good strength, low melting temperature, and low forging temperature)
- C360 Brass (low forging temperature)
- Pure copper (baseline material, commonly employed for signal wire attachment)

2.2.2 Stud Design

A stud design (Figure 25) was developed to allow for implementation of a "fusible link" approach to force failure of the wire-to-stud joint rather than the stud-to-rail joint. This approach was based on the results of TTCI and industry studies that indicated such a design minimizes the risk of rail damage.[5] This approach was further developed to address the need for an easily removable connection. The hex shape allows the stud to carry torque loads.

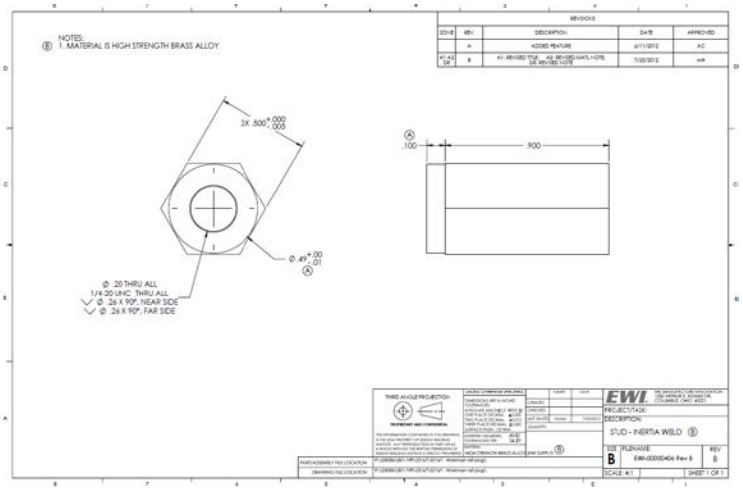

Figure 25. Stud Design used to Produce C360, C172, and C464 Welding Studs

2.2.3 Welding Trials

Once a working process and material combination were identified, a Design of Experiments (DOE) study was conducted to examine the effects of changes in process parameters and gage the robustness of the process. The best suited parameters identified in the DOE were developed to provide strength in the weld joint and tolerance for variability in the delivered speed and thrust load without forming martensite. Process development continued with 360 brass, commercially pure (C110) copper, C172 copper alloy, and the C464 copper alloy.

Initially, welding trials were conducted using an air-driven Ramstud R104 welder—the currently available off-the-shelf portable friction welding system. Because of thrust load limitations, surface velocity limitations, and stud stability inadequacies, the work was moved to an Manufacturing Technology, Inc. (MTI) Model 120 Inertia Welder to gain better control and parameter flexibility. The MTI unit provided a much broader variation in loads, speeds, and inertia which were advantages for this process development task.

The inertial welding process uses a spinning flywheel of fixed mass to provide rotational energy to the stud. When the flywheel reaches a predetermined rotational speed, the spinning stud is brought into contact with the stationary rail steel. The friction between the stud and rail steel elevates the temperature of both pieces. A thrust load forges the stud to the rail steel. The process ends when there is no more energy (rotational force) in the flywheel.

The initial parameters used for the welding trials were:

- Flywheel speed—6000 RPM

- Thrust Load—2000 lb
- Flywheel size—approximately 1 wk^2 (a measurement of the total moment of inertia of the flywheel)^2

These parameters proved to be marginal starting points for producing welds. As such, the work and welding trials were shifted to a hard tool MTI 120B machine which allowed for wider variation of the welding parameters. The weld processing for each material is detailed below in the following sections. The MTI machine is a nonportable inertia friction welder.

Samples of standard rail steel were cut 2-inches by 2-inches by 0.5-inches thick from rail sections to simplify developmental welding trials. This strategy allowed for easy setup for each trial and simplified subsequent metallurgical and mechanical analysis after welding. IFW trials were conducted varying the inertial mass, rotation speed, stick out, and thrust load.

After welding, EWI performed mechanical tensile tests and metallurgical analyses on the weldments. The metallurgical samples were etched with 2 percent Nital to examine the steel microstructure for martensite or some other transformed product. Scanning electron microscope (SEM) analysis of the weldments was conducted in specific cases to examine the microstructure in greater detail for the presence of deleterious phases in the steel.

2.2.3.1 360 Brass Welding Trials

No welds with any appreciable strength could be produced with the 360 brass using the initial parameters listed above.

The 360 brass has excellent melting point suppression and forging characteristics. However, the free machining additions in the 360 brass appear to suppress friction, dramatically reducing the heating at the joint. during the friction welding heating phase. The research showed that, compared with the other materials examined, the upset or forging achieved with identical welding parameters produced strengths roughly 10 percent those of the higher strength materials. This finding indicated that heating was minimal using normal welding parameters.

EWI attempted to increase weld strength by increasing weld force. These trials are summarized in Table 2.

Table 2. Welding Trials 360 Brass Stud

Trial Number	Speed (RPMs)	Thrust Load (lb)	Upset (in)
360-1	8400	2000	0.020
360-2	9400	4000	0.241
360-3	8400	1500	0.020
360-4	8400	600	0.010
360-5	4000	5000	0.250
360-6	7000	2400	0.281
360-7	7500	3200	0.178
360-8	8500	3200	0.180
360-9	8500	2400	0.125

No significant improvement in weld strength was attained using these parameters. The parent metal strength of the 360 brass was not sufficient to support the increased thrust load applied.

No metallographic sections were taken of 360 brass studs since no joints were produced with sufficient strength. Based on the level of upset, and the fact that a high RPM was required to create upset, martensite was expected in the rail steel below the failed joints. The research suggests that the 360 brass material achieved limited success because of the high level of lead and sulfur in the alloy.

2.2.3.2 Commercially Pure (C110) Copper Welding Trials

Welding trials conducted on the standard material for attachments, C110 copper or commercially pure copper, were successful at achieving a weld joint.

Table 3 shows the welding parameters and trial results for C110 copper. In general, upset occurred easily with the C110 copper because of its low yield strength. The low yield strength raised concerns regarding fitness of the C110 copper for use in service. It is difficult for weaker materials to hold threads after repeated bolt application. The alloy's high thermal conductivity required the process to be driven at higher surface velocities (RPMs) such that a low energy input weld could not be made.

Table 3. Welding Trials C110 Copper Stud

Trial Number	Speed (RPMs)	Thrust Load (lb)	Upset (in)	Notes
C110-1	8400	600	0.020	Not tested
C110-2	8400	300	0.241	Not tested
C110-3	8400	1500	0.020	Not tested
C110-4	8400	600	0.020	Not tested
C110-5	8400	5000	0.250	Not tested
C110-6	8400	2400	0.281	Not tested
C110-7	8400	3200	0.178	Not tested
C110-8	7000	2400	0.253	Red glow too hot

Figure 26 shows the cross section of a weld at low energy produced with C110 copper. Note that the depth of martensite in this weld exceeded the depth observed with other materials. This difference was likely due to the higher surface velocity required to join the very conductive C110 material to the rail.

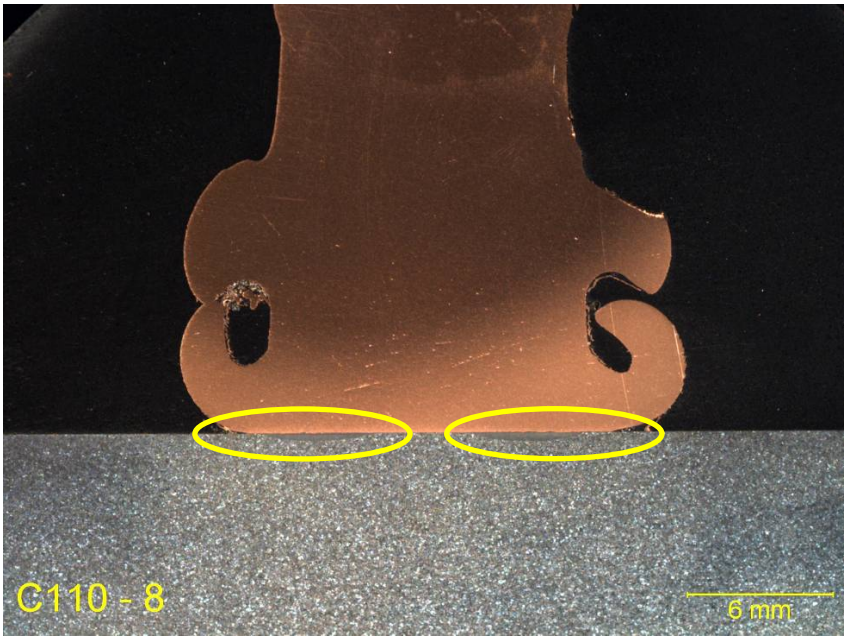

Figure 26. Cross Section of C110 Weld Produced with Inertia Friction Welding

Because of its high conductivity, the copper can extract heat from the joint at a very rapid rate. This leads to an imbalance in heating between the two sides of the joint. It is believed that this conductivity mismatch drives the need for lower weld forces and/or higher surface velocity to generate higher temperatures at the interface. These two parameters must be shifted upward to create a sound joint, creating the higher peak temperatures in the joint necessary to successfully join the C110 to the steel. As previously mentioned, the goal of the process development was to make joints with minimal heat input to avoid the steel transformation temperature.

The upset achieved in this weld was near the minimum required to make a weld with the C110 material. The depth of the martensite was nearly twice that of a weld made with C464 alloy (shown later in this report), suggesting that even if successful parameters could be developed, they would offer only a very narrow region of acceptable welding parameters leading to a less robust process overall. Based on these trials and observations, work on C110 was discontinued. The critical observation made in these welding trials is that lower material conductivity was critical to reducing heat input into the rail.

2.2.3.3 C172 Copper Welding Trials

C172 copper, or Class 4 copper, is a very high-strength copper with melting point suppression due to alloy additions. It is in a class of "precipitation-hardened" copper alloys. When C172 copper is heated above its solutionizing temperature, the precipitates dissolve and it loses strength, making it ideal for a friction welding application without melting.[10] This process reduces the flow stress of the material at the weld joint interface. In general, welding trials with this material produced high joint strengths. The parameters are listed in Table 4.

The C172 alloy required high weld forces. This is likely due to the material's inherently high strength and the short heating time required for joining. This short duration allows the precipitates to remain somewhat intact, thus maintaining the material's high strength. The material produced sound welds, but it also produced very shallow HAZ in the rail steel with martensite formation at the bondline, as shown in Figure 27.

Table 4. Welding Trials C172 Class 4 Copper Stud

Trial Number	Speed (RPMs)	Thrust Load (lb)	Upset (in)	Notes
C172-1	8400	2400	0.010	Not tested
C172-2	9400	4000	0.241	Not tested glow
C172-9	5000	4400	0.150	Not tested glow
C172-11	5000	4000	0.092	Martensite
C172-12	9000	6000	0.325	Not tested
C172-13	8000	6000	0.276	Martensite

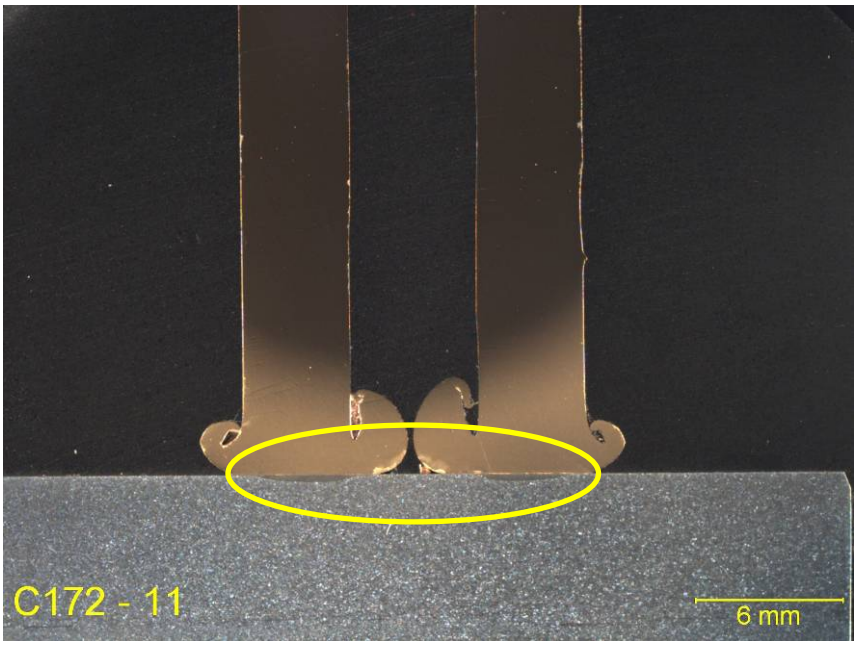

Figure 27. Cross Section of C172 Weld 11 Showing Small Areas of Martensite below Weld Joint

Use of lower surface velocity (i.e., lower RPMs) was possible with this alloy because of its low conductivity, and the heat generated tended to stay at the weld joint interface, creating a bond with lower upset levels. However, the lower surface velocity used in the welds required additional rotational mass in the form of weights to be added to the inertia welding system. This in turn increased the heat input into the weld joint. The strength of the material itself is close to that of the rail steel. High torque levels were required to create the shearing and upset needed to make a friction weld joint. Overall, this material would be difficult to use in the field because of the high thrust loads and larger rotating mass requirements. Higher thrust loads add weight to the inertia welding system and the additional energy required to form a joint with the material risks forming martensite. Figure 28 shows a weld made with the approximate limit to thrust load, 6,000 lb, in C172 where a notable band of martensite was still present under the joint in the rail steel.

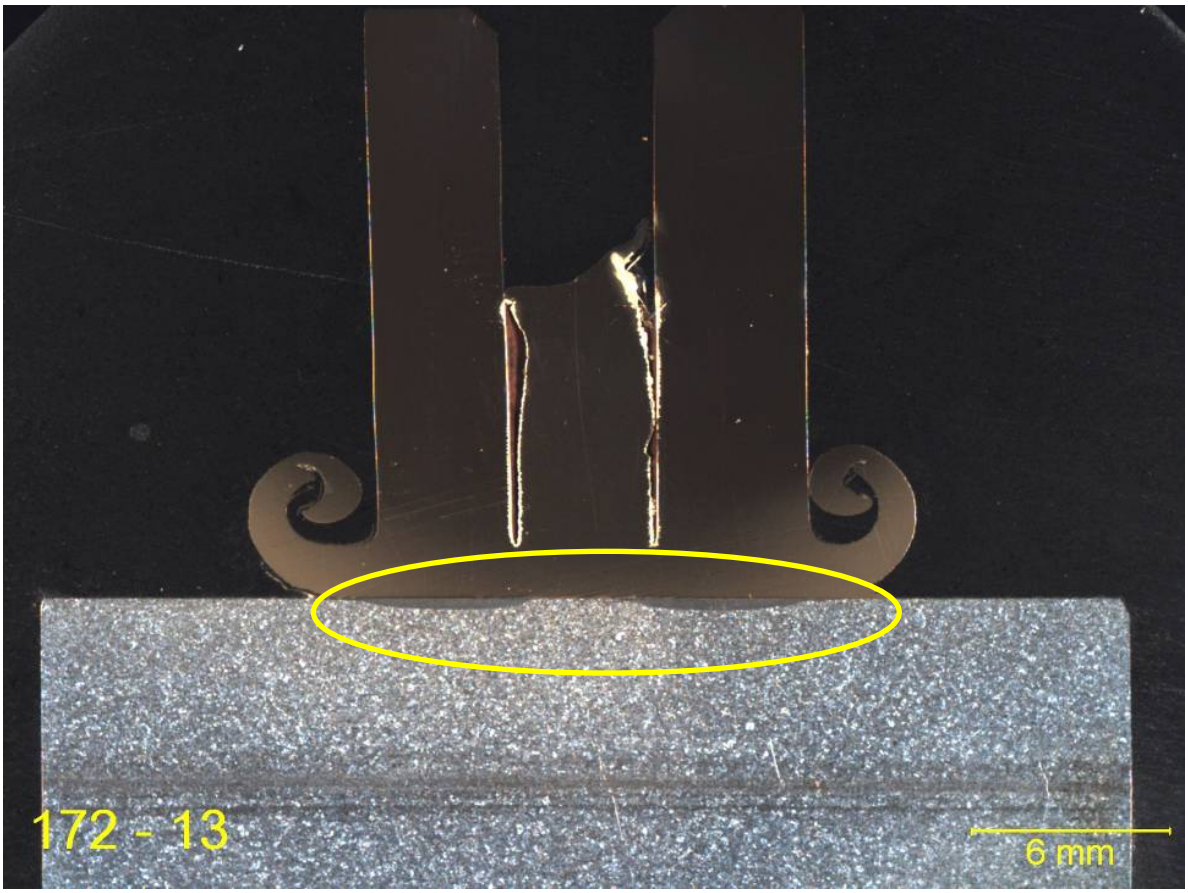

Figure 28. Weld Made with Maximum Allowable Thrust Load in C172 Alloy with Heavy Martensite Present under Joint

This alloy showed promise, but in order to keep the weight of the in-field equipment to a manageable level, the thrust load required to make a weld would have to be below 6,000 lb. No martensite-free welds were produced with the thrust load below this level. It is assumed that higher thrust loads with this alloy would produce martensite-free welds, but in order to focus the work on a field deployable solution, we concluded that other alloys provide a better solution. Work was discontinued on this alloy.

2.2.3.4 C464 Naval Brass Welding Trials

Initially, welding trials with the C464 naval brass showed martensite under the joint in the rail steel just like the other alloys exhibited (see Figure 29). Table 5 shows the welding trials conducted on the C464 alloy with a variety of speeds and thrust loads.

Table 5. Welding Trials C464 Naval Brass Stud

Trial Number	Speed (RPMs)	Thrust Load (lb)	Upset (in)	Notes
C464-1	8400	600	0.010	Not tested
C464-2	8400	900	0.021	Not tested
C464-3	8500	4000	0.375	Not tested
C464-4	7400	3200	0.358	Not tested
C464-5	4500	2800	0.342	Excess upset
C464-10	8400	2400	0.281	Not tested
C464-14	8400	3200	0.403	Martensite
C464-15	7000	2400	0.379	Martensite
C464-19	4500	5200	0.250	No martensite
C464-20	4000	5200	0.170	No martensite

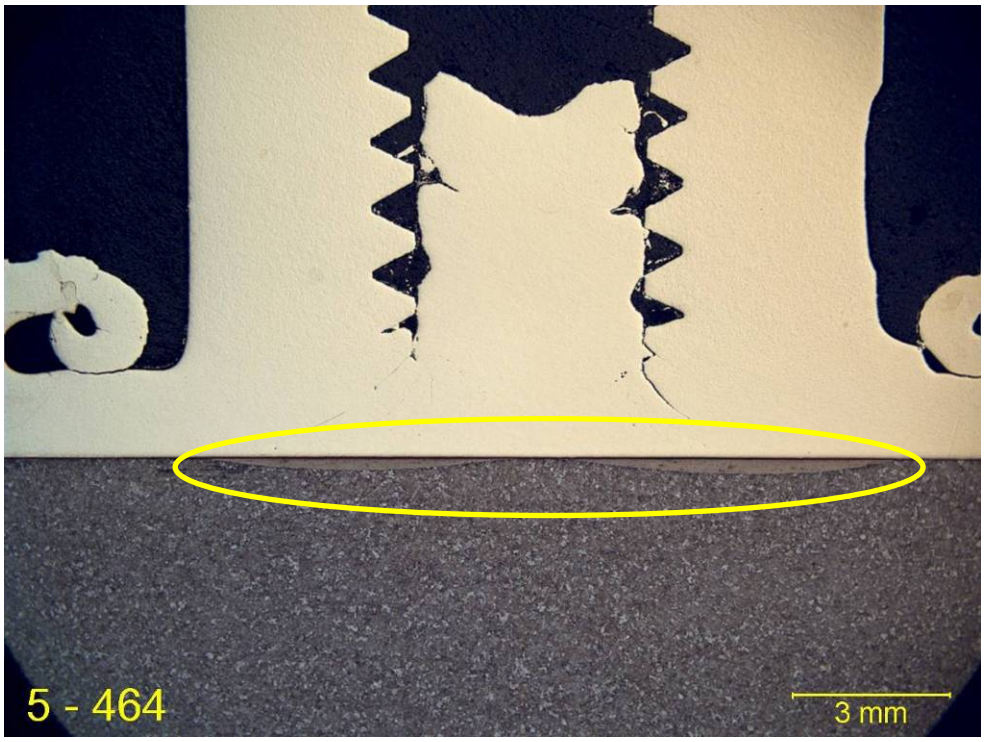

Figure 29. C464 Naval Brass Weld Exhibiting Narrow Band of Martensite in Rail Steel during Early Development

As welding thrust load was increased and total energy in the weld was decreased, the size of the martensite layer shrank notably. The C464 alloy was unique in that the size of the martensite layer could be modified through changes in process parameters. Figure 30 shows a section of a weld taken with higher thrust load and reduced energy welding parameters. Note the size change in the martensite layer.

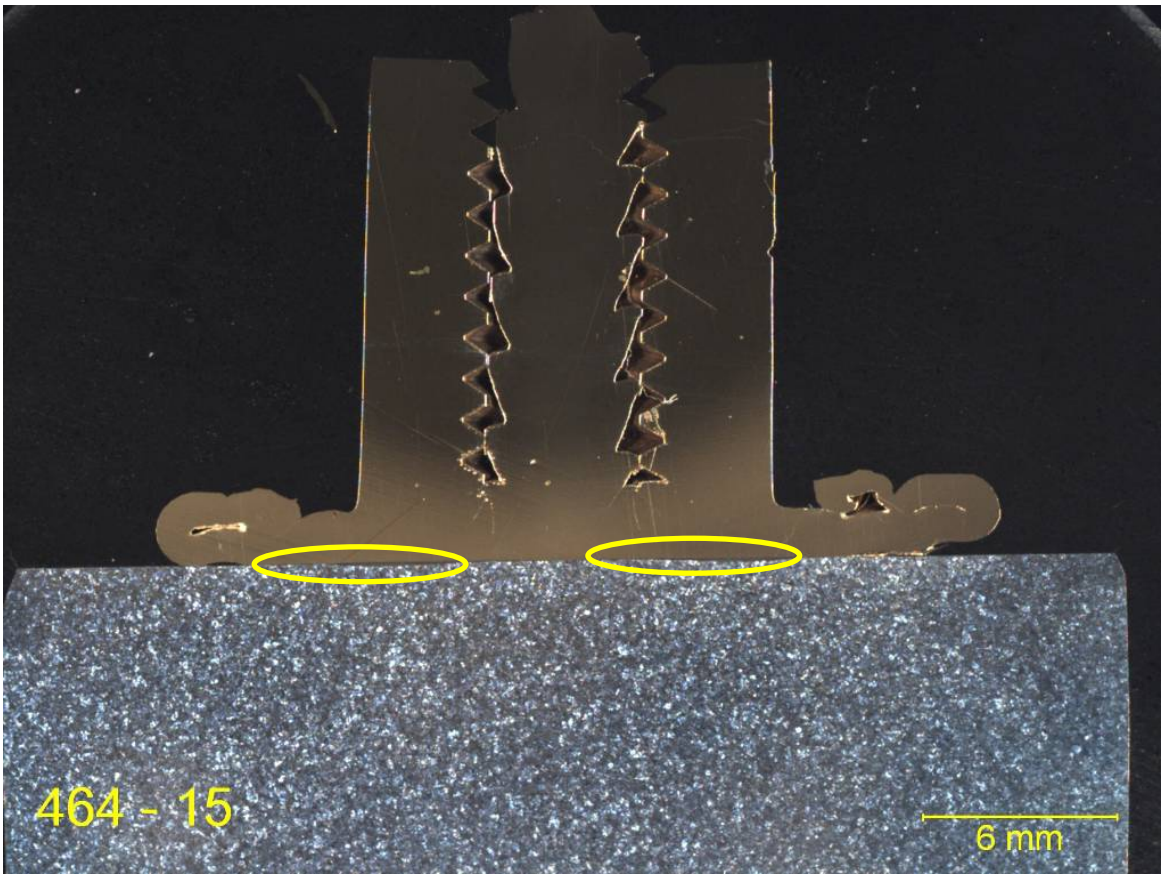

Figure 30. C464 Alloy Weld Showing Different Sized Layer of Martensite Responding Significantly to Parametric Changes

In the welding trials, it was noted that a minimum surface velocity was required to form a weld with each material. In the C464 alloy, that surface velocity or speed in RPMs was approximately 4,500 RPMs. Welding trials were conducted at 4,000 and 4,500 RPMs in Welding Trial Numbers 19 and 20. Figures 31 and 32 show the welds in macro view, respectively. No martensite was present in these welds at higher magnification, as shown in a detail of the bondline in Weld 19 (Figure 33). SEM analysis of the bondline area is shown in Figure 34. The deformation of the lamellae in the pearlite of the steel is apparent without the presence of martensite.

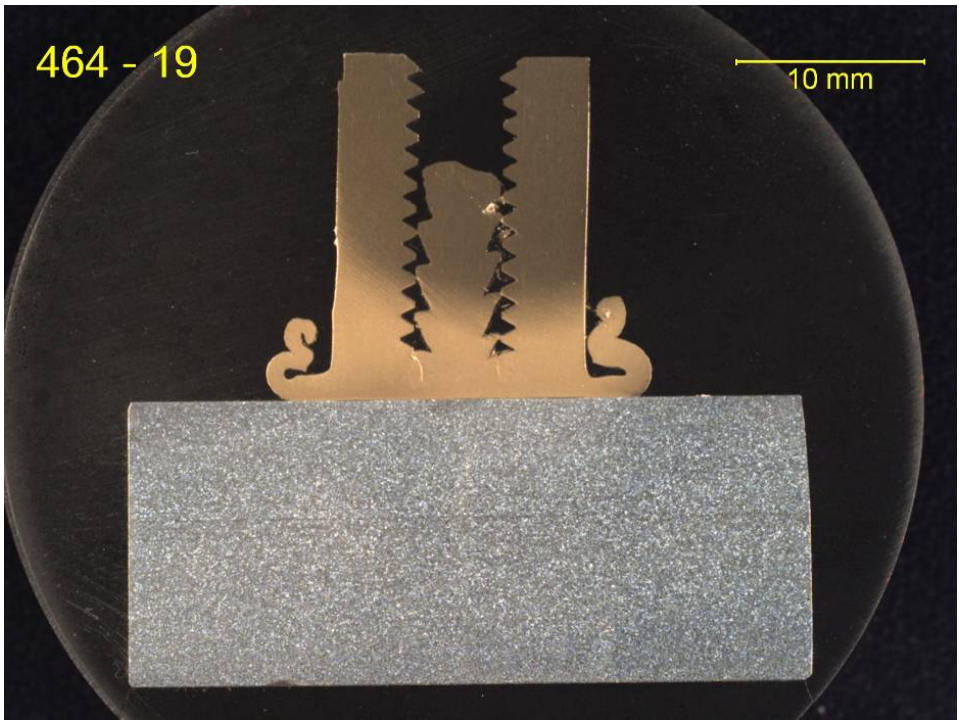

Figure 31. Macro View of Weld 19 in C464 Showing Martensite-Free Joint

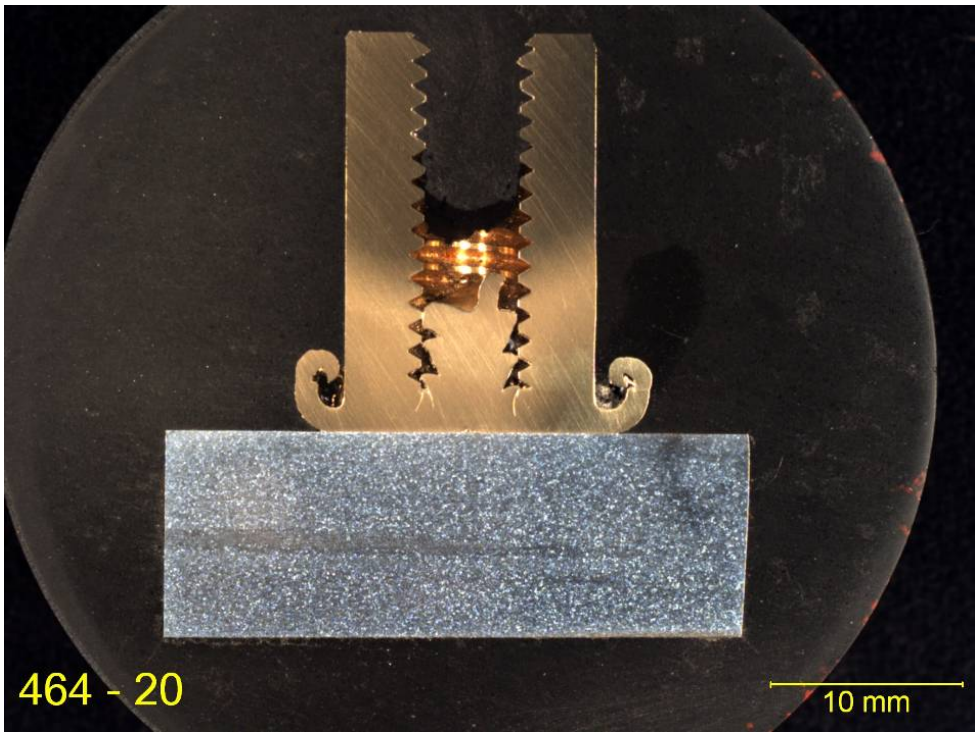

Figure 32. Macro View of Weld 20 in C464 Showing Martensite-Free Joint

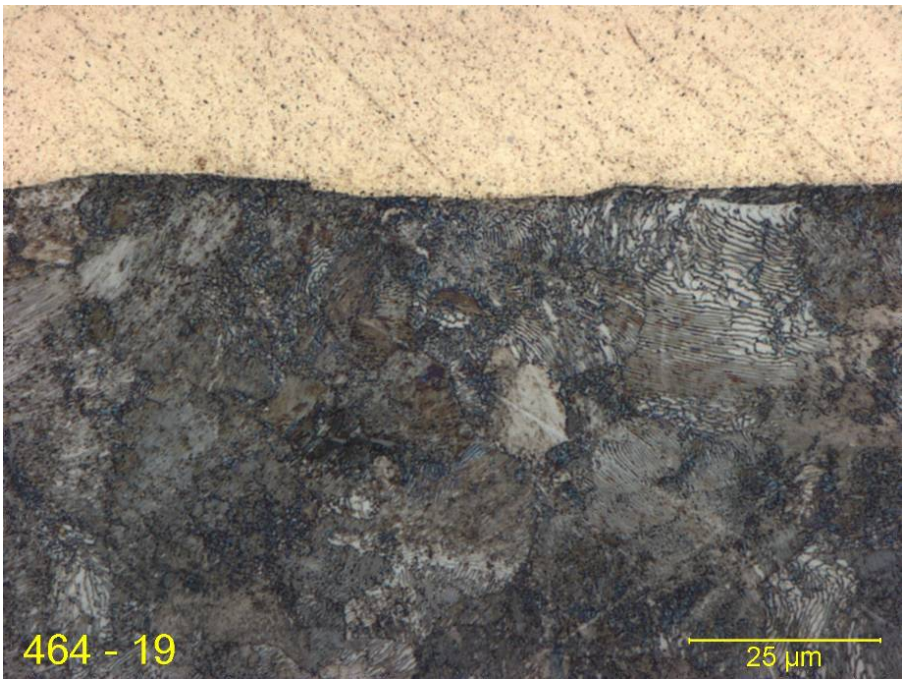

Figure 33. Close-Up of Weld 19 in C464

SEM analysis of the welds was conducted in order to verify that no martensite was present in the weld joints. In Figure 34, it is obvious that the lamellae of the pearlite lay immediately adjacent to the bondline and the C464 alloy in the joint.

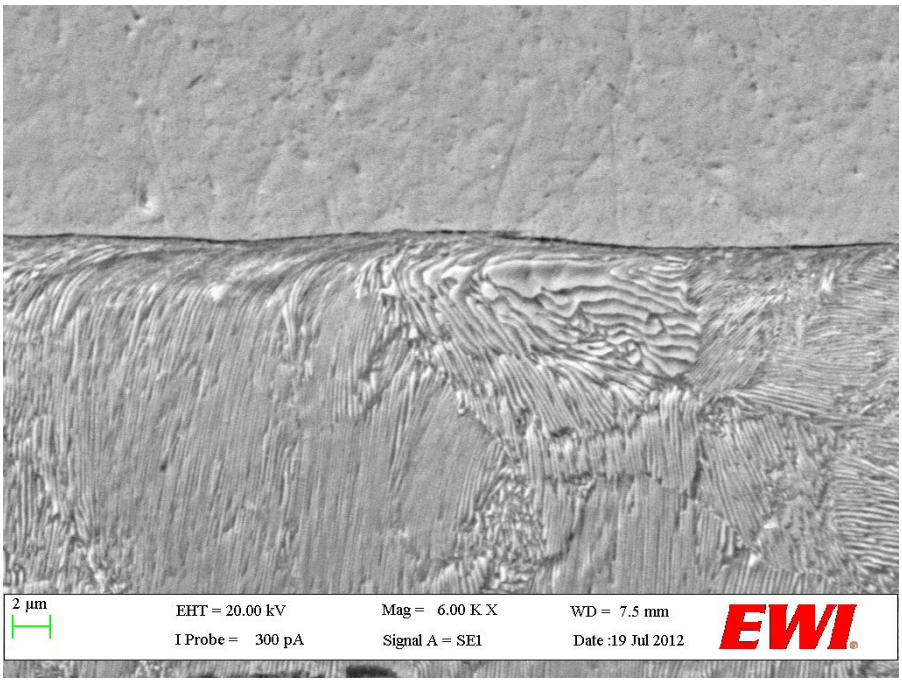

Figure 34. SEM Image of Bondline Showing No Martensite in Weld Joint

Several key findings were made during the weld trials. First, the use of a material with a low melting and forging temperature does not guarantee that a weld can be produced with sufficient strength. Second, there is no direct correlation between forging temperature and the formation of martensite. Finally, the best alloy must also fit operational conditions for field deployment. These findings meant selecting an alloy that would allow for low energy and low thrust loads in the welding process such that a lightweight portable IFW could be used. The attributes of each alloy investigated are shown in Table 6.

Table 6. Comparison of Materials Performance in Study

Material	Martensite Propensity	Thrust Load Required	Energy Required	Commercial Availability	Weld Strength
C464	Lower	Low	Low	Common	Good
C172	Moderate	High	High	Common	Excellent
360 Brass	Unknown	Lower	Lower	Common	Very poor
C110 Copper	High	Low	High speed	Common	Good

The C464 naval brass allowed the objective outlined in the plan to be achieved. Additionally, it responded favorably to changes in the welding parameters, resulting in a strong, martensite-free weld.

2.2.3.5 C464 Naval Brass Welding Process Study

C464 naval brass showed the best process characteristics of the alloys examined. A DOE study was conducted to determine the range of weld parameters that produce a strong, martensite-free weld joint with this alloy. Welding parameters were chosen to assume the existing parameter sets as a maximum energy. Thrust loads were increased to examine the tolerance of the process to changes.

Table 7. DOE Test Matrix and Results

Thrust Load	3500 RPMs	4000 RPMs	4500 RPMs
600 PSIG	DOE # 1 n/g	DOE # 4 Tensile 4153 lb, 4349 lb No martensite	DOE # 7 Tensile 3745 lb, 4750 lb No martensite
650 PSIG	DOE # 2 n/g	DOE # 5 Tensile 100 lb, 350 lb No martensite	DOE # 8 Tensile 3581 lb, 4750 lb No martensite
700 PSIG	DOE # 3 n/g	DOE # 6 Tensile 2750 lb, 2980 lb Martensite present	DOE # 9 Tensile 3795 lb, 3745 lb Martensite present

Table 7 lists the strength results for each set of conditions for varying RPM and thrust loads. The thrust load is calculated by multiplying the pound per square inch gage (PSIG) value by 8 as the cylinder area is 8 square inches.

Note that several parameter sets produced welds with more than adequate strength and free of martensite. Martensite layers in these welds were not visible in the macro views of the cross sections; however, 100× magnification views showed very slight formation (approximately 35 micrometers deep) of martensite in two of the weld joints that had appreciable strength. These are shown in Figures 35 and 36 for Welds DOE 8 and 9, respectively.

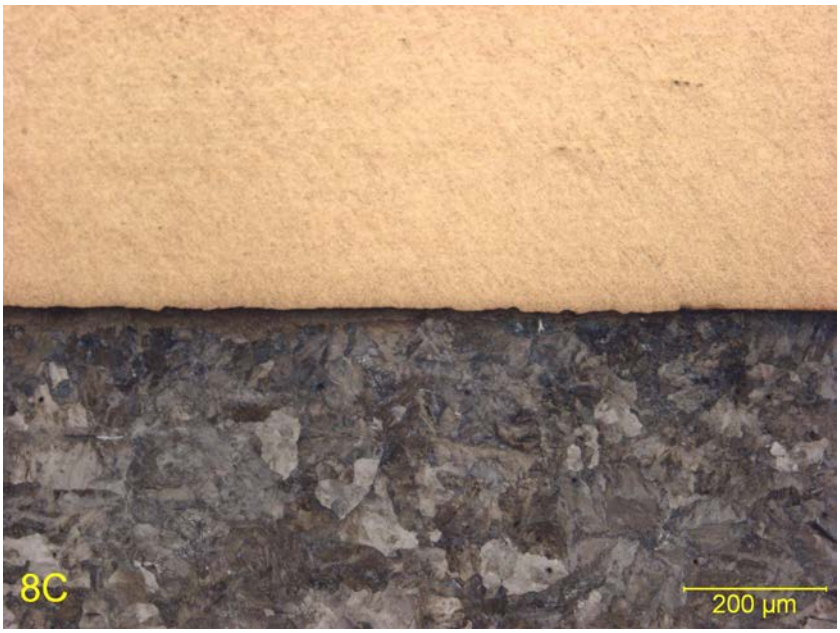

Figure 35. Detail of Bondline in DOE Weld 8

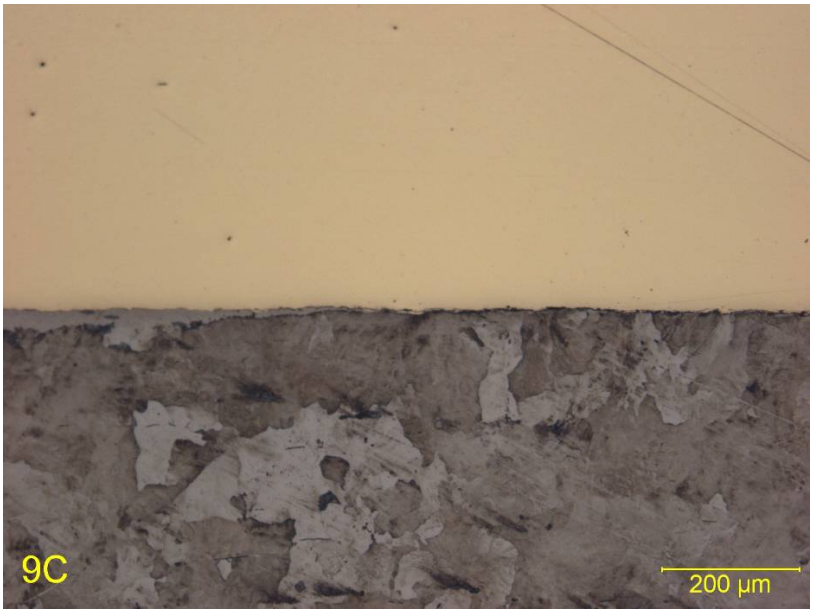

Figure 36. Detail of Bondline in DOE Weld 9 Showing Minimal Presence of Martensite

Rotational speeds below 4000 RPM did not produce welds with adequate tensile strength. Higher surface velocity or speed, combined with higher thrust loads, produced strong welds, but the increased thrust load produced higher frictional heating. This resulted in the weld joint exceeding the critical temperature and forming martensite in the joint, as shown in Figures 35 and 36. In Figure 37, Weld 7 shows no martensite and produced a weld with appreciable strength.

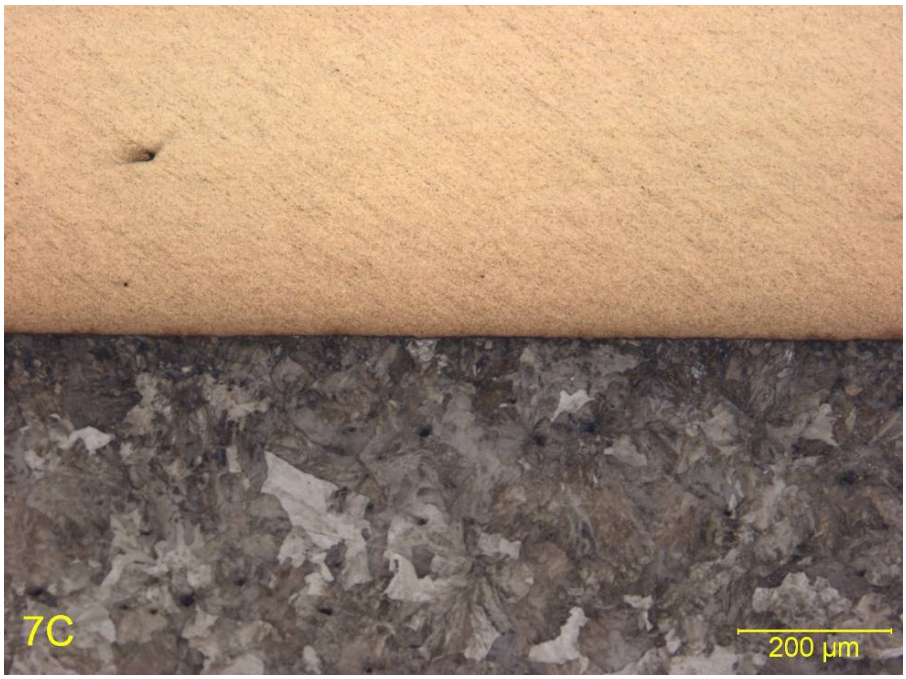

Figure 37. Section from DOE Weld 7 Showing No Martensite along Bondline

EWI performed a regression analysis on the DOE results to estimate a range of acceptable weld parameters. This analysis revealed that there is no correlation between the rotational speed of the flywheel and the formation of martensite in the rail steel and that there is a correlation between the tensile strength of the weldment and the rotational speed of the flywheel. Based on these results, EWI established the baseline weld parameter range:

- Flywheel speed—4000–5000 RPM
- Thrust load—600–650 psig (4800–5200 lb)
- Flywheel size—2.2 wk^2

The DOE results revealed that the IFW parameters must be followed in order to produce good welds without martensite. However, the DOE also showed that there was sufficient latitude in the parameters to allow the development of a welding tool to produce field welds if the equipment could control thrust loads and RPMs.

2.2.3.6 Reparability Study

One of the testing goals was to show that welds could be repaired, repeatedly if necessary, without the subsequent formation of martensite. Signal lugs can be broken or removed for reasons other than insufficient attachment strength; for example, the need to move the location or

removal prior to MOW activities. EWI tested welds made with the developed process using C464 alloy to ensure that repeated application of the process would not result in development of martensite in the rail. Ten welds were repeatedly made at the same location. The parameters used in the study were 4600 RPMs, 2.2 wk^2, and a 625 PSIG (or 5000 lb) thrust load.

The first weld was produced then forcibly removed and a second weld was produced over the same spot. This process was repeated until the ten welds were completed. The repair welds all showed repeatable weld strength and no indication of martensite in the underlying rail steel. The metallographic sections are shown in Series 1 through 10 in Appendix B. For comparison, the first weld is shown in Figure 38 and the tenth weld is shown in Figure 39. In addition, the tensile tests results from the first, fifth, and tenth weld all remained similar at 4650, 4720, and 4800 lb, respectively.

These results are demonstrative of a properly developed friction welding process. A good process exhibits excellent repeatability. The total heat input to the rail steel from the repeated welds was low, thus minimizing the risk of damage to the underlying base materials.

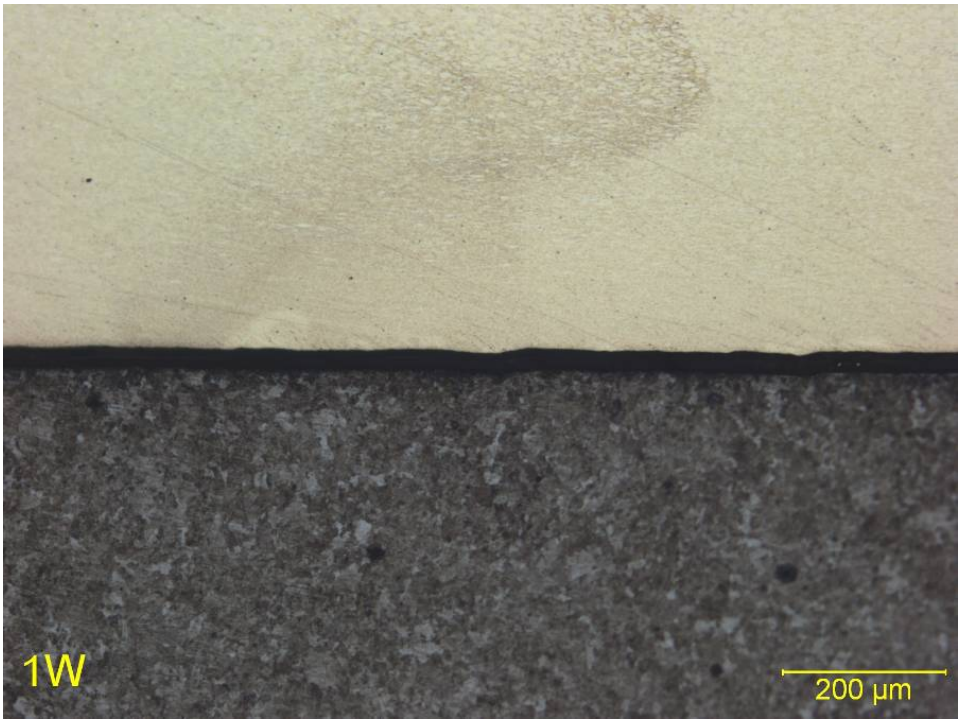

Figure 38. Initial Weld Made in Reparability Study

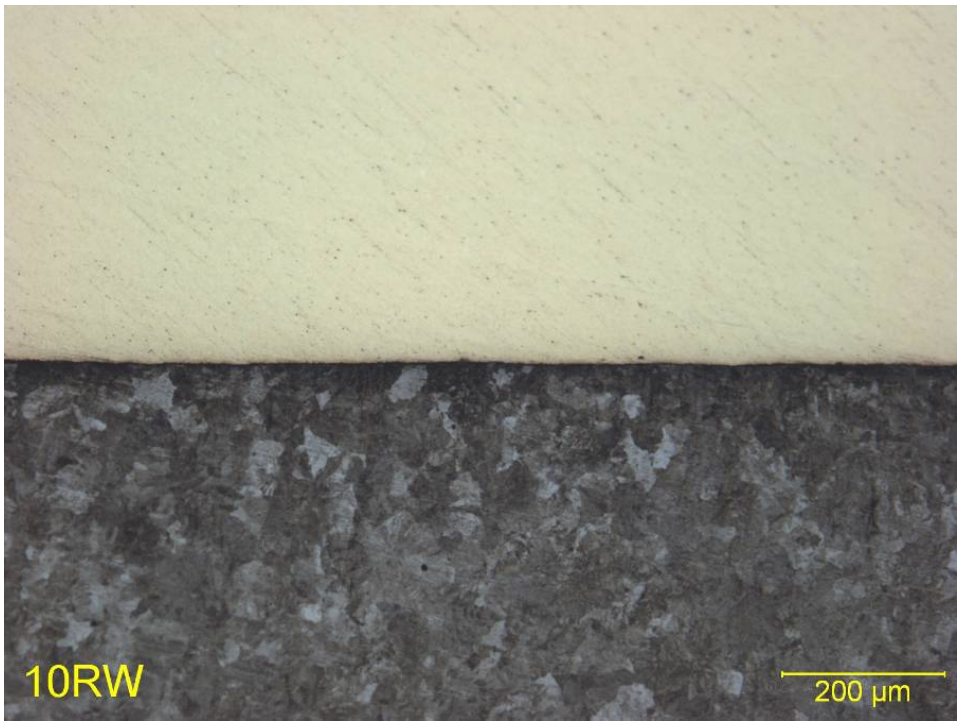

Figure 39. Tenth Repair Weld Made in Reparability Study

2.2.3.7 Experimental Variations of Inertia Friction Welding

EWI tested friction soldering and brazing as a possible alternative to friction welding. A C464 Stud was pre-tinned with a 0.150-inch-thick layer of tin-silver alloy (95 Sn/5 Ag). A test was conducted at speeds ranging from 4500 to 6500 RPMs and thrust loads from 2400 to 3000 lb. A completed joint was obtained with a 3000-pound thrust load at 6500 RPMs; however, the bond strength was very low. The required joining process was complex, requiring many steps in specific order. Although many of these steps could be completed, the application of flux and hold time after solder required particular attention. Given that a simple, field method was the goal for this project, no further development was made to this technique.

2.3 Phase 3 Joint Performance Verification

The EWI developed a mechanical test matrix to verify the weld properties for multiple welds and compare the IFW weld with an industry standard exothermic process (Table 8).

The initial weld parameters used were 5200-pound thrust load at 650 psig with 2.2 wk^2 flywheel and 4800 RPMs. These parameters were within the acceptable range as determined by the DOE regression analysis. Upon inspection, however, these welds contained a thin layer of martensite. The root cause of the martensite appears to be related to geometric high spots on the rail head surface after grinding. Welding forces are elevated in these areas, creating excessive heat build-up and the formation of martensite. The initial weld trails showed that high force and heat drive the formation of martensite. EWI improved the surface finish requirements for grinding and adjusted the weld parameters to eliminate the risk of martensite. A new set of samples was produced with the following weld parameters:

- Flywheel speed—4200 RPM
- Thrust Load—600 psig (4800 lb)
- Flywheel size—2.2 wk^2

The exothermic CAD welds were produced using Erico die and clamp kit # SBTBT21C, SB25 weld material, and SBTBB34 bootleg wires 3/16-inch diameter with a 1-inch tab. The rail and dies were preheated to 250 °F to drive off any moisture. EWI followed the manufacturer's standard procedures to attach the wire bonds to the neutral axis of the rail. The surface temperature of the rail was measured using a tactile temperature probe.

EWI sourced rail material from rail resellers and new rail suppliers. All rail was 136 RE. The standard rail chemistry used in welding trials was Evraz 2012 and Steel Dynamics 2012 in almost new condition. The high performance rail was Evraz RMS 2010. The hyper-eutectoid rail used in welding trials was Nippon HE400 2007. In all testing, the standard chemistry rail is referred to as SS grade, the high strength grade is referred to as DS grade, and the hyper-eutectoid chemistry is referred to as HE grade.

Table 8. Test Matrix for Welded Samples

Testing Procedure	Joining Process	Standard Chemistry (SS)	Hyper-Eutectoid (HE)	Premium Rail (DS)
Corrosion SAE J2234	CAD	5	5	3
Corrosion SAE J2234	IFW	5	5	3
Fatigue Testing	CAD	3	2	1
Fatigue Testing	IFW	3	2	1
Tensile Tests (pulled on embedded wire strand)	CAD	5	5	5
Tensile Tests (not possible because of geometry)	IFW	X	X	X
Metallurgical Examination with Vickers Micro-Hardness Traverse from Stud to Rail	CAD	2	2	2
Metallurgical Examination with Vickers Micro-Hardness Traverse from Stud to Rail	IFW	2	2	2
Impact Test Joint to Rail Interface	CAD	3	3	3
Impact Test Joint to Rail Interface	IFW	3	3	3
Shear Testing of Welded Joints	IFW only in lieu of tensile	3	3	3
Re-Weld Testing with Metallurgical Testing after 10 Repeated Welds at Same Location	IFW only	1	1	1
Total Samples		35	33	28

2.3.1 Conductivity Testing

Conductivity testing of the weld joints showed nearly identical results from both processes. EWI took resistance measurements between the wire connection point to approximately 1 mm outside the joint on the surface of the rail using a micro-Ohm-Meter. This insured that only the conductivity of the joint was measured. A sample of the test results is shown in Table 9. The results indicate no significant difference between the joint types.

Table 9. Conductivity Measurements Taken on Samples from Corrosion Test Piece

Joint Type	Micro-Ohm Resistance	Joint Type	Micro-Ohm Resistance
SS IFW	27	SS CAD	32
SS IFW	24	SS CAD	33
SS IFW	32	SS CAD	32
SS IFW	33	SS CAD	28
SS IFW	36	SS CAD	32
HE IFW	24	HE CAD	21
HE IFW	32	HE CAD	29
HE IFW	33	HE CAD	31
HE IFW	47	HE CAD	28
HE IFW	37	HE CAD	26
DS IFW	27	DS CAD	31
DS IFW	30	DS CAD	37
DS IFW	42	DS CAD	30
DS IFW	39	DS CAD	37
DS IFW	42	DS CAD	34

2.3.2 Corrosion Testing

Corrosion testing was conducted using SAE J2234 cyclic corrosion test procedures. This test is accepted by the military and automotive industry as an accurate predictor of real-time corrosion for painted exposed surfaces in harsh environments. A 5-year life was simulated.

The goal of the test was to identify any galvanic corrosion at the interface between the rail steel and signal wire joint. Galvanic corrosion can occur between dissimilar metals in the presence of moisture. This type of corrosion would appear as an area of increased corrosion like a ditch or groove around the perimeter of the joint.

A photograph of each bond type prior to corrosion testing is shown in Figures 40 and 41.

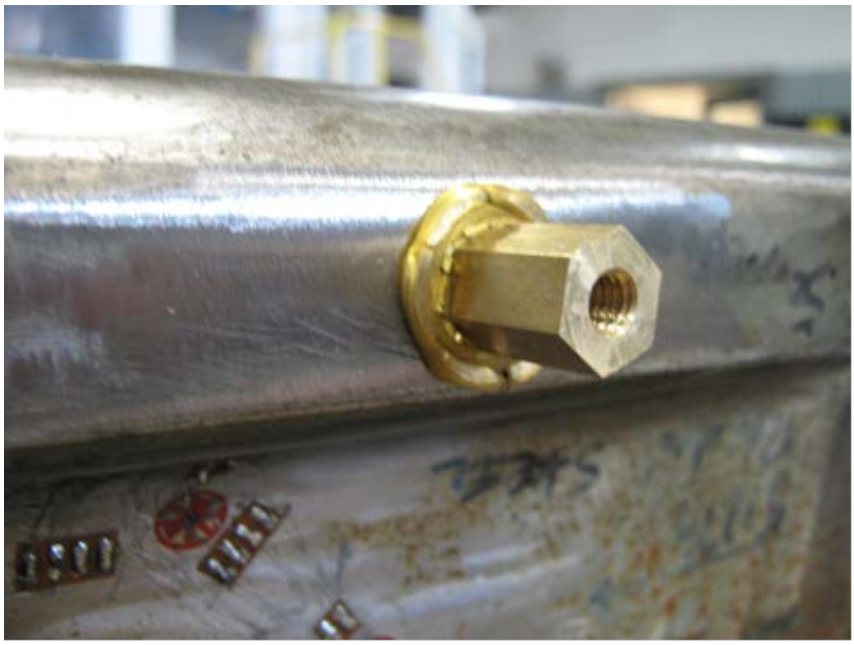

Figure 40. IFW Joint Prior to Corrosion Testing

Figure 41. CAD Joint Prior to Corrosion Testing

EWI measured approximately 0.200 in loss of material in the rail head width. The loss of material is obvious in Figure 42. The corrosion products are apparently scabbing away from the parent rail.

Figure 42. End View of Rail Showing Corrosion Products' Accumulation on Rail Web

Photographs of the corroded test samples are shown in Figures 43 and 44.

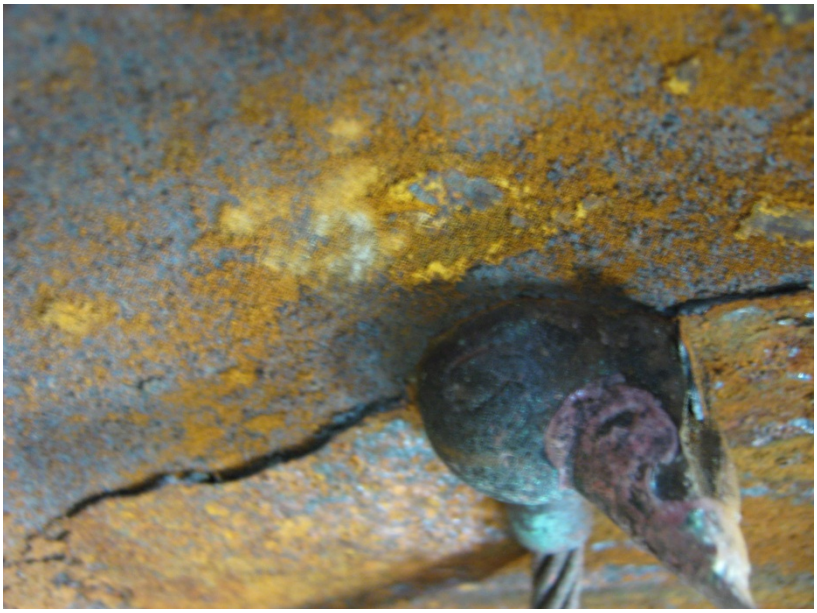

Figure 43. CAD Weld after Corrosion Test

Figure 44. Inertia Friction Weld after Corrosion Testing

No evidence of galvanic corrosion was observed in either joint type. Some IFW samples fell off during testing. This was attributed to a lack of weld coverage caused by the irregularly shaped rail head and the alignment of the IFW machine. There is a slightly radial surface on the side of the rail head which was not accounted for in the alignment of the IFW machine. In addition, the surface of the rail was slightly rough, which caused inconsistent fusion. These issues resulted in failure of some of the weld joints. There was very little metallic bond to seal out the corrosive media; consequently, the steel simply corroded away from the weld joint. A photograph of a failed joint surface is shown in Figure 45. EWI is currently working to resolve these issues.

In summary, neither welding process displayed any type of crevice or galvanic attack around the weld joints because the corrosion products stopped at the weld joints for each weld joint type. This test confirmed that neither process suffered any deleterious effects from exposure to a corrosive environment when a good quality weld was made.

Figure 45. Low Quality IFW Joint due to Misalignment

2.3.3 Fatigue Testing

EWI designed a four-point bending setup to perform fatigue testing on both joint types. Figure 46 provides a diagram of the fixture. The setup mimics an EU-designed rail fatigue test with loading similar to the AWS standard.[10,11] High-frequency strain oscillations are used to load the joint. The moment, or bending stress, applied to the rail section is equivalent to the stress applied during a standard rolling load fatigue test.

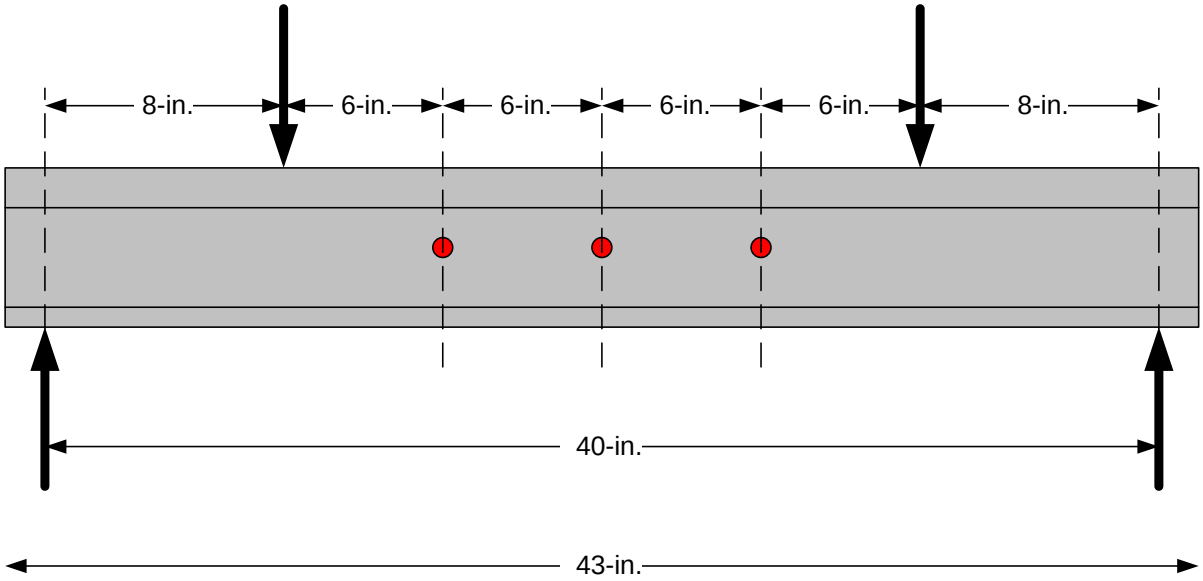

Figure 46. Fatigue Test Layout Showing Specimen Locations and Loading Scheme

EWI employed a stepped loading scheme for the fatigue test. Cyclic loads were increased after 1 million cycles until failure was observed. The test results are presented in Table 10.

Table 10. Summary of Fatigue Testing Results

Sample No.	Process	Step 1 88,000 lb Cycles	Step 2 106,000 lb Cycles	Load 3 124,000 lb Cycles	Load 4 142,000 lb Cycles	Load 5 160,000 lb Cycles	Failure Initiation Site
SS-1	CAD	1 mil	1 mil	981,000			Head surface
SS-2	CAD	1 mil	1 mil	764,000			Head attach
SS-3	CAD	1 mil	1 mil	639,000			Head attach
HE-1	CAD	1 mil	1 mil	1 mil	1 mil	154,000	Head surface
HE-2	CAD	1 mil	1 mil	17,000			Head attach
DS-1	CAD	1 mil	1 mil	1.4 mil			Head surface
SS-1	IFW	1 mil	1 mil	314,000			Head attach MS
SS-2	IFW	1 mil	1 mil	298,000			Head attach. MS
SS-3	IFW	1 mil	1 mil	726,000			Head surface
HE-1	IFW	1 mil	1 mil	1 mil	94,269		Head surface
HE-2	IFW	1 mil	1 mil	1 mil	790,000		Head surface
DS-1	IFW	1 mil	1 mil	1 mil	562,000		Stud proximity

MS = Martensite observed in microstructure

Most of the observed failures originated at surface defects on the rail head. Most failure initiated from the surface of the rail where tiny corrosion pits acted as stress risers, as shown in Figure 47. In normal track service, it is unlikely that these pits would initiate cracks because the constant rolling friction of the train wheels acts to close the pits.

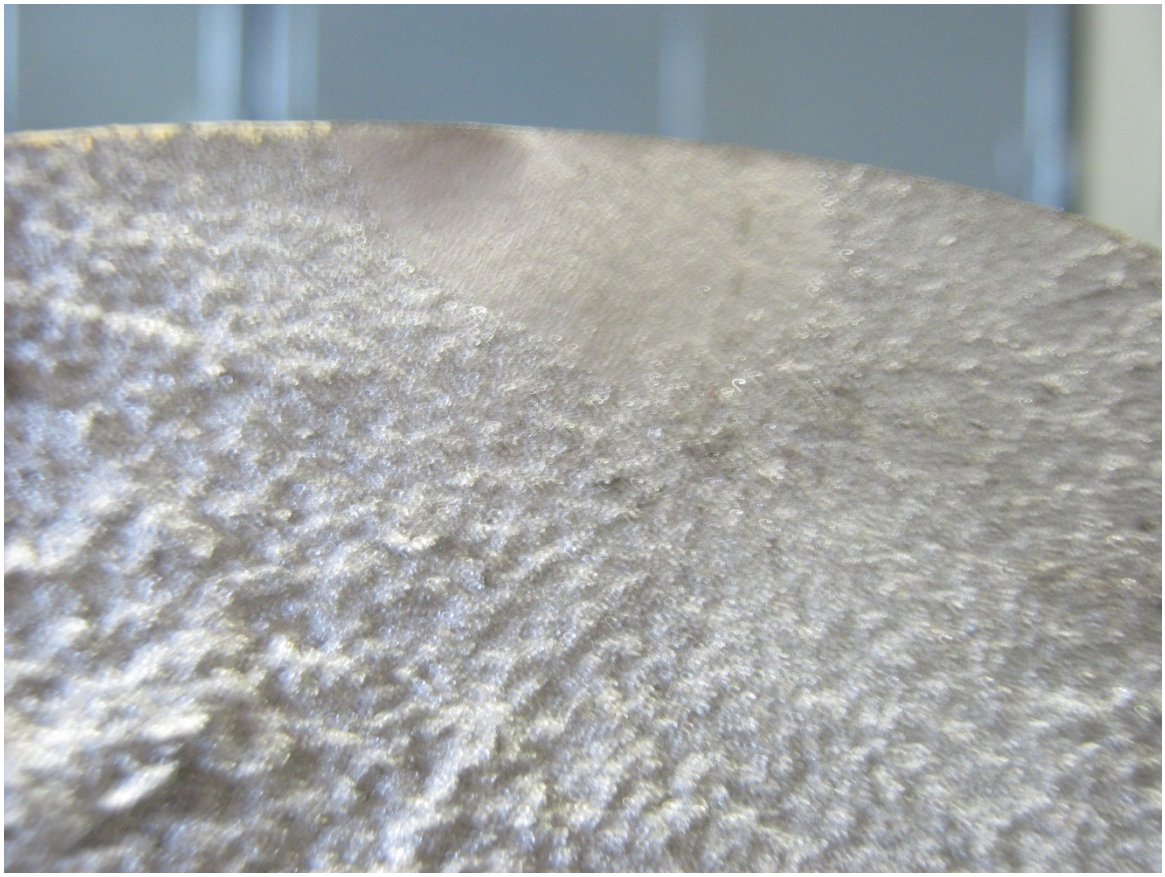

Figure 47. Fatigue Failure Driven by Surface Pitting on Rail Head

Several of the fatigue failures resulted from stress concentrations associated with the joining process. In the case of the CAD welds, the fatigue failures were attributed to the development of martensite from the welding process where the critical temperature in the rail was exceeded. A photograph of a CAD weld failure caused by the formed martensite is shown in Figure 48. With the IFW joints, the martensite was associated with an out-of-plane condition that created both martensite and a zone of upset in the side of the rail head as it forged into the rail. This is the same issue that caused some problems with the corrosion test. Figure 49 shows a photograph of an IFW joint failure. The presence of martensite in either joint reduced the fatigue life. In general, the rails failed in the 140 percent load range of the bending stress applied in the rolling load test for 136 RE rail. When martensite was present, the cycles to failure were achieved at lower loads.

It should be noted that failures at the signal wire joint location were expected. This location experienced the highest cyclical loads during the test. In general, the cycles-to-failure was very similar to that measured from plain rail.

Figure 48. CAD Weld Driven Failure due to Formation of Martensite

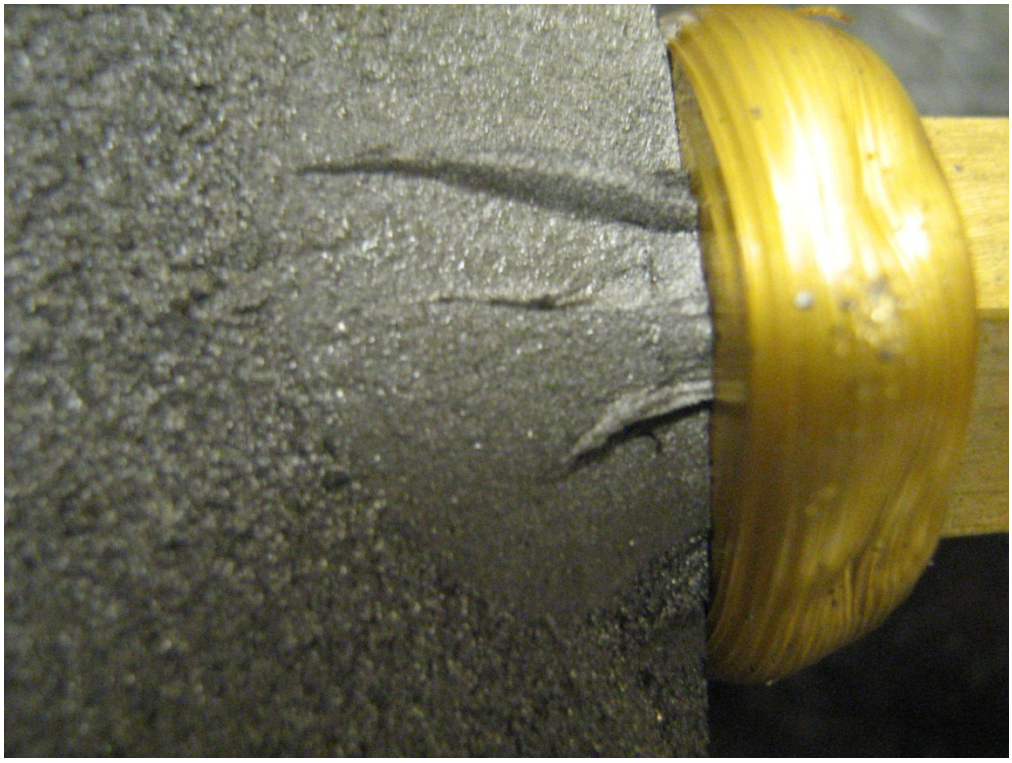

Figure 49. IFW Joint with Martensite Present

2.3.4 Tensile Testing

EWI completed tensile testing of CAD joints by applying tension to the cable. Tensile testing of the IFW joints was not possible on the rail head because of geometric limitations. Additionally, because of the stud size, it was not possible to grip the stud and rail simultaneously and bolts inserted into the stud pulled out the threads in the stud before stressing the joint. Table 11 shows the tensile test results of the CAD weld joints. The cable consistently broke away from the joint at approximately 500 lb of tension. Nothing remarkable was noted in these tests. The wires failed at a fairly consistent load, and no fractures were found in the rail surface.

Table 11. Tensile Testing Results from CAD Welds

Specimen	Maximum Load		Displacement at Maximum Load	
Identification	(kips)	(kN)	(in)	(mm)
SS-1	0.496	2.21	0.098	2.49
SS-2	0.511	2.27	0.098	2.49
SS-3	0.489	2.18	0.105	2.67
SS-4	0.495	2.20	0.140	3.56
SS-5	0.596	2.65	0.125	3.18
HE-1	0.490	2.18	0.099	2.51
HE-2	0.462	2.06	0.105	2.67
HE-3	0.632	2.81	0.073	1.85
HE-4	0.500	2.22	0.121	3.07
HE-5	0.595	2.65	0.114	2.90
DS-1	0.439	1.95	0.079	2.01
DS-2	0.532	2.36	0.105	2.66
DS-3	0.541	2.41	0.089	2.26
DS-4	0.485	2.16	0.089	2.26
DS-5	0.521	2.31	0.097	2.46

Figure 50 shows the resulting failure of a CAD weld joint where the wire has simply pulled out of the CAD weldment. All joints in the CAD welds failed in this manner. This failure mode acts as a fusible link application in a RWI joint.

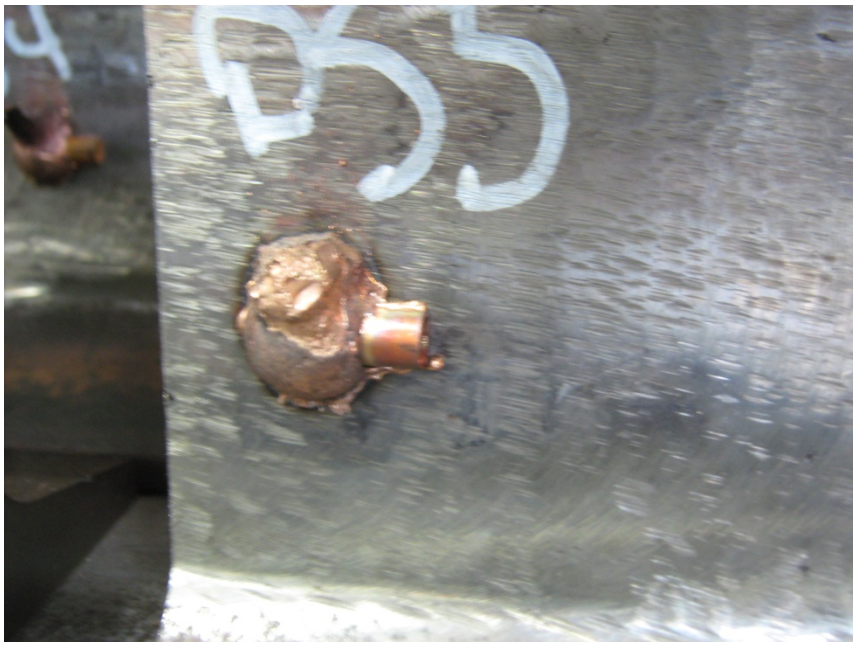

Figure 50. CAD Weld Typical Failure Showing Wire Strand Pullout

2.3.5 Shear Testing

Shear testing was completed on the IFW joints, in lieu of tensile testing. The IFW joints are capable of supporting shear loads as an appurtenance device, and they may carry both shear and tensile in service, depending on the direction of the load. EWI constructed a hard tool, as shown in Figure 51. This tool was then attached to an Instron machine and the machine applied a shear load to the weld joint at its mating surface with the rail. Peak load data was collected. This loading to the stud is analogous to the loading applied to the exothermic bonds in the tensile testing. The testing replicates the shearing action of the wire pulling on the joint in a direction parallel to the rail.

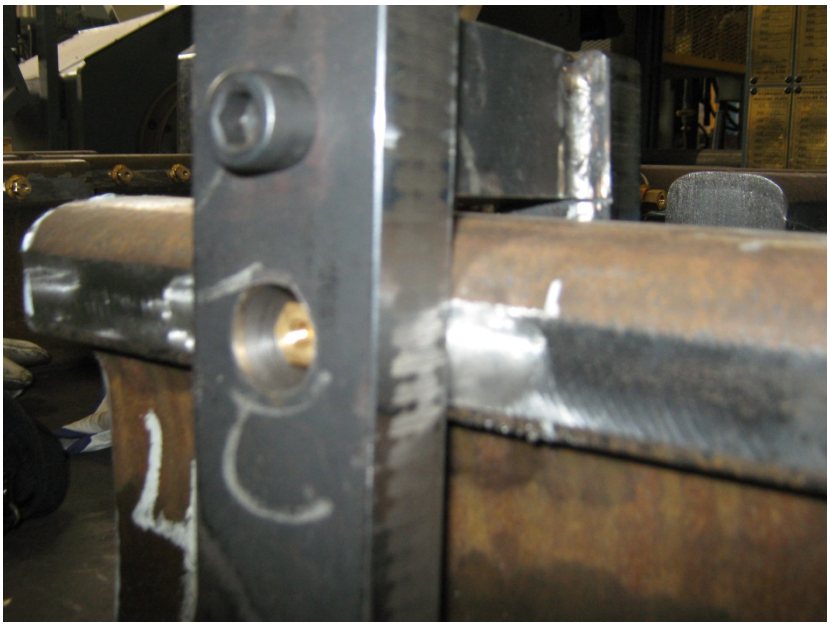

Figure 51. Shear Testing Tool Used to Assess IFW Joint Shear Strength

Table 12. Shear Test Results of IFW Weld Joints

Identification	Shear Strength (kips)	Shear Strength (kN)	Displacement (in)	Displacement (mm)
DS-1	7.089	31.53	0.111	2.82
DS-2	4.782	21.27	0.083	2.11
DS-3	6.432	28.61	0.142	3.61
HE-1	~0 bad weld joint			
HE-2	0.864	3.84	0.020	0.51
HE-3	0.643	2.86	0.017	0.43
SS-1	4.166	18.53	0.111	2.82
SS-2	6.730	30	0.142	3.61
SS-3	1.857	8	0.037	0.94

Figure 52 shows a typical failure from a shear test of the IFW joints. It is apparent in the photograph that the rail surface was irregular—leading to a lower load failure of the weld joint. This conclusion is evidenced by irregular areas of the stud material transfer onto the rail and the apparent peak on the rail surface. The high strength joints show that the IFW joint is at least as strong as the exothermic weld joints, from a wire restraint standpoint. Additionally, they show that the stud can pull away from the rail without damaging the underlying rail material while providing a high strength joint.

Figure 52. IFW Shear Test Failure Surface

2.3.6 Impact Testing

EWI conducted impact testing to determine the toughness of the rail-to-bond interface. Impact testing measures the amount of energy required to forcibly remove, or break away, the signal wire attachments from the rail itself.

Figure 53 shows the impact the test fixture installed in a drop tower applied to the IFW joint. Figure 54 shows the test fixture as applied to the CAD weld joint. The fixture was designed to apply the load energy directly to the welded joint, approximately 0.030 in from the interface.

Figure 53. Impact Fixture Applied to IFW Joint

Figure 54. Impact Fixture Applied to CAD Joint

There is a significant difference between the IFW and CAD joints in the bond area. The CAD weld joints have a larger cross-sectional area attached to the rail than the IFW joints. To account for this difference, the energy applied to the joint is normalized per unit area to allow for a direct comparison between the two techniques. The maximum amount of impact energy available from the testing device was 330 foot-pound force (ft-lb). In some cases, the joints did not fracture under the first test. In Tables 13 and 14, when two loads are shown for the sample, it signifies that the joint did not fracture at the first impact loading, and a second impact loading was required to fracture the joint from the rail.

Table 13. Impact Load Testing of IFW Joints

Sample	Rail Material	Impact Energy, ft-lb	Normalized Energy ft-lb/in^2	Failure
1	SS	80	543	Yes
2	SS	64	434	Yes
3	HE	64	434	Yes
4	HE	127	862	No
	HE	~330	2242	Yes
5	HE	~330	2242	Yes
6	DS	127	862	Yes
7	DS	127	862	No
	DS	~330	2242	Yes
8	DS	127	862	No
	DS	~330	2242	Yes
9	DS	127	862	No
	DS	~330	2242	Yes
10	DS	~330	2242	Yes
11	HE	~330	2242	Yes
12	HE	~330	2242	Yes
13	HE	127	862	Yes
14	SS	127	862	No
	SS	~330	2242	Yes
15	SS	127	862	Yes
16	SS	127	862	No
	SS	~330	2242	Yes

Table 14. Impact Load Testing of CAD Weld Joints

Sample	Rail Material	Impact Energy, ft-lb	Normalized Energy ft-lb/in^2	Failure and Location
A	SS	~330	538	No
B	SS	~330	538	No
C	SS	~330	538	No
D	SS	~330	538	Yes into rail

The energy absorbed by the two processes was very similar. Many of the lower energy fractures in the IFW joints were the result of poor welds. Some samples suffered from the misalignment and surface roughness issues previously mentioned. These joints displayed the typical partial bonding area pattern described in the following section. All but one of the CAD welds absorbed the maximum impact force without failure. The CAD weld that did fail is shown in Figure 55. In this case, the fracture path migrated into the steel. All the IFW joints fractured in the brass

material and did not progress into the rail material. These results correlate well with work completed by TTCI and other authors.[5]

Figure 55. Fractured CAD Weld

2.3.7 Metallographic Analysis

EWI prepared cross-sections from each of the rail steels to microscopically verify the underlying microstructure. In addition, a Vicker's micro-hardness traverse was taken along the weld butt line into the HAZ in the rail steel. By conducting metallographic analyses, EWI was able to obtain data pertaining to the expected performance of the joint and compare the two methods against each other.

2.3.7.1 Standard Chemistry Rail (SS)

The standard chemistry rail sections (SS) are shown in Figures 56 and 57 for the IFW joints and Figures 58 and 59 for the CAD joints. In these sections, the naval brass is apparent on one side of the joint, and the other side is the unaffected steel. An area of martensite is apparent in the CAD sections shown in Figures 58 and 59.

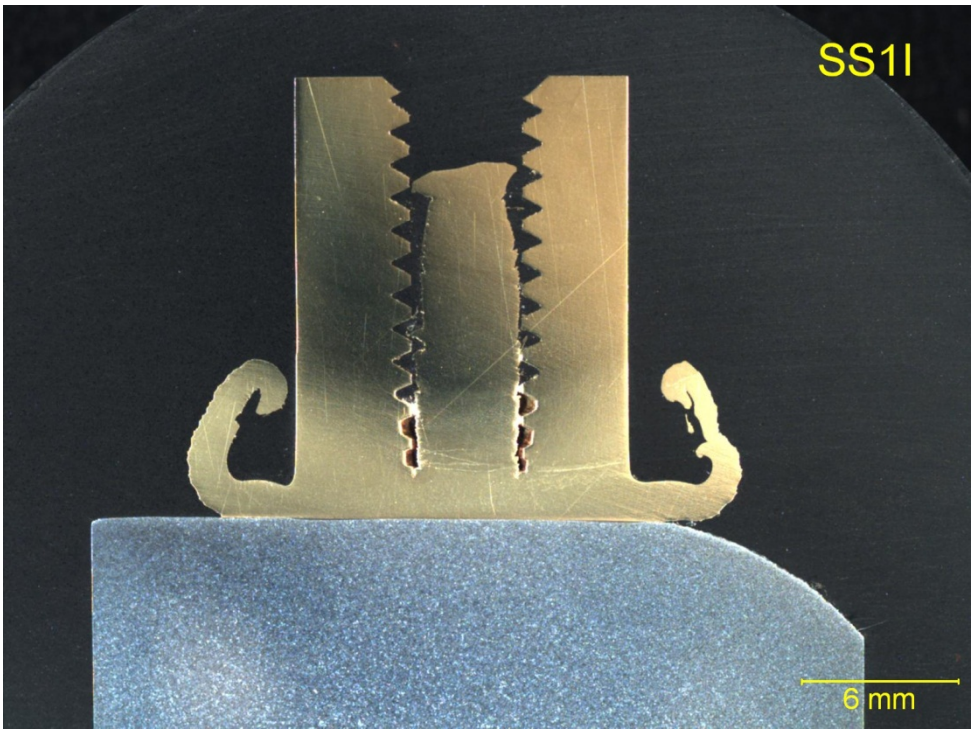

Figure 56. IFW Weld Joint Standard Chemistry Rail #1

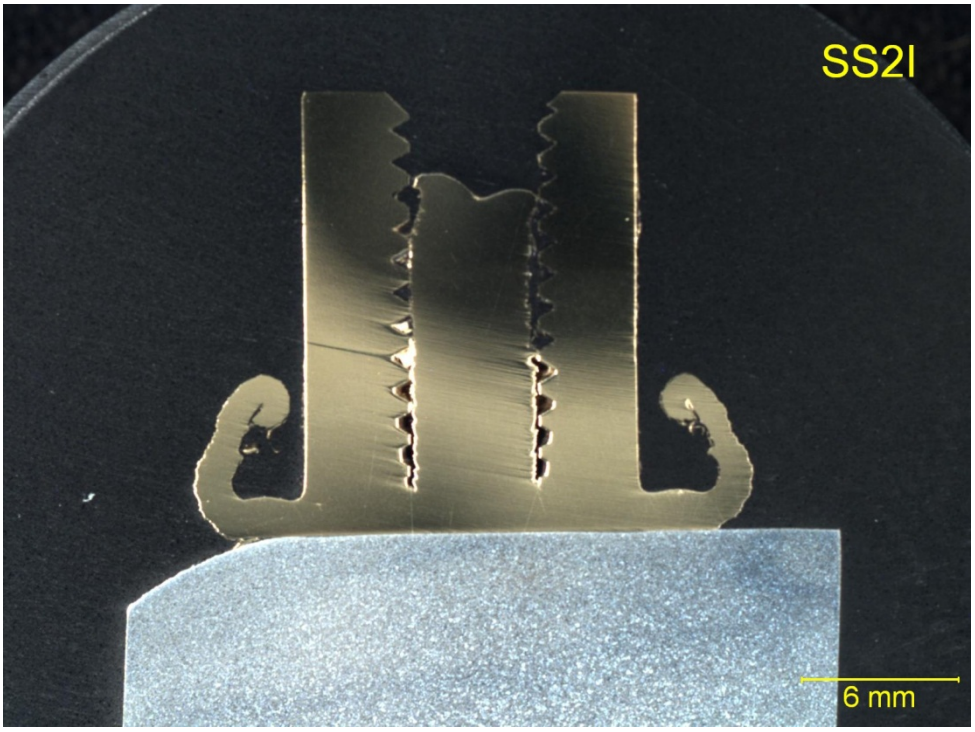

Figure 57. IFW Weld Joint Standard Chemistry Rail #2

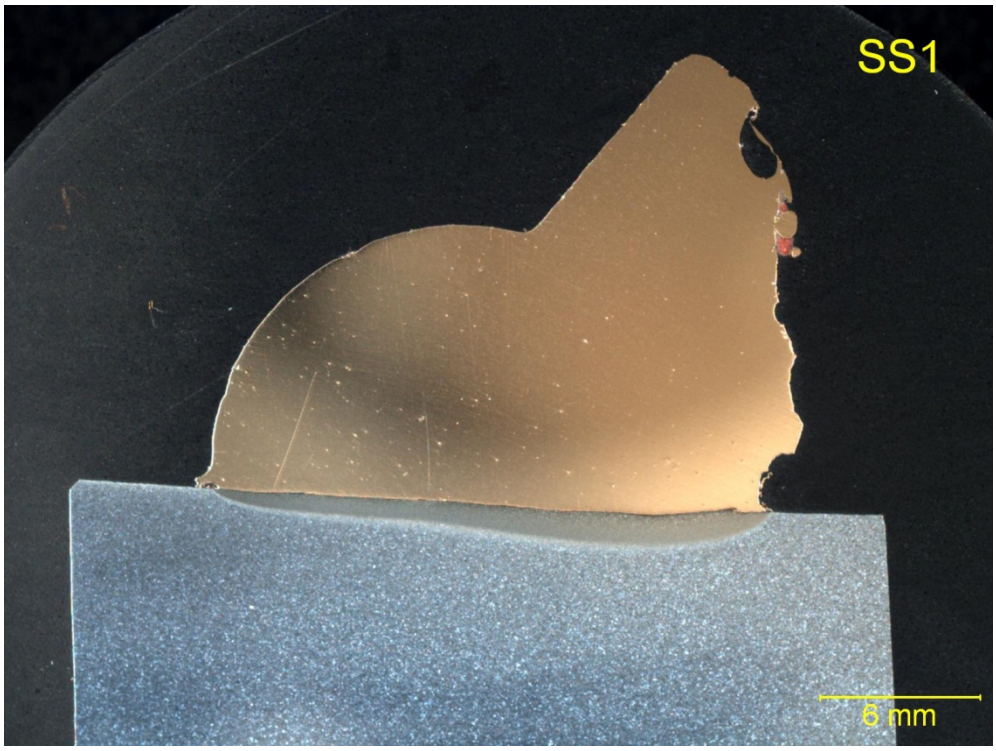

Figure 58. CAD Weld Joint Standard Chemistry Rail #1

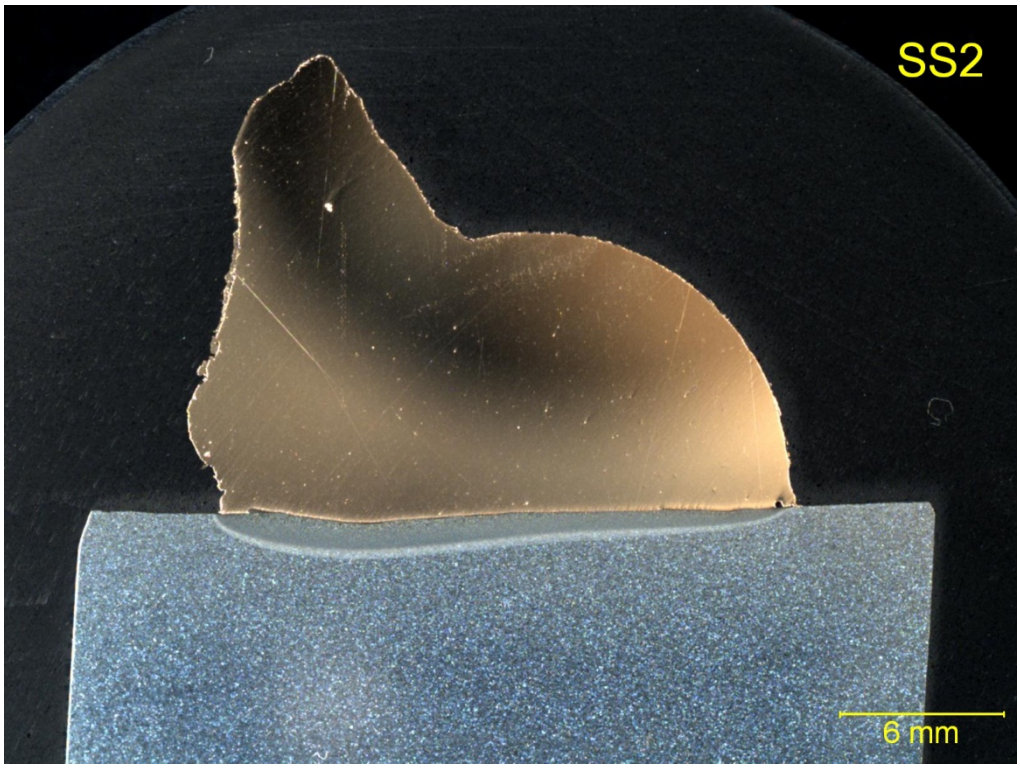

Figure 59. CAD Weld Joint Standard Chemistry Rail #2

A micro-hardness traverse was also completed with the first point taken at the weld joint and the remaining points traversing into the rail material away from the weld joint. The micro-hardness traverses are shown graphically in Figure 60 for the standard chemistry rail. This depicts the changes in hardness near the weld joint and the differences between the two processes.

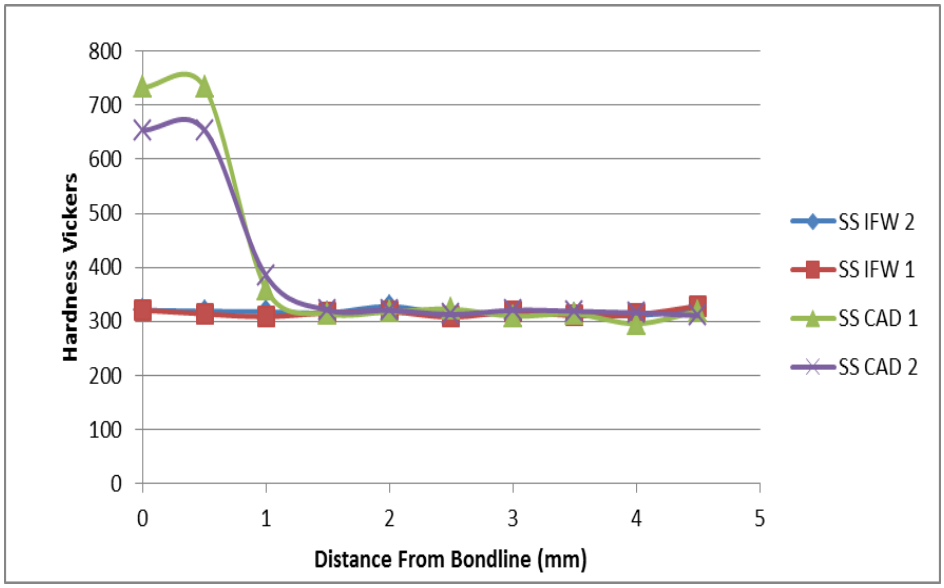

Figure 60. Microhardness Traverses in Standard Chemistry Rail

2.3.7.2 Hyper-Eutectoid Chemistry Rail (HE)

The hyper-eutectoid chemistry rail sections (HE) are shown in Figures 61 and 62 for the IFW joints and Figures 63 and 64 for the CAD joints. In the IFW joints, Figures 61 and 62, the naval brass is apparent on one side of the joint and the other side is the unaffected steel. In the CAD joints in Figures 63 and 64, the HAZ in the steel is much more obvious with both a hardened zone up close to the attachment and a softened zone further away from the attachment.

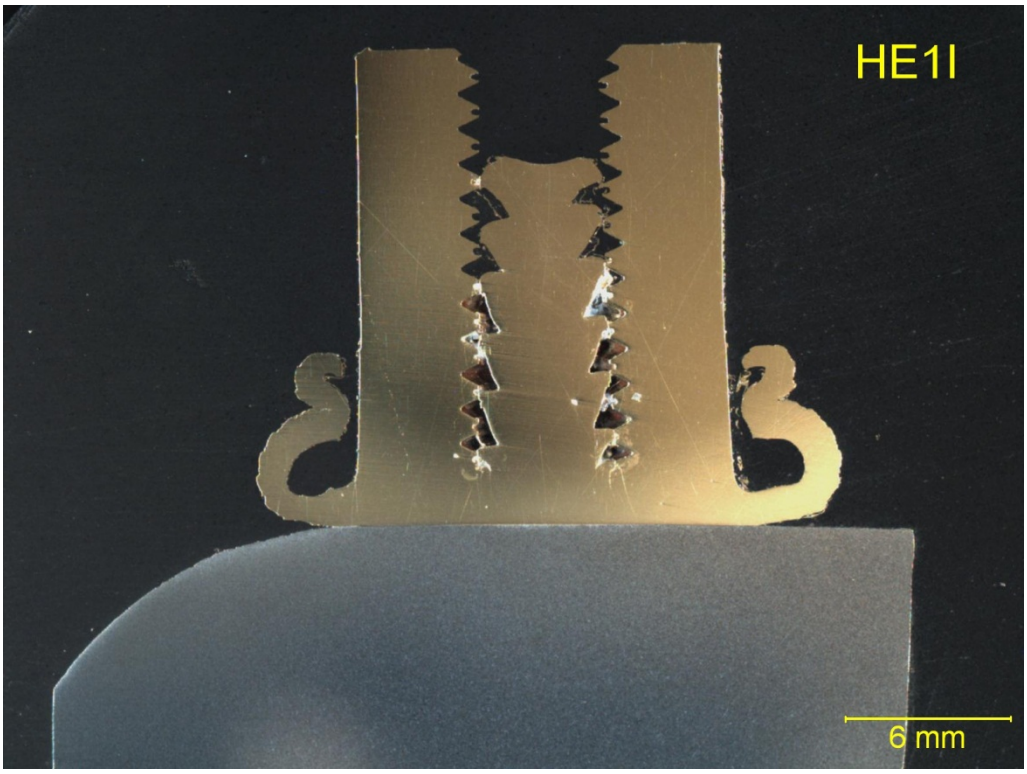

Figure 61. IFW Weld Joint Hyper-Eutectoid Rail #A

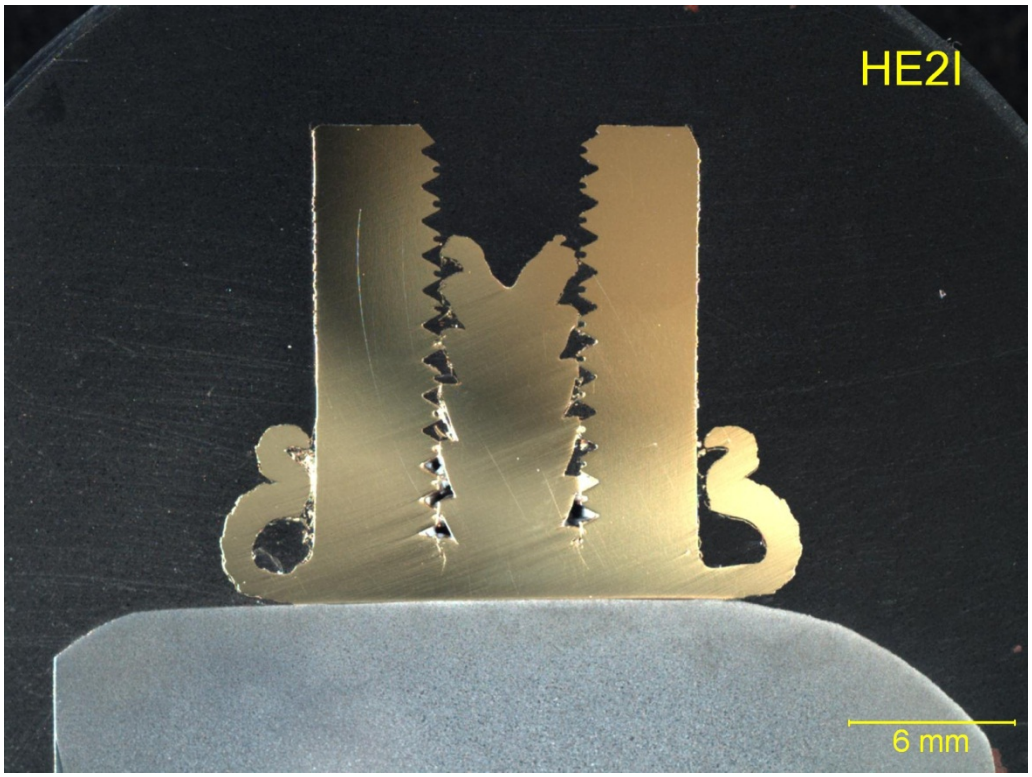

Figure 62. IFW Weld Joint Hyper-Eutectoid Rail #B

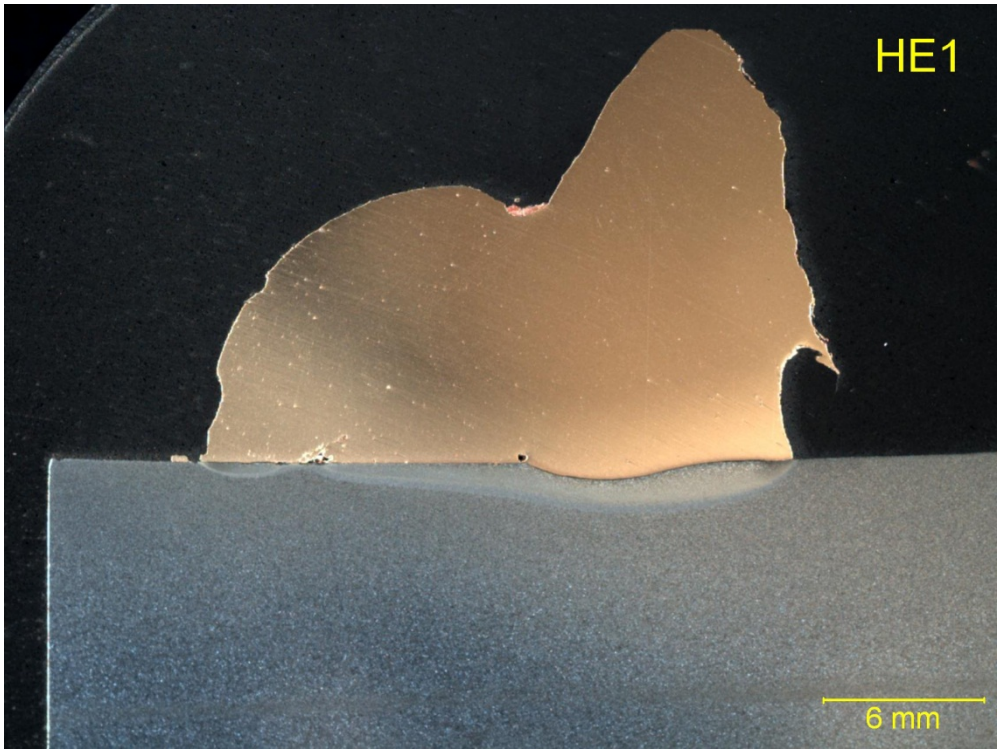

Figure 63. CAD Weld Joint Hyper-Eutectoid Rail #1

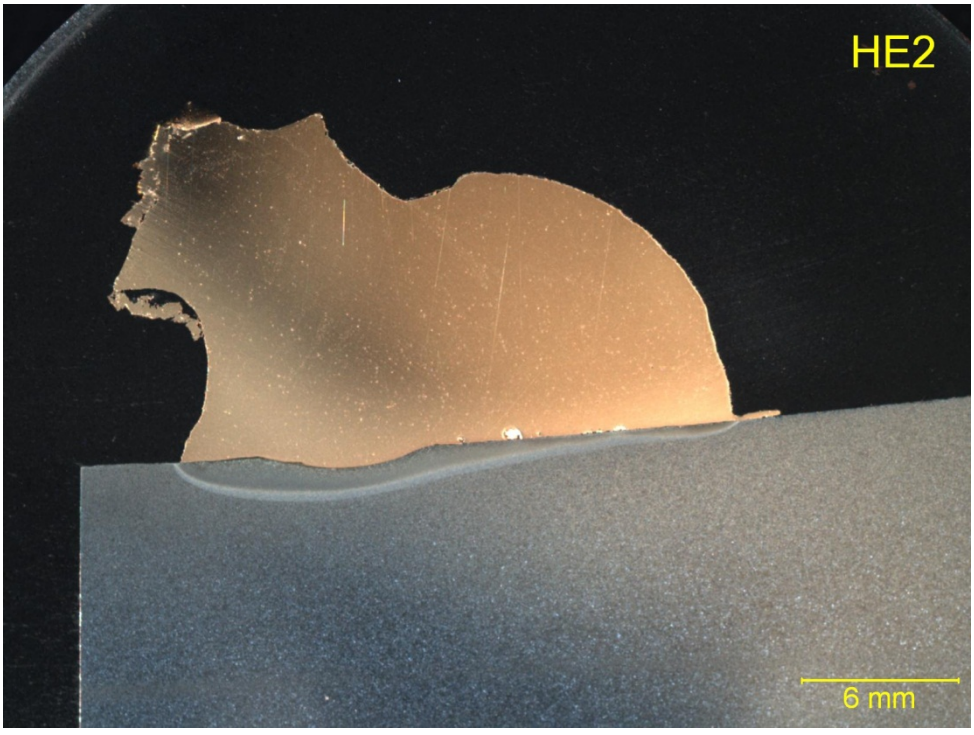

Figure 64. CAD Weld Joint Hyper-Eutectoid Rail #2

EWI also completed a micro-hardness traverse with the first point taken at the weld joint and the remaining points traversing into the rail material away from the weld joint. The micro-hardness traverses are shown graphically in Figure 65 for the hyper-eutectoid chemistry rail with all sections shown in one plot for easy comparison.

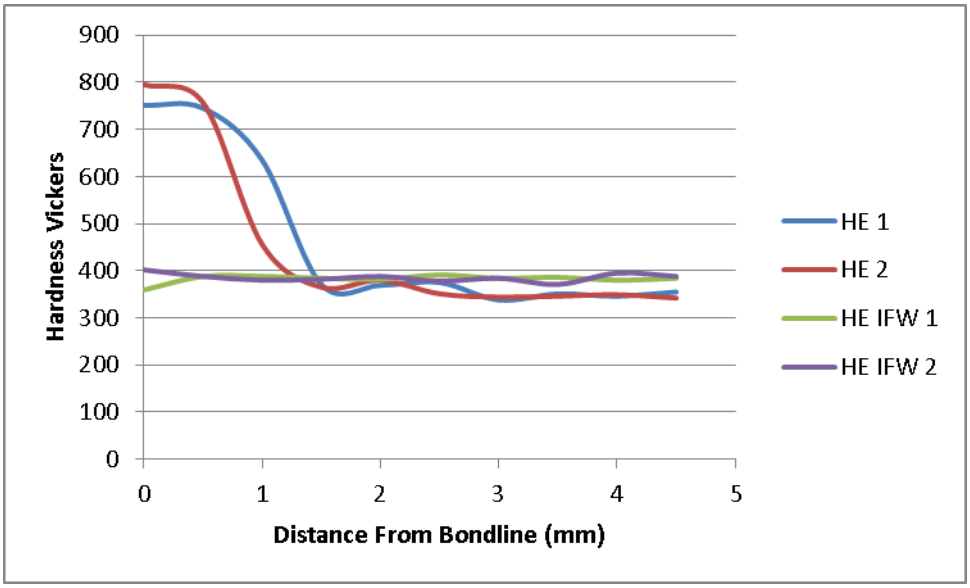

Figure 65. Microhardness Traverses in Hyper-Eutectoid Chemistry Rail

2.3.7.3 High-Performance Rail (DS)

The high-strength rail chemistry rail sections are shown in Figures 66 and 67 for the IFW joints and Figures 68 and 69 for the CAD joints. In these sections the naval brass is apparent on one side of the joint in the IFW welds and the other side is the unaffected steel. In the CAD weld joints, the HAZ in the steel is much more obvious. No HAZ is apparent in the IFW joints.

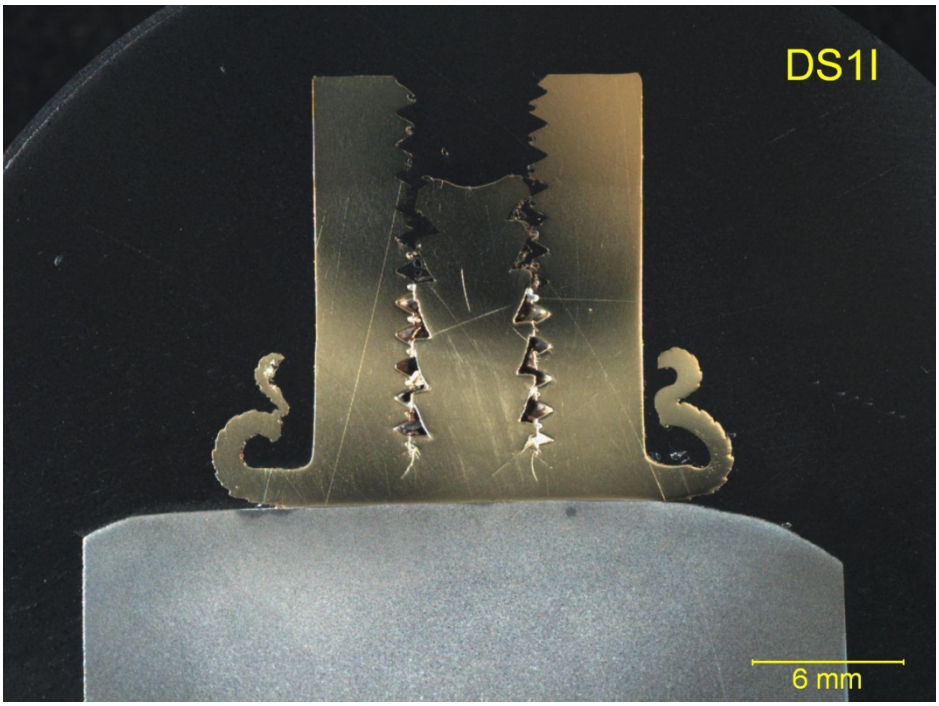

Figure 66. IFW Weld Joint High-Strength Chemistry Rail #1

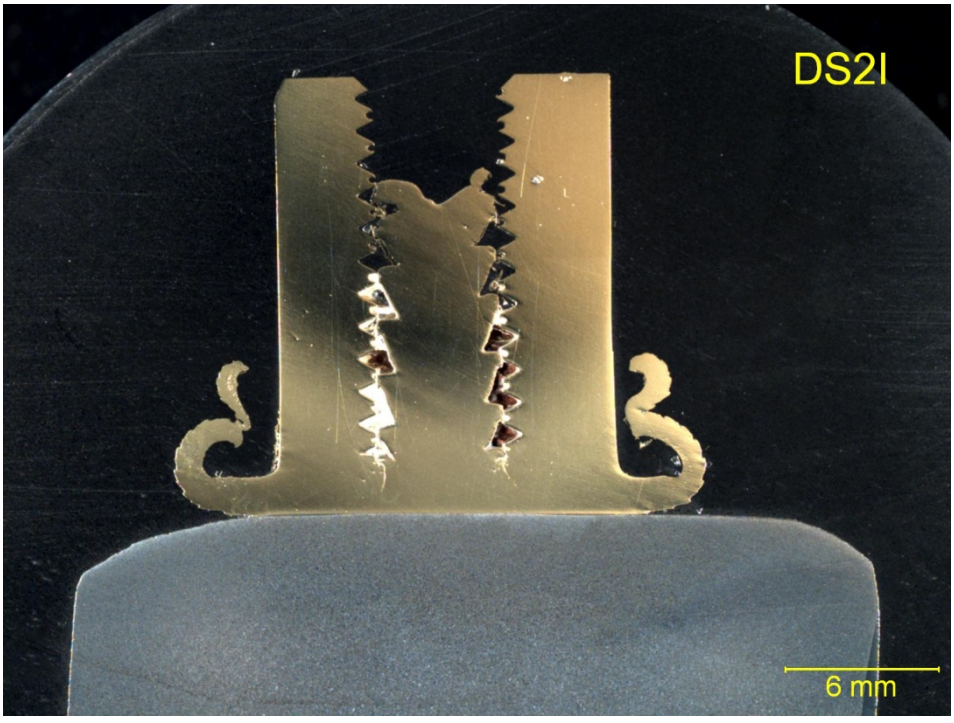

Figure 67. IFW Weld Joint High-Strength Chemistry Rail #2

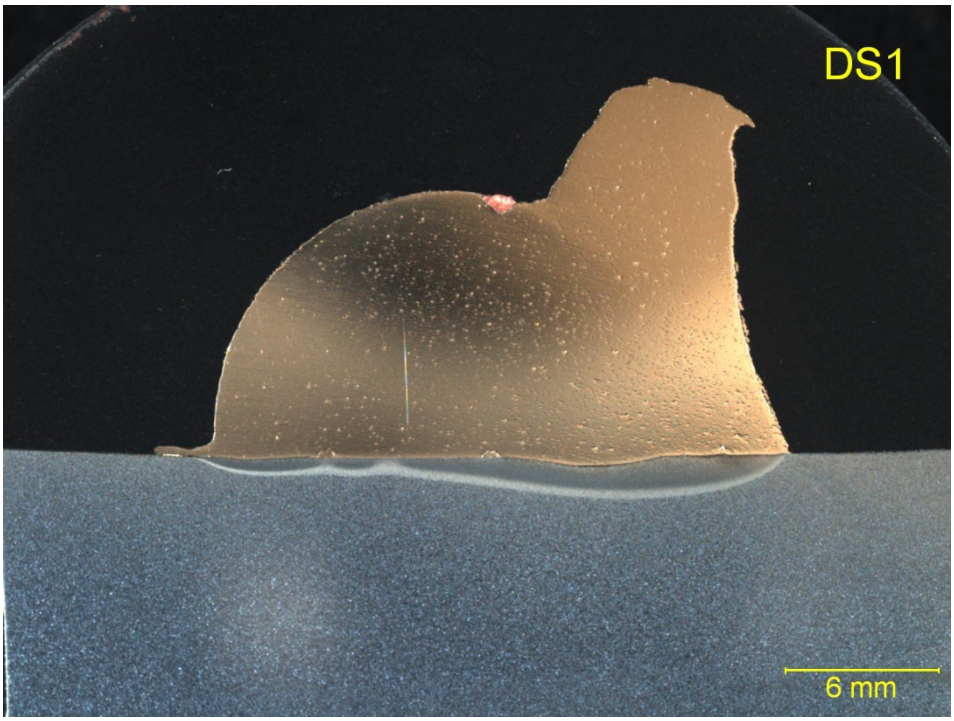

Figure 68. IFW Weld Joint High-Strength Chemistry Rail #1

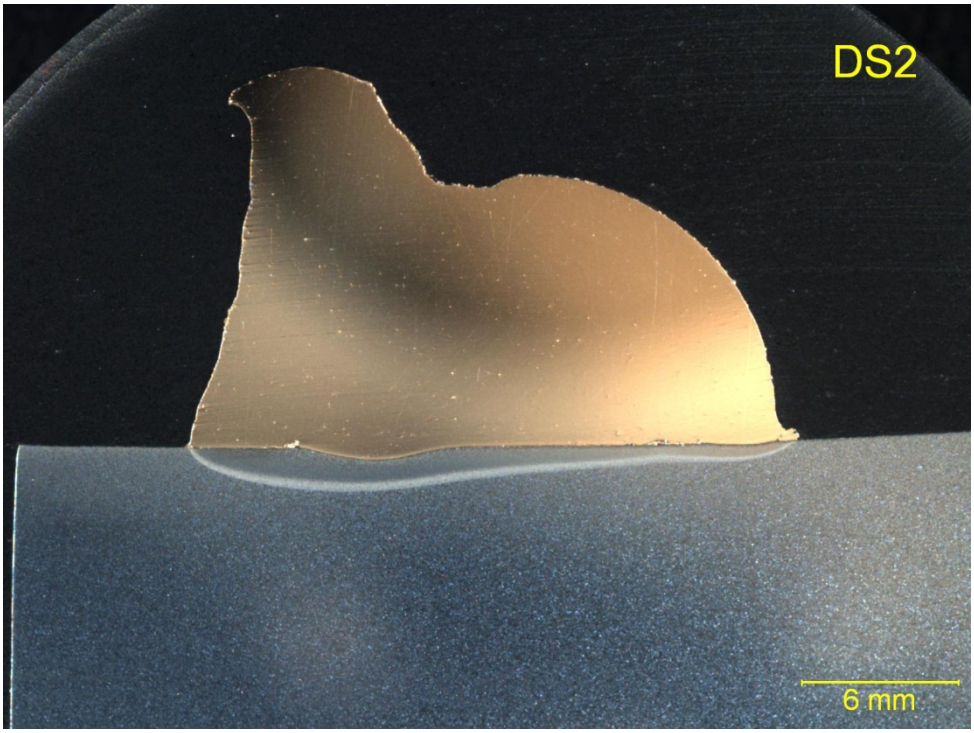

Figure 69. IFW Weld Joint High-Strength Chemistry Rail #2

A micro-hardness traverse was also completed with the first point taken at the weld joint and the remaining points traversing into the rail material away from the weld joint. The micro-hardness traverses are shown graphically in Figure 70 for the high-strength chemistry rail.

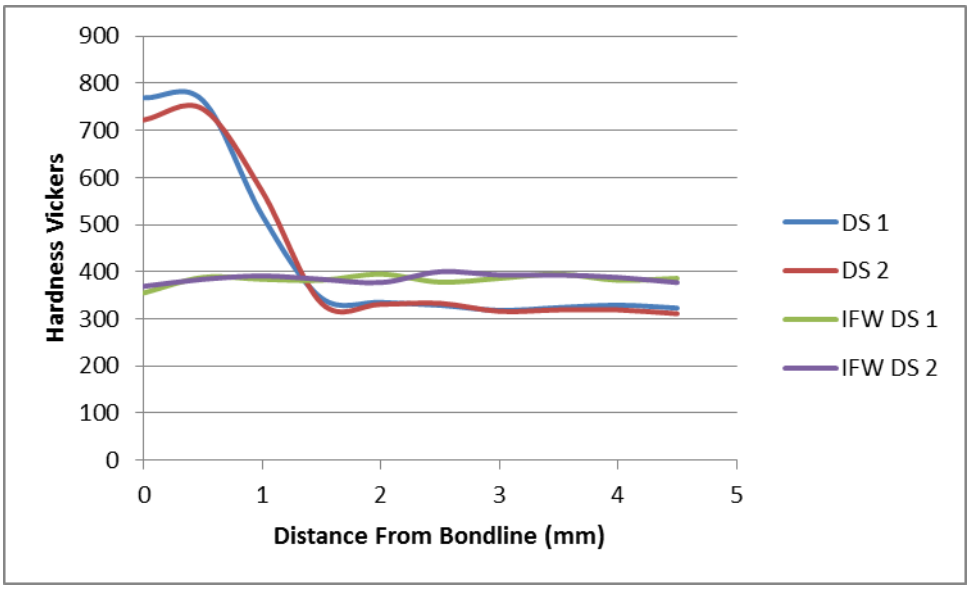

Figure 70. Microhardness Traverses in High-Strength Chemistry Rail

In all the metallographic analyses, it appears that the IFW attachment method creates a joint without producing martensite in the rail. The exception to this is when the surfaced preparation is not correct and the machine is not aligned properly on the rail. The following section discusses the features incorporated into the portable machine design to prevent this occurrence. The effect of these features on the weld quality can be visually observed and the hardness traverses confirm that the HAZ is much smaller and less severe in the IFW joints.

By preventing the formation of martensite, the rail material will carry the fatigue loads, and the joint can be made on the rail head without the risk of microstructural degradation that can lead the formation of a crack in the rail.

2.3.7.4 Detailed Microstructural Findings

Detailed analysis of the welds shows an even bigger difference between the IFW and the exothermic weld joints. The IFW joints produce a clean bond because the rail steel is not melted, nor is it exposed to temperatures in excess of the transformation temperature. The exothermic weld joints are exposed to both a high enough temperature to transform the material and the liquid copper, which can lead to LME, as detailed below.

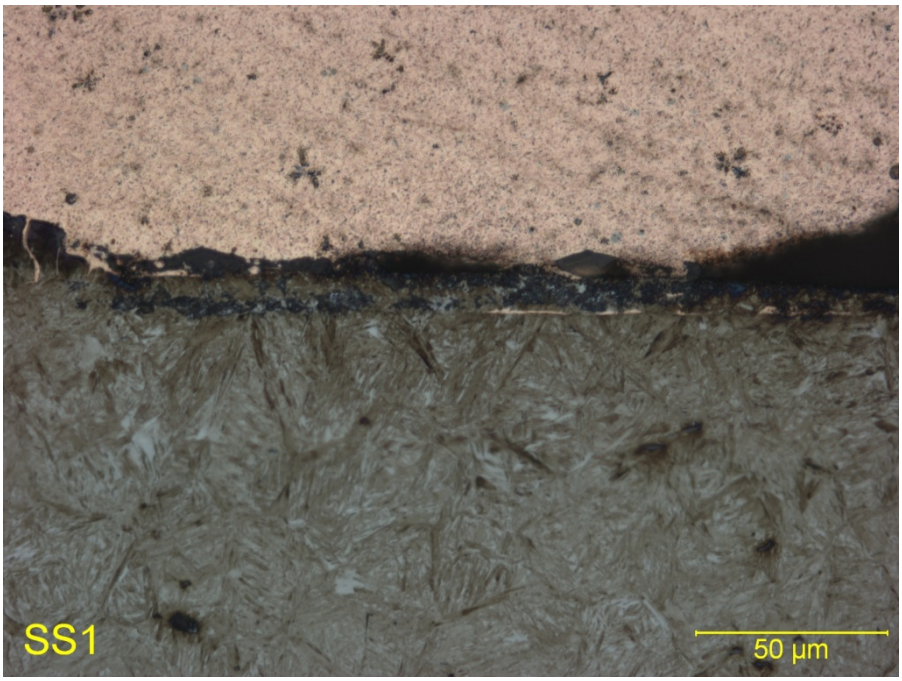

Figure 71. Bondline of Exothermic Weld onto Standard Chemistry Rail

Figure 71 shows a cross section of the fusion boundary between the rail steel in the bottom and the exothermic material in the top. Several items are apparent in this section. First, the steel is fully martensitic. Second, the copper has infiltrated the steel at the fusion boundary, as shown by the copper strands in the steel at the interface.

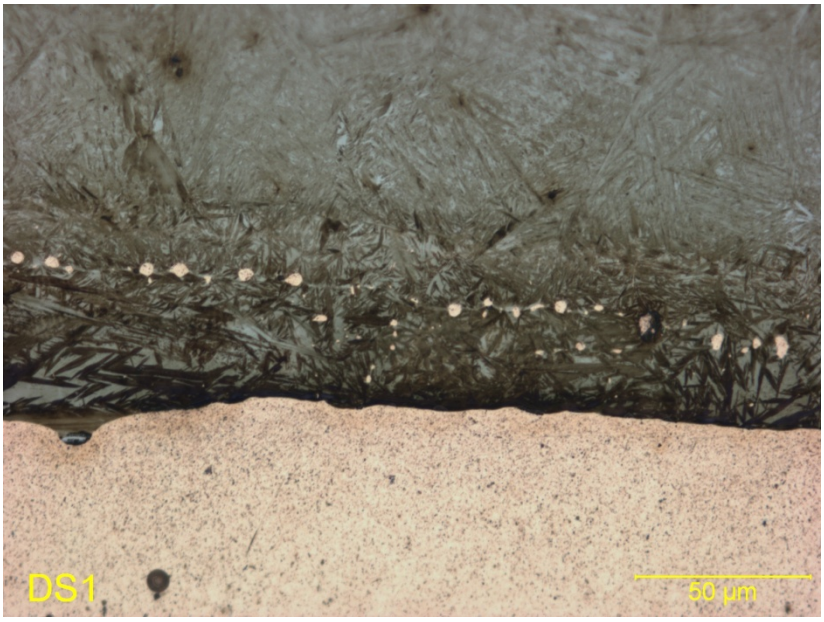

Figure 72. Section at Fusion Boundary Showing Resolidified Copper Globules in Resolidified Rail Steel

Figure 72 shows in greater detail that the molten copper coming out of the exothermic process is hot enough to melt the steel and dissolve copper into the steel matrix, as evidenced by the small copper balls apparent in the resolidified steel. The molten copper is in fact penetrating the steel, a key characteristics of LME. LME was cited in the failure analysis as one of the contributing factors to the creation of the UT indication.

Further analysis of the metallographic sections showed a larger LME-driven crack in the rail steel which is shown in Figure 73 and Figure 74. Note that the cracking extends from the fusion boundary into the parent solid rail steel section. When this LME occurs, a crack of much larger size is created during the welding process. This crack may have initiated in a fusion zone in the steel, or simply ran into the base metal, as there was both tensile stress and liquid metal available in the weld joint.

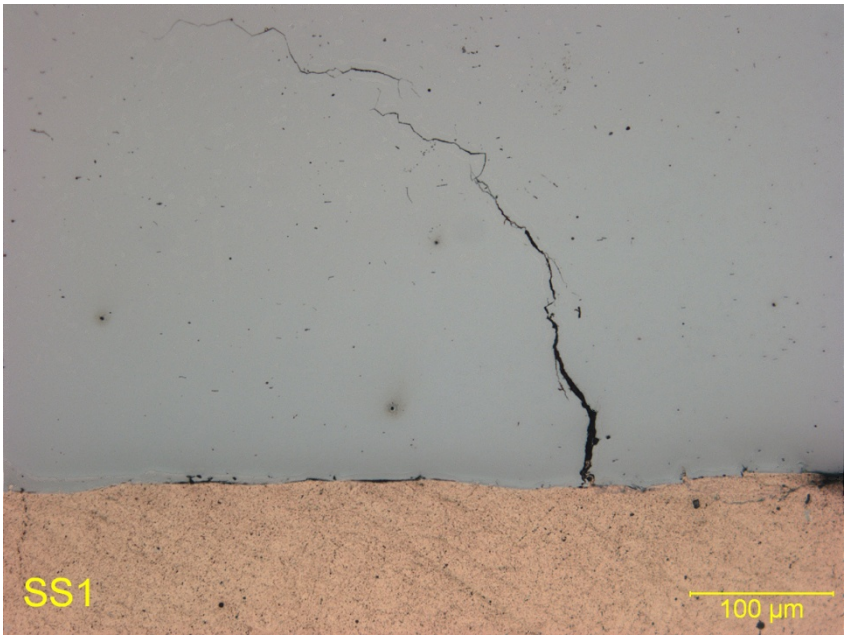

Figure 73. LME Crack into Parent Standard Chemistry Rail Steel

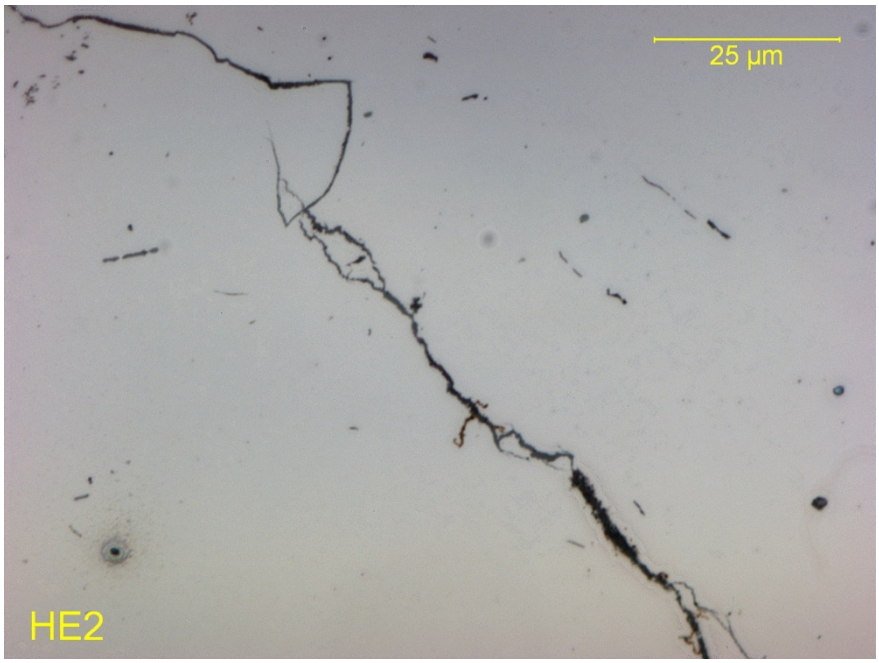

Figure 74. LME Crack in Detail in Standard Chemistry Rail showing Copper Coloring within the Crack

In reviewing the metallographic sections, several key issues can be observed. The exothermic welds all display a layer of hard martensite at the fusion boundary that extends into the base metal rail. No martensite was observed in the improved IFW joints. The exothermic welds typically display copper globules in the molten rail steel zone, suggesting that the rail steel melted and resolidified. The IFW process operates below the melting temperature of both the stud material and the rail steel; therefore, no solidification defects can be observed. Most importantly, however, a LME crack was found, which shows that this cracking mechanism can occur in rail at a neutral stress state due to the residual stress in the rail itself.

3. Summary and Conclusions

3.1 Summary of Results

EWI developed a new intertial friction welding process and wire mounting stud to attach signal wires to the rail head without the need for a liquid metal to form during the operation and without leaving a residual martensite layer in the weld joint. The mechanical performance of the new IFW joint is nearly identical to that of the current exothermic methods. With a proper setup for the weld, no microstructural damage to the underlying rail steel was detected in the welding trials. The physical testing data reveals very similar performance from existing attachment techniques in terms of tensile strength, fatigue performance, impact resistance, electrical performance, and corrosion resistance. The biggest difference observed is the formation of a very hard layer of martensite with the current approach whereas with the IFW process (when using the appropriate material and method) no martensite formed.

Based on this work, EWI believes that a high quality, repeatable, solid state weld process and associated tooling can be developed that will eliminate the need for operator-control of the weld and will allow single wire attachment on all standard rail types and sections.

3.2 Conclusions

Signal wire attachment failures occur at higher-than-desirable rates which lead to safety concerns and train delays. The root cause of these failures can be traced to current attachment location requirements and metallurgical issues. The goal of this research is to develop an improved signal wire attachment method.

Based on interviews conducted on this project and previous TTCI research in the area of signal wire attachment, the following conclusions can be drawn. A welded or brazed joint is desired at the RWI location for durability and corrosion resistance. MOW equipment snags still account for many wire or RWI interface failures due to wire location requirements. In the work conducted by TTCI, it would appear that approximately 50 percent of the required wire repairs can be traced to MOW activity. The current CADWELD weld and pin brazing systems used in the field can produce martensite in the RWI joint. This martensite can lead to rail section failure, even though it is on the neutral axis of the rail. Additionally, the RWI joint can lead to formation of a hard disk at the attachment point, which may in turn lead to a dishing or planar failure releasing the RWI from the rail web because of the underlying brittle nature of the attachment. Cleaning and preheat are reportedly required for best use of the CADWELD attachments systems; however, it is unclear whether signal crews have the tools and training to regulate and use preheat effectively.

The failure analysis of the RWI joint with a crack indication showed both overheating of the steel to the point of melting resulting in martensite formation and LME in the joints. In particular, the crack face itself was decorated with copper. The most critical flaw in this joint, or the flaw that initiated failure, cannot be positively identified with the material provided; however, two issues capable of initiating crack development and growth were observed. From a safety perspective, it is believed that melting of the copper alloy or RWI alloy onto the rail can

lead to the formation of LME. LME will eventually create some sort of fatigue-type failure if there is any strain in the RWI region.

A weld process must be developed that creates a solid-state bond while controlling the peak temperature in the rail steel. The process must require very few preparation steps and should be very portable. It would be ideal for the process to eliminate the need for preheating, as this feature of all welding and brazing processes used in welding on rail is cited as undesirable.

An IFW process was developed to attach threaded nuts to rail steel with appreciable joint strengths and without the formation of martensite. C464 Naval Brass studs showed the best characteristics of all alloys reviewed, from an inertia welding perspective, for attachment to rail steel. This attachment or stud is part of a signal wire attachment technique that would allow for placement of a wire onto the head of the rail. An internally threaded stud used in the trials also allowed for the use of a fusible mechanical link or breakaway in the assembly of signal wires to prevent damage to the rail if the wire was snagged.

Basic research was conducted to identify candidate alloys for the IFW approach. Four alloys were identified that exhibited the required commercial availability, corrosion resistance in combination with rail steel, and forging characteristics which allow the IFW process to be developed. IFW process development was conducted on all four alloys: C110 copper, C464 Naval Brass, C172 Copper, and C360 Brass. C464 Naval Brass allowed welds to be made with parameters such that a portable IFW system could be designed.

With C464 Naval Brass, the process exhibited tolerance for change in the parameters without compromising strength or forming martensite in the rail. A reparability study was conducted where the welds were made and removed ten consecutive times to show that the process did not degrade the underlying microstructure of the rail. No changes in rail microstructure or grain growth were observed in these trials.

The process developed appears to have met all the objectives of the program:

(1) No formation of martensite or deleterious phases;
(2) No risk of liquid metal embrittlement;
(3) Reliance on the equipment to guarantee weld quality; no preheat, no special preparation, no flux, no changes required for each weld; and
(4) Adequate strength that allows a fusible link to fail before the stud weld fails in order to minimize pull-away from the rail and reduce repair times.

The testing conducted on the IFW stud welds and comparison with the CAD process show very similar performance. The most notable difference is that the IFW process shows the ability to produce welds on rail steel without the formation of martensite or liquid metal embrittlement occurring. Strength, fatigue resistance, corrosion performance, and impact resistance are all similar in the welds.

One major issue was identified in the testing that will require further research and testing to confirm that it has been resolved. The IFW weld requires planar joint preparation. This implies that the grinding techniques used in these welding trials were not adequate, and the grinding or

surfacing operation should be integrated into the portable IFW unit. The conceptual welder design incorporates a spot facing tool into the machine so that the axial alignment and surface smoothness conditions required to create martensite free high-strength welds can be accomplished without operator dependence.

3.2.1 IFW Process Challenges

In some samples, the IFW weld quality was not sufficient. Poor quality welds exhibited less than desirable performance in many of the test series. The root causes of this poor weld quality are the rail head surface roughness and the angular misalignment of the IFW stud and rail head. When the surface of the rail head was irregular, the weld temperatures were elevated above specification, resulting in an inconsistent bond. Figure 75 shows just such an occurrence where upset or forging of the rail head is apparent at several locations denoted by a lip in the rail at the edge of the weld joint.

Figure 75. IFW Joint Displaying Evidence of Irregular Surface Preparation

The second challenge is aligning the IFW machine axially normal to the rail head surface. When misaligned, areas of the IFW joint are subjected to higher localized thrust loads leading to the formation of an irregular bond. This type of failure is shown in Figure 76. Misalignment also results in a “hot spot” in the weld joint which increases the risk of martensite formation. In this joint, the bond is apparently stronger where more stud material is deposited on the rail surface. More material is deposited on the lower portion of the joint than on the upper portion of the joint in this photograph.

Figure 76. IFW Joint Displaying Characteristics of Axial Misalignment

In order to address these issues, the portable welder unit was designed to incorporate a spot facing tool to set the plane of stud to rail interaction as desired and to dress the surface where the bond will be produced. This spot facing tool will engage the IFW unit in the same manner as the stud.

3.2.2 Conceptual Design of Portable Welder

EWI completed a conceptual design for the IFW stud welder. The design objectives included:

- Lightweight, portable design—15 lb weight target
- Minimal external power requirements—battery or spring
- Solid state welding process—no operator-dependent variables. The machine controls all weld parameters
- Accurate weld alignment and surface preparation

Figure 77 shows a conceptual drawing of the IFW stud welder in an isometric view. The welder applies force using force stored in a stack of Bellville washers. The flywheel is shown immediately adjacent to the chuck which holds the rail stud. An electric motor at the opposite end of the welder is used to accelerate the flywheel to the correct welding speed. Once the correct speed is reached, a switch releases the stored force in the Bellville washers, and the process begins as the stud engages the rail surface.

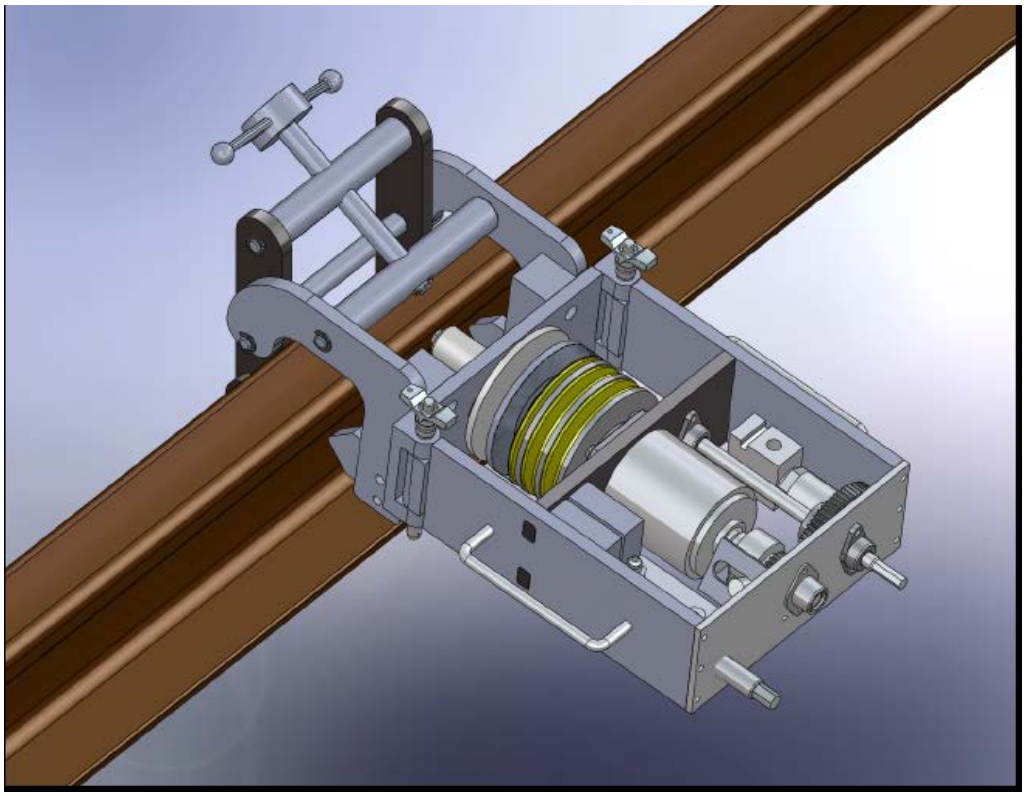

Figure 77. Isometric View of Portable Inertia Friction Welder

The welder itself is initially located on the rail and locked in position with a clamping device. The spot facing step is accomplished by inserting the spot facing tool or sanding disk in the welder and using a reduced force application to dress the face of the rail to accept the stud weld joint. This step, which was not possible in the no-portable welder, is expected to address the issues observed with variations in strength and martensite formation. After the face is prepared, the welder is opened up on a hinge without affecting the set plane of the base, and the stud is placed in the welder and then closed for welding. Figure 78 shows the mechanism in place to allow the welder to be opened to guarantee axial alignment without moving the plane of the welder.

The features detailed in the conceptual design should allow the welder to achieve the outlined goals. The welder itself will of course require some modification based on field trials. Plans for the initial build of the welder have not been firmed up at this date.

3.2.3 Presentation of Concurrent Results to Public

Results of the research were presented at the ASME Joint Rail Conference (JRC 2012) held April 2012 in Knoxville, TN. Questions were answered and further confirmations regarding the development of UT indications at the CAD weld locations were discussed. Others present in the audience were interested in the ability of the process to attach to rail with little risk of martensite development. The risk associated with the current technologies and the ability to move the attachment point back onto the rail head seemed to peak interest within the community.

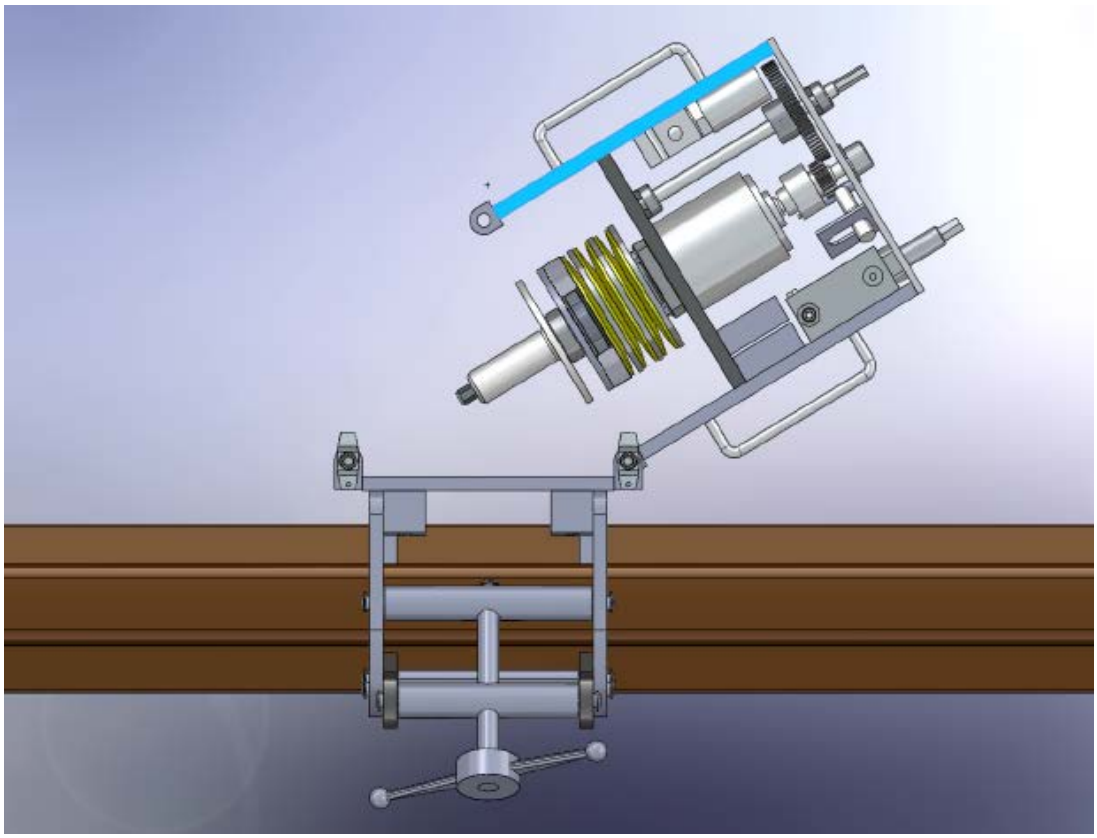

Figure 78. Top View of Welder Opened for Change from Spot Face to Weld Setup

3.3 Future Work

Currently, the number of UT indications associated with signal wire attachments at the web are not tracked effectively enough to capture the total number of indications found per year. These defects are known to the industry, and identified using scans of the web area, but not specifically tracked. This data may enlighten the industry to the number of rail replacements and downtime associated with the process. The downtime and capacity lost due to signal wire failures is captured and most of this time is associated with placement of the wire in the web, which allows MOW equipment to interfere with the signal wires. Some of the downtime is because of RWI failures, but it is difficult to determine what the exact ratio is between failures and snags. A change in reporting procedure may allow for better determination of the root cause of signal wire downtime.

The IFW technology developed and tested in this work shows the ability to produce a martensite-free weld, which should ideally allow for placement of the signal wire bond or connection onto the rail head. The technology should also dramatically reduce the number of wire snags attributed to MOW equipment. The strength of these welds is fully capable of withstanding any loads expected in the field without damage to the rail. Additionally, the breakaway concept mentioned in the TTCI report could be employed easily to the IFW joints either via a bolt-on connection or a solder-on connection to the stud.

In order to deploy this technology, the portable IFW welder needs to be refined, built, and field tested from a user standpoint. Key to this development would be incorporating a self-dressing or grinding mechanism into the welder so that a reliable surface for the stud welding could be produced. Field testing will allow for careful analysis of the weld joints in more realistic conditions. It is likely that employment of this new technology will result in a reduction in wire snags, simplified wire replacement during MOW activities, and improved track circuit reliability.

4. References

(1) Hawken, T., Davis, D., and House, M., "Improved Signal Reliability: Rail-to-Wire Bonding," Technology Digest, TTCI, Pueblo, CO, TD-08-016.

(2) Read, D., House, M., and Davis, D., "Rail-Wire Interface Performance Issues," Technology Digest, TTCI, Pueblo, CO, TD-08-058.

(3) Koch, K., Reiff, R., and Davis, D., "Evaluation of the Effects of Track Wire Connections on Rail Fatigue Life," Technology Digest, TTCI, Pueblo, CO, TD-10-025.

(4) Reiff, R., Hawken, T., and Davis, D., "Maintenance Resistant Track Wire Connections," Technology Digest, TTCI, Pueblo, CO, TD-11-010.

(5) Reiff, R., Hawken, T., and Davis, D., "In-Service Evaluation of Track-to-Wire Connections for Signals," Technology Digest, TTCI, Pueblo, CO, TD-11-026.

(6) Derailment of Canadian National Freight Train M33371 and Subsequent Release of Hazardous Materials in Tamaroa, IL, February 9, 2003. NTSB/RAR-05/01, PB2005-916301, Notation 7686, Adopted January 25, 2005.

(7) Honeycombe, RWK, Steels Microstructure and Properties, pp. 76-78.

(8) Steele, Roger, K, "Steel Alloys with Lower Bainite Microstructures for use in Railroad Cars and Track," DOT/FRA/ORD-01/15

(9) V.I. Vill', "Friction Welding of Metals," American Welding Society, Reinhold Pub. Co., 1962, pp. 20-23.

(10) Copper Development Association, Properties of C172 Class 3 copper: http://www.copper.org/

(11) ANSI / AWS D15.2-94, Recommended Practices for the Welding of Rails and Related Rail Components for use by Rail Vehicles.

(12) EN 14587-2, Railway Applications-Track-Lash Butt Welding of Rails- Part 2: New R220, R260, R260Mn, and R350HT grade rails by mobile welding machines at sites other than a fixed plant, Annex C, April 2009.

Appendix A. Estimation of Number of RWI Joints in Used Track

Major Sources of Signal Wire Attachment or RWI Joints

The following data and calculations were used to calculate the estimated signal wire failure rate.

- Number of miles of rail in the United States: 140,000 miles
- Average length of rail section: 1440 feet
- Number of joints per section: 4 joints per section
- RWI joints at rail joints: 2,053,333 = 140,000 miles × 5280 feet/mile ÷ 1440 feet per section × 4 joints per section.

- Number of monitored crossings in the United States: 65,000
- Number of RWI per crossing: 8
- RWI at signaled crossings: 520,000 = 65,000 × 8

- Miscellaneous RWI attachments for frog, switch, and pullout controls 2,500,000

- Estimated RWI joints in track: 5,000,000 = 2,053,333 + 520,000 + 2,500,000
- Estimated failures per year: 50,000
    - These are considered in aggregate as they can result in a system signal of a failure.
- Estimated failure rate: 1% = 50,000 breaks ÷ 5,000,000 joints

Sources:

1. http://people.hofstra.edu/geotrans/eng/ch3en/conc3en/usrail18402003.html, citation for miles of U.S. rail 2010.

2. http://www.fra.dot.gov/eLib/Details/L02691 . # of signaled crossings in the United States.

Appendix B. Reparability Study Metallography

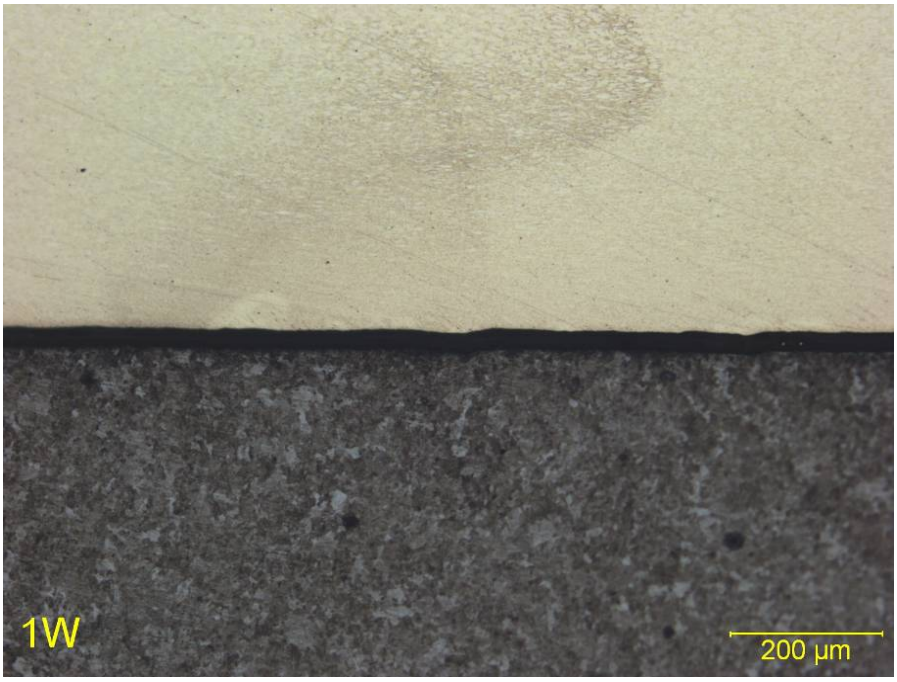

Figure B1. Initial Weld

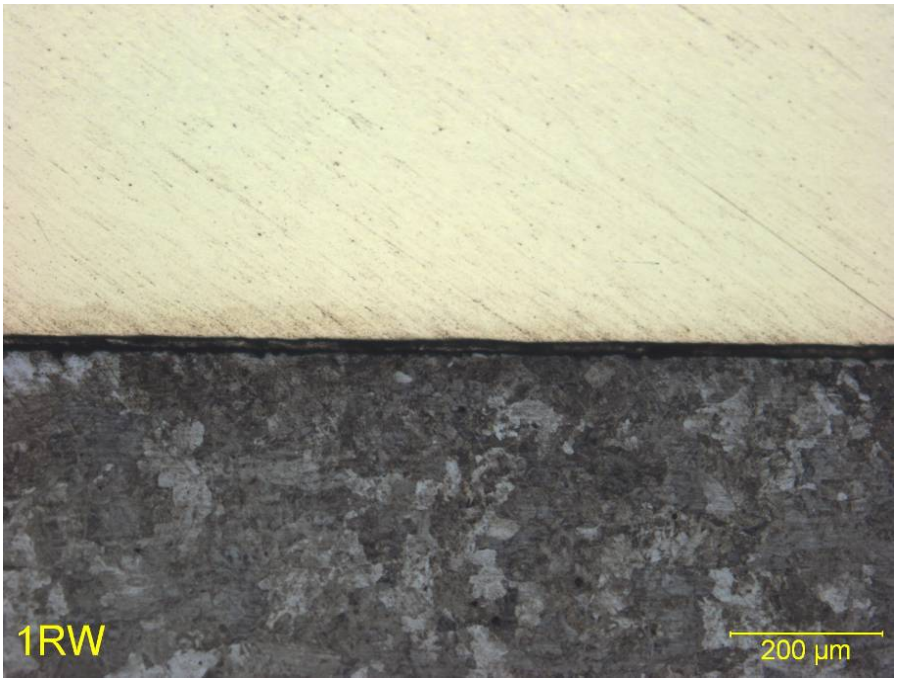

Figure B2. Reweld 1

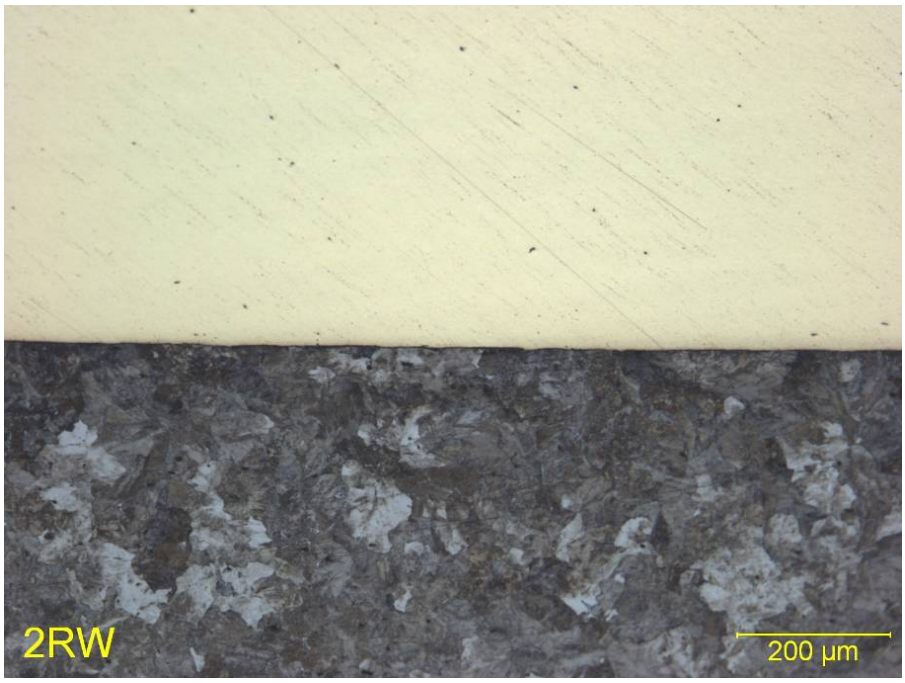

Figure B3. Reweld 2

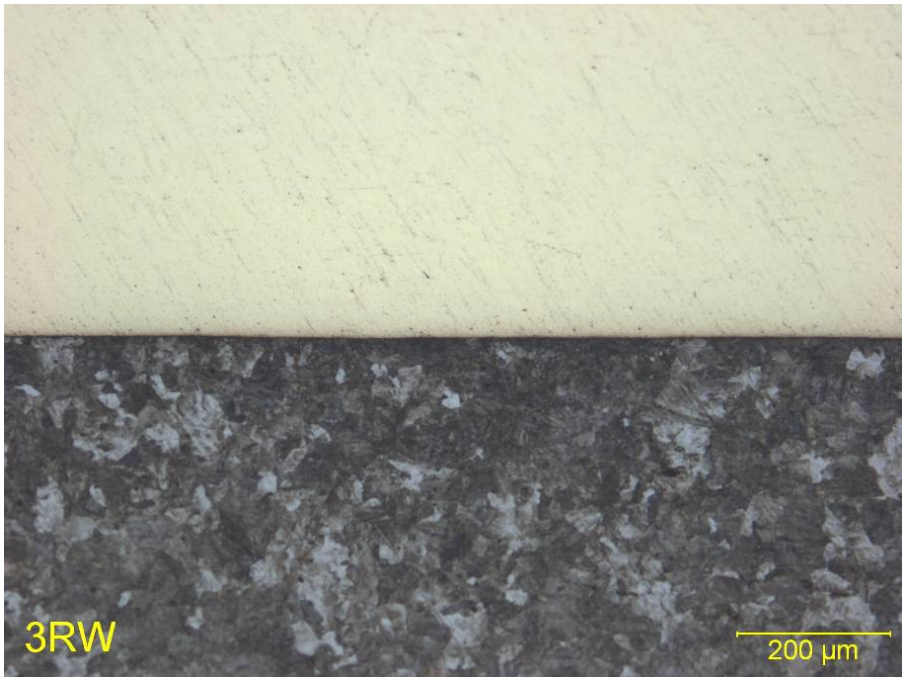

Figure B4. Reweld 3

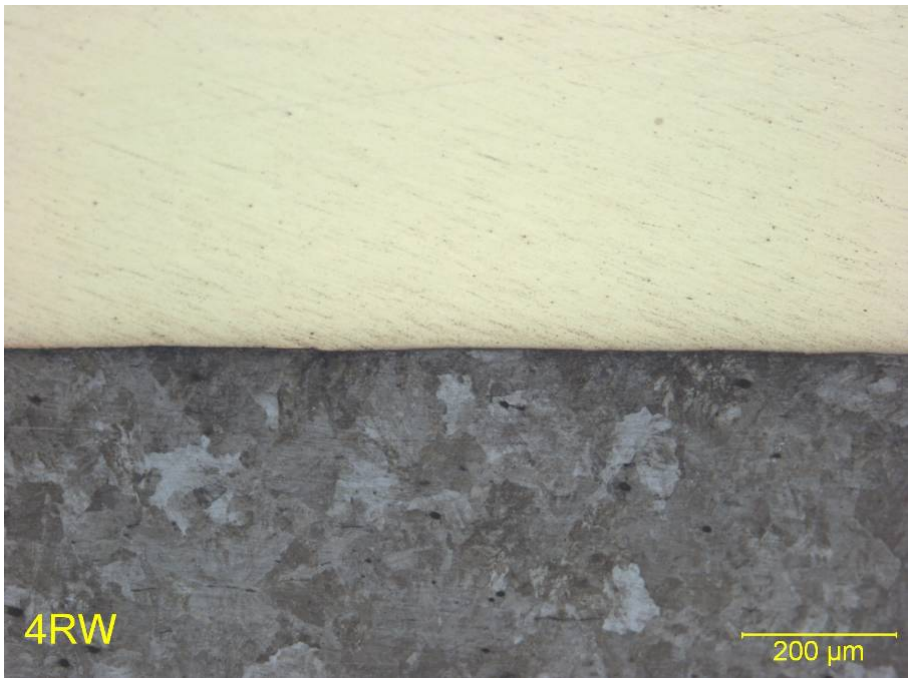

Figure B5. Reweld 4

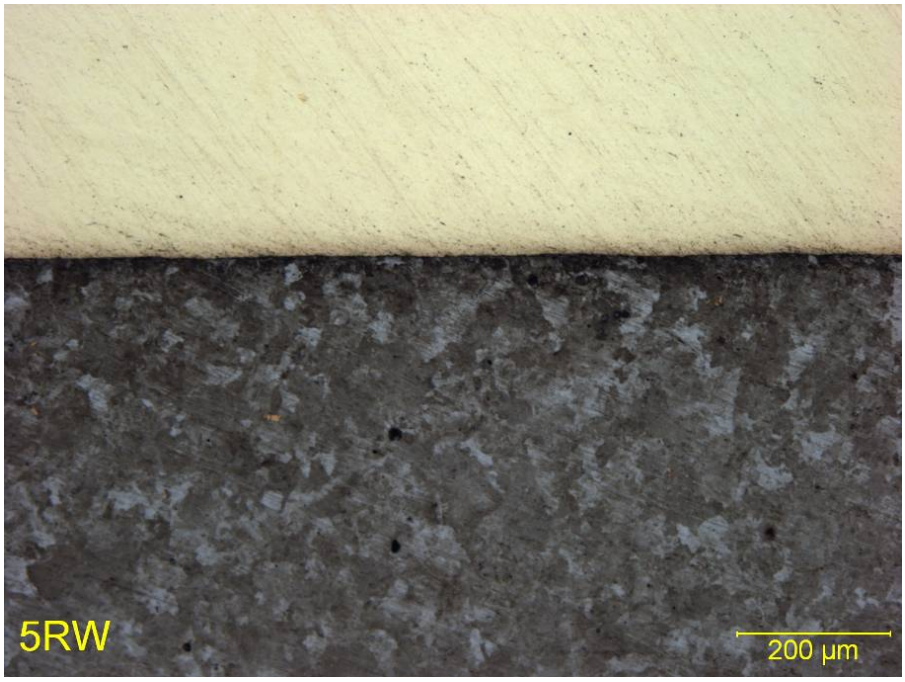

Figure B6. Reweld 5

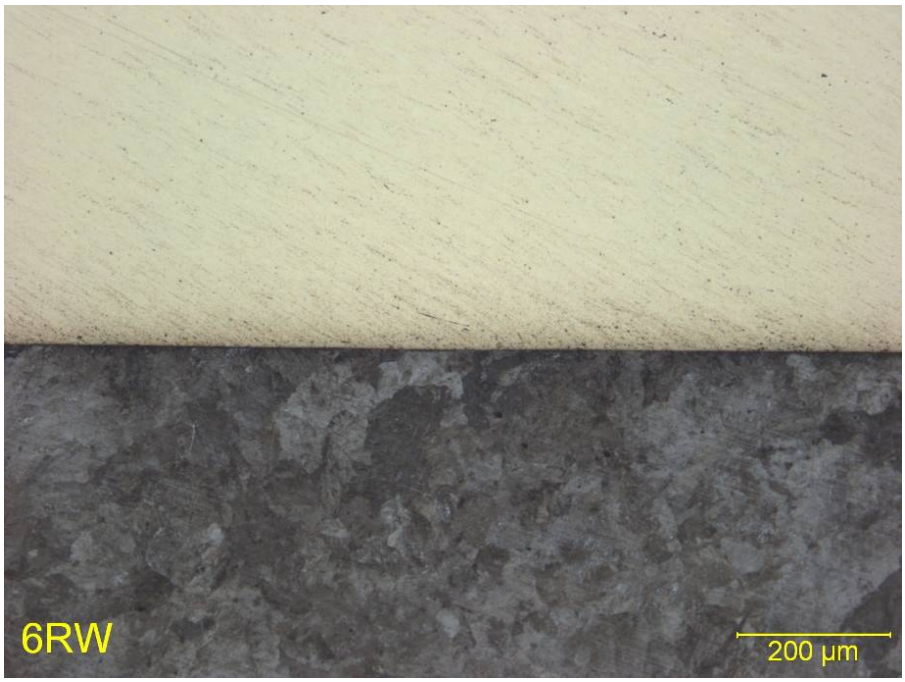

Figure B7. Reweld 6

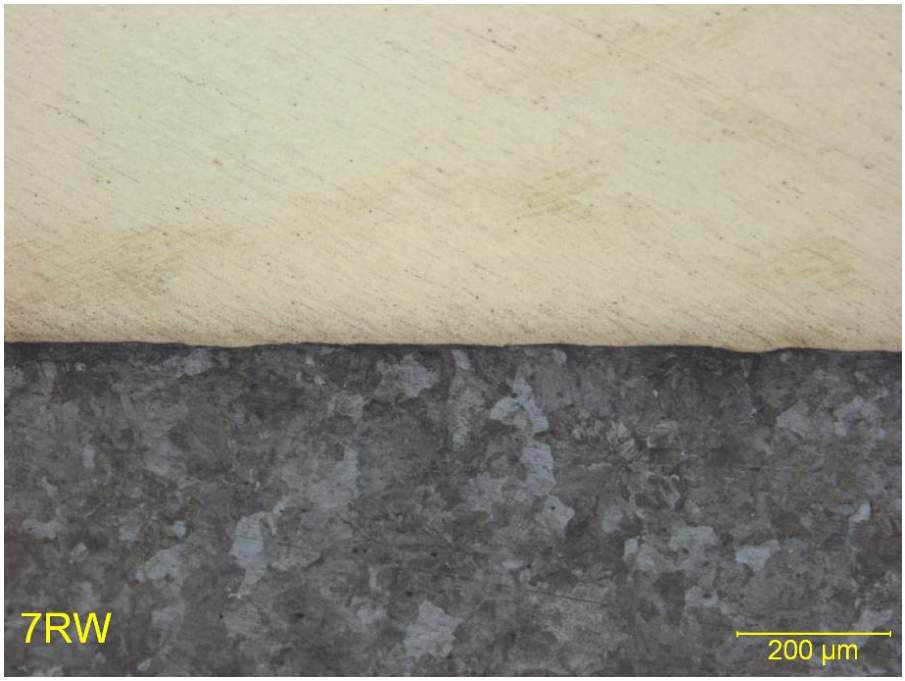

Figure B8. Reweld 7

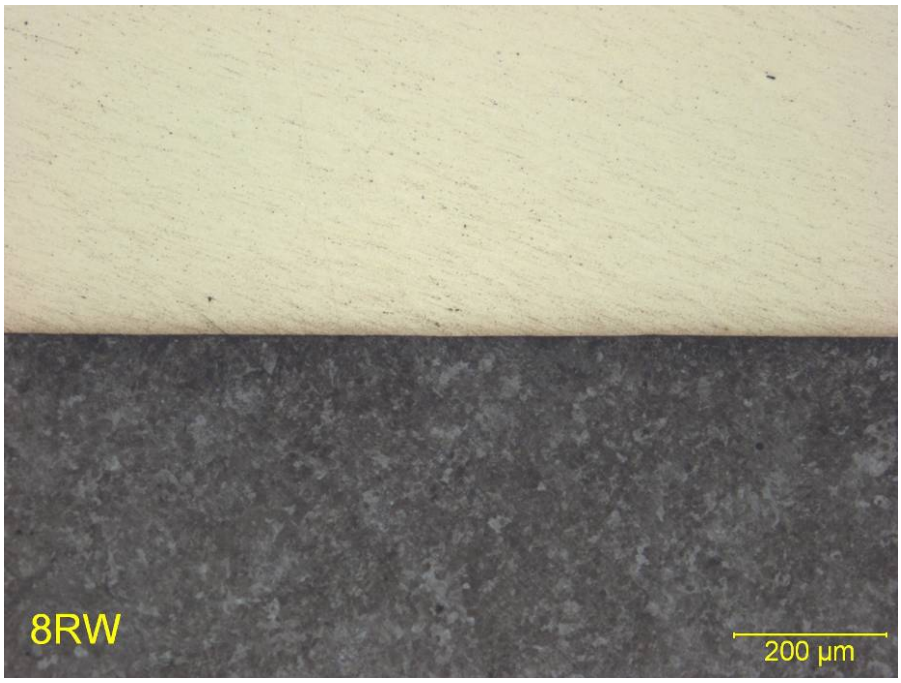

Figure B9. Reweld 8

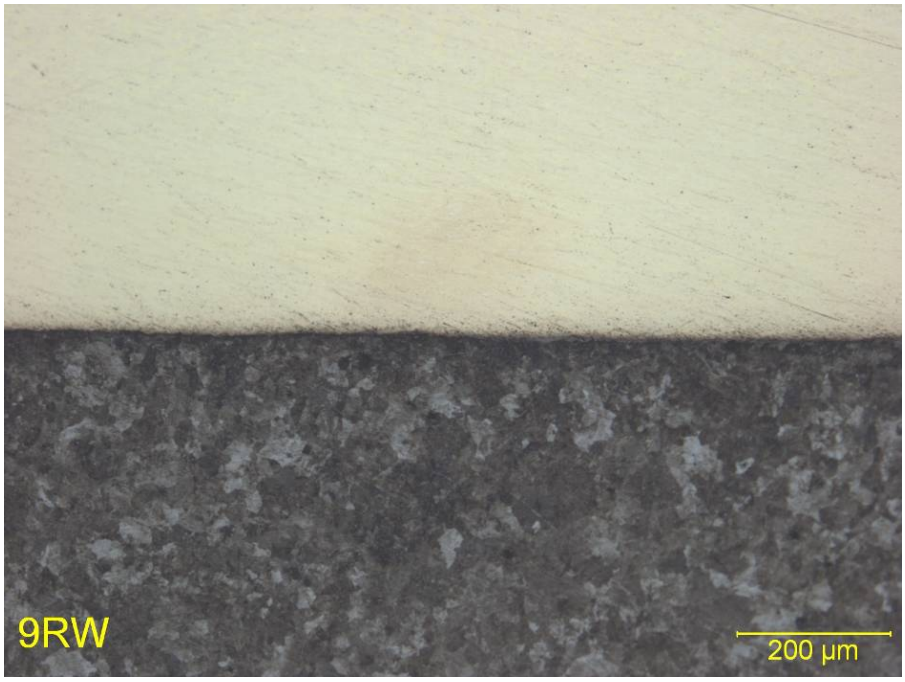

Figure B10. Reweld 9

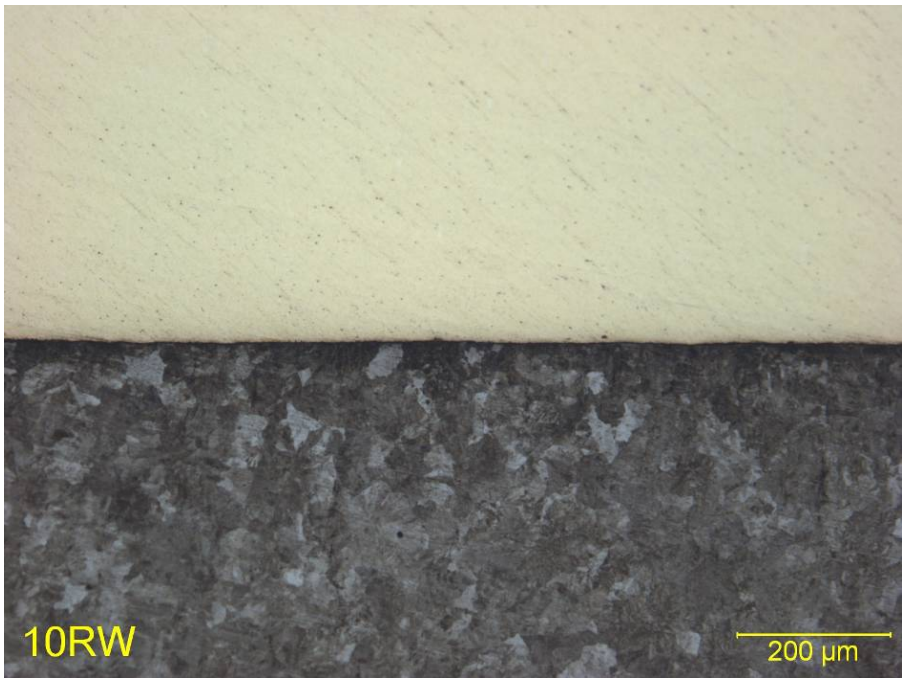

Figure B11. Reweld 10

Abbreviations and Acronyms

AAR	Association of American Railroads
AREMA	American Railway Engineering and Maintenance-of-Way Association
DOE	Design of Experiments
FAST	Facility for Accelerated Service Testing
FRA	Federal Railroad Administration
HAZ	Heat-Affected Zone
IFW	Inertia Friction Welding
LME	Liquid Metal Embrittlement
MOW	Maintenance of Way
NDE	Nondestructive Evaluation
NTSB	National Transportation Safety Board
PTC	Positive Train Control
SEM	Scanning Electron Microscope
TTCI	Transportation Technology Corporation Inc.
UT	Ultrasonic Testing
UTS	Ultimate Tensile Strength